ELECTROMAGNETIC STEREOTACTIC COMPUTER-ASSISTED NAVIGATION IN MINIMALLY INVASIVE SURGERY

A PhD THESIS

Submitted
By

Dr. Ronald Andrew von Jako

In Partial Fulfillment of the Requirements
For the Degree of

Doctor of Philosophy

In

Experimental Surgery

Advisor:
Professor Gyorgy Weber

Program Leader:

Professor Erzsebet Roth

University of Pecs, Faculty of Medicine
Department of Surgical Research and Techniques

2009

CONTENTS

LIST OF TABLES

LIST OF FIGURES

ABBREVIATIONS

ANSI	American National Standards Institute
CAES	Computer-assisted endoscopic surgery
CAS	Computer-assisted surgery
CHS	Compression hip screw
CLS	Cannulated lag screws
CF	Conventional fluoroscopy
CT	Computer tomography
CTQ	Critical to quality
DF	Degrees of freedom
DRA	Dynamic reference array
DRF	Dynamic reference frame
DS	Depuy Spine
EM	Electromagnetic
EMG	Electromyography
EMF	Electromagnetic field-based
ENT	Ear Nose and Throat
ESS	Endoscopic spine surgery
EER	Entrance exposure rate
FESS	Functional endoscopic sinus surgery
FID	Field integrity distortion
FOV	Field of view
Gy	Grays

ABBREVIATIONS CONTINUED

HMD	Helmet mounted display
ICU	Intensive care unit
IEEE	Institute of Electrical and Electronic Engineers
IGS	Image-guided surgery
Ii	Image intensifier
IRB	Institutional Review Board
JAC	John Anthony Carrino
J&J	Johnson & Johnson
LED	Light-emitting diode
MR	Magnetic resonance
MVA	Motor vehicle accident
NAV	Navigation
OR	Operating room
PACS	Picture Archiving Central System
PMMA	Polymethylmethacrylate
PPS	Pulse per second
RSNA	Radiological Society of North America
SSEP	Somatosensoric Evoked Potentials
TLD	Thermoluminescent dosimeter
RVJ	Ron von Jako
VCF	Vertebral compression fracture

PREFACE

My involvement in medical research started two decades ago when I was involved with laser surgery experiments combined with histological evaluations at the Boston University School of Medicine. This work was presented to the University of Pecs Medical School in 1990 as my Medical Doctoral Thesis.[208] It received a grade of 5/5.

My continued work involved both preclinical and clinical surgical research related to minimally invasive surgery for new concepts of instrumentation and techniques I had the opportunity to coin as “Minimally Invasive Direct Access Surgical Techniques” (MIDAST™). The preclinical work for MIDAST™ started at the Moritz Kaposi Medical Center followed by: The University of Pecs Faculty of Medicine, Semmelweis Medical University, The University of Debrecen Medical Faculty, and The Medical University of Szeged hospitals in Hungary. The Medicor hand Instrument Company of Debrecen manufactured the instruments for MIDAST™ surgery in which I played a significant role in design development. Pre-clinical and clinical work was also performed in the United States at the Minimally Invasive Surgical Research Laboratories of Harvard and Boston University affiliated hospitals: Brigham and Woman’s hospital, Beth Israel Hospital, The Massachusetts General Hospital, and The Lahey Clinic. The development involved general surgery and ten other subspecialties from urology to cardiac surgery. This research resulted in several publications and presentations, as well as seven scientific exhibitions at the annual meetings of the American College of Surgeons and other notable medical congresses listed in the personal publications list.

In the last decade, a new horizon opened in the advancement of minimally invasive surgery known as “Stereotactic Computer-Assisted Surgical Navigation.” I was fortunate to be one of the original participants in its development as a member of the surgical research team at Visualization Technology, Inc (VTI). Shortly after, the Healthcare segment of the General Electric Company, a Fortune 10 Company, acquired VTI. My research continued, and I worked with physicists, engineers, and numerous leading clinicians in the United States, Germany, and Hungary. Five years ago, I was appointed clinical research leader of GE Healthcare’s surgical development efforts providing direction for the progress of minimally invasive navigation and organizing research at prestigious academic centers in the U.S. and abroad. Data evaluation was performed in our corporate science laboratories in cooperation with physicists and engineers working at my direction.

This Thesis presents my own individual research efforts with my colleague team members. It covers work and results relating to paranasal sinus surgery, spine surgery, and femoral bone surgery. For the paranasal sinus investigation, we used ten human cadaveric heads. We used 47 human cadavers for research in the spine and five human cadavers for experiments in femoral bones. All these clinical applications involve computer tomography (CT) scanning with specially formatted data sets. This exposes the patient to excess ionizing radiation when compared with simple radiographs. Since CT scans are taken in advance of surgical procedures and not at the time of surgery, the physician cannot update the surgical progress of altered anatomical landmarks and structures during dissection or drilling. Therefore, I instituted a research effort to address this issue by applying intraoperative C-arm fluoroscopy for real-time image updates. This potentially reduces radiation exposure in comparison to CT. Parallel to this, instrumentation was improved to accomplish this goal. I designed and built over a dozen custom instruments for spine surgery that were submitted for patents by the General Electric Corporation. Some of these research aims, performance limitations, and results are also included in this Thesis. Because these procedures require further refinements, the future needs are also mentioned.

My original interest and work with laser surgery also prompted me to investigate new approaches to enhance the already clinically recognized techniques of percutaneous laser discectomy. I combined it with navigation to improve technique accuracy and minimize x-ray exposure. This preclinical research was performed at a Hungarian laboratory where all CT/MR/X-ray resources and specific equipment needs were available in one central location. This laser-Nav project was coauthored by von Jako and Cselik and supported by Professors G. Weber and E. Roth. It was published in the Journal of Lasers in Medicine and Surgery with an impact-factor of 2.771 and is presented here in more detail. A second collaboration was performed with Professor G. Weber and the Experimental Surgery Department to investigate minimal access approaches to the spine. This research was accepted for publication in the Journal of NeuroImage with an impact-factor of 5.5 and presented in the Thesis.

In the interest of medical progress it is expected that the field of surgical navigation will expand to new areas, including the field of vascular surgery. Further collaborative investigations with institutions in Pecs and Hungry would be welcome in these future preclinical and clinical research efforts.

CHAPTER 1. General Introduction

The use of modern stereotactic surgical guidance technologies has been an exciting and growing field in the past 20 years. Its successful combination with axial computed tomography (CT), magnetic resonance (MR) imaging, and intraoperative C-arm fluoroscopy, which provide direct and detailed radiological views of orthopedic and neuroanatomy, prompted an expansion in the use of stereotaxis. This technical field of computer-assisted surgery (CAS) for anatomical navigation, also known as image-guided surgery (IGS) and surgical navigation (SN), lets a surgeon track the position of instruments and implants relative to the patient's anatomy in a quasi virtual-reality mode displayed on a color monitor. The aim is to guide the device safely and precisely to its target in two or three dimensions and to reduce the invasiveness of procedures. For instance, navigated otorhinolaryngologic surgery makes it easier to perform complicated sinus and temporal bone surgeries. Navigation in orthopedic spine and hip surgery ensures that hand instruments and implants are precisely positioned and in the field of cranial neurosurgery, that a biopsy can be accurately targeted with instruments while circumventing critical and sensitive neurovascular structures. Its enhanced use with new electromagnetic (EM) tracking technology in surgical subspecialties is being evaluated and is the focus of this research.

1.1 History Of Stereotactic Surgical Navigation

Surgeons continuously strive to improve the safety and effectiveness of their interventions throughout every operation. A surgeon must maintain a precise sense of complex three-dimensional (3D) anatomical relationships. To accomplish this, a surgeon needs to be able to visually track or navigate the actions of instruments relative to the surrounding anatomy. The term "navigate" as defined by Webster's dictionary means, "to steer or direct the course of a ship or aircraft." The earliest forms of navigation utilized sailing along coastal lines with visual landmarks to move from one place to another. Through the centuries, early navigators created charts, compasses, and instruments like the sextant and an accurate marine clock to measure the altitude of stars and planets for positional localizations. In medicine, over a century ago, surgeons began to discover new techniques for localizing anatomy, starting in the mapping of the brain and based off of René Descartes' mathematical coordinate system for determining a point in 3D space.[142,190]

The earliest instruments for brain localization were designed to reference the surface of the skull and its relationship with the brain. Deeper brain structures were explored accurately when a precise coordinate reference system was established and a true stereotactic instrument was designed. The term "stereotactic" comes from "stereo," the Greek word for 3D and "taxic" Greek for system or arrangement and the Latin verb "tactus," which means to touch.[88] In medicine, "stereotactic" navigation involves the use of an external framework attached to the patient (Figure 1.1.) to allow for the correlation of geometrically determined vectors to internal points of anatomical interest.

Courtesy of Integra NeuroSciences-Radionics

Figure 1.1 Stereotactic Brown-Roberts-Wells frame for cranial surgery circa 1980.

The first use of modern image guidance or navigation came only eight days after Roentgen's announcement of the discovery of X-rays.[135] An emergency suite surgeon in Birmingham, England named J.H. Clayton in 1896 used a radiograph to surgically remove a needle buried in a woman's hand. The image guidance helped determine the trauma, the shape and size of the surgical target, and the location of the needle relative to other anatomical structures in the patient. Still, because the simple radiograph compressed the 3D spatial relationships into a 2D image, a degree of positional uncertainty existed in regard to the thickness of the patient's hand.[216] The radiograph also showed only the bony landmarks clearly, so the surgeon still needed to rely on his understanding of general anatomy for the location of tendons, vessels, and other structures to minimize unnecessary harm. Even today, surgeons must operate with this principle among their guiding tenets.

1.2 Technical Background Of Surgical Navigation

In 1908, twelve years after Clayton's surgery, Horsley and Clarke[88] described a device that allowed the placement of electrodes into precise positions within an experimental animal's brain when the device was fixed to anatomical landmarks. In this paper, Horsley and Clarke coined the term "stereotactic" and described techniques for establishing a positional brain atlas to aid in the exact placement of electrodes. Their device was predicated on the assumption that by affixing the frame relative to certain external anatomical landmarks such as the orbital rims and the external auditory canals, the internal target points of the skull could be consistently and reproducibly localized for electrode or needle placement. In experimental animals, the device performed well by applying rectilinear topography to the animal brain and using a stereotaxic instrument to pass needles to desired points in the brain, although placement was confirmed by sacrifice of the animal at the end of the experiment. Horsley and Clarke's frame principles are what later enabled various head and extremity fixation devices to work in the evolving field of surgical navigation. The next major step was the development of computer science, which was pioneered by Hungarian scientists John von Neumann and John Kemeny at Princeton University.[149] Later, Edward Teller developed initiatives for military aerospace navigation.[206-208]

1.2.1 Framed-Based Stereotaxis

Following the works of Horsely and Clarke, methods continued to evolve in the space of stereotactic neurosurgical techniques using instruments and procedures to target the brain. In the 1940s, Spiegel and Wycis[198] first used stereotactic methods in humans for neurosurgical ablation procedures. Some of these evolving stereotactic techniques included what is known as a frame-based stereotaxis, combining radiography and anatomic atlases. After Spiegel and Wycis, in 1949, Leksell included an arc system attached to a patient's head; this was ultimately developed into a well-known frame named after him. Talairach and team also followed with a different version, as did Todd and Wells; from this, the Kelly-Goerss frame was later derived. This target-centered frame became known as the COMPASS system.[128,129,137,205] Roberts and Brown developed a frame-based system called the Brown-Roberts-Wells (BRW system) for CT in the late 1970s and later modified it for use with MRI.[174] Wells and Cosman created a less complex version of the BRW in the 1980s by developing an arc guidance frame similar to the Leksell frame that became known as the Cosman-Roberts-Wells (CRW) system. This system directs a probe isocentrically around a planned target without the need of a fixed entry point. It was later used with optical infrared navigation systems such as the Radionics OTS frameless image guidance system, providing the target and trajectory calculations (personal communication, Chris von Jako, Integra Neurosciences–Radionics). Other known frames included the Zamorano-Dujovny multipurpose head frame and the Patil frame, which allows a surgeon to measure coordinates directly from a scanner screen and allows the surgeon user to acquire intraoperative images to confirm procedural accuracy.[155,233] In practical use, these frames involve a rigid housing and multiple skull pins used with local anesthesia. The frames create a bond between a patient's skull and fiducial markers to localize intracranial targets with precision trajectories for spatial accuracy, speed, and reliability of stereotactic instrumentation used for functional and stereotactic radiosurgery.[8] The frames are also used in multiple procedures that involve the need for both diagnostic and therapeutic goals. Biopsy is one of the most common uses for indirect image-guided stereotactic methods and prior to the development of frames and radiography, targeted access to the head required free-hand approaches to craniotomy procedures to guide various instruments such as needles for aspiration.

1.2.2 Frameless Stereotaxis

With the introductions of advanced CT and MR imaging over the past decades, stereotactic-assisted craniotomies for tumor, vascular, and other deep lesions became available, and work by Kelly and others[110,111] helped to evolve frameless systems by converting volumetric information from CT scans into stereotactic space.[112,173,197] The frameless systems differ in that they do not require a fixture to the head; in this way they eliminate the drawbacks of a bulky apparatus that requires local anesthetics to control discomfort prior to patient attachment. Frameless systems eliminate field obstructions that later enabled spinal navigation procedures.[77,214,215] Furthermore, many of the frame-based systems limit surgeons to a straight trajectory line and do not offer real-time feedback. Roberts and Friets[67,173] used frameless stereotactic systems in the 1980s to define points in a radiographic image and also in the patient to map the two to each other. In this correlation process, the pre- or intraoperative radiographic image of the anatomic structure of interest is shown in one frame of reference. The instruments are visible in a second frame of reference that is established by a localizing device whose position and orientation are known (to the computer) in 3D space.

Frameless units are used for different reasons than the frame-based systems. They are also mechanically designed to hold instruments for a planned tumor target. The frameless system cannot provide a mechanical containment of surgical instruments to target a lesion or other tissue. The frameless navigation system uses different localization methods to indicate its position in space for tracking on CT/MR fused cranial procedures or CT data sets in the spine (FIG 1.2).

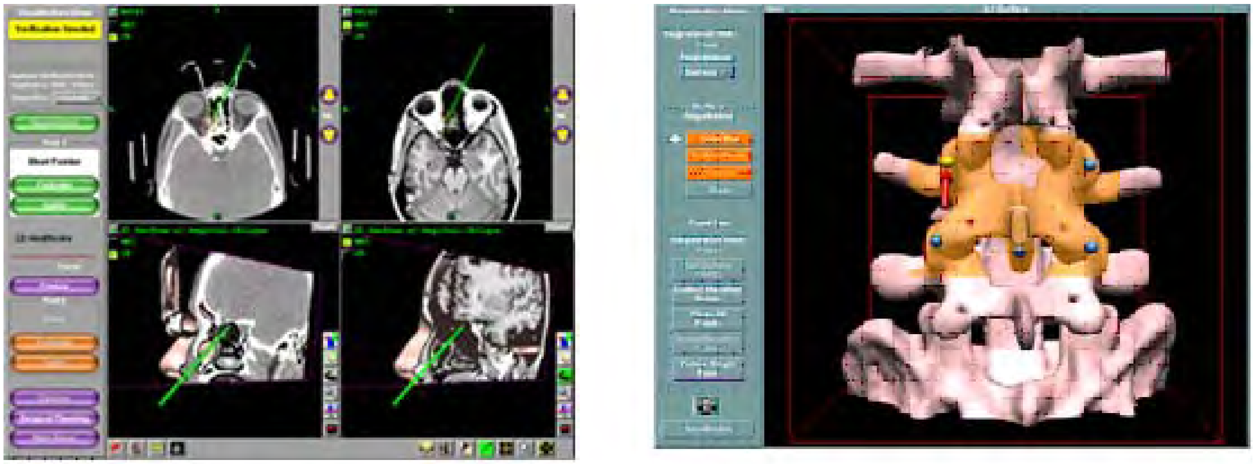

Figure 1.2 (A) CT/MR registration of the head and brain; (B) CT paired-point registration of the spine.

The development of frameless stereotactic systems enabled the integration of stereotactic devices into spinal surgery, which had been inhibited because an external frame of reference (i.e., stereotactic frame) could not be applied easily to the spine and the skin encompassing the torso was too mobile for the application of reliable external surface markers. These problems were overcome by the development of the frameless systems, which use two common methods for registration of the external markers with the internal points. The first uses a surface-based registration to fit a set of points from the outlines of one image to a surface-rendering outline of a patient's anatomy or other images. The second method is a point-based registration technique that requires the user to select corresponding points in different images and on the patient's anatomy using fiducial markers and the instruments.[18,162,211,224] These points could be anatomical landmarks or artificial and mobile markers. The mobile markers can be glued, clamped, or driven into the bone for a temporary and rigid fixation (Figure 1.3). The mobile markers (described later) are what we used in our experiments with what is called manual and automatic registration.[120] Then, the coordinates from each set of points are defined and a geometric transformation is calculated between them.

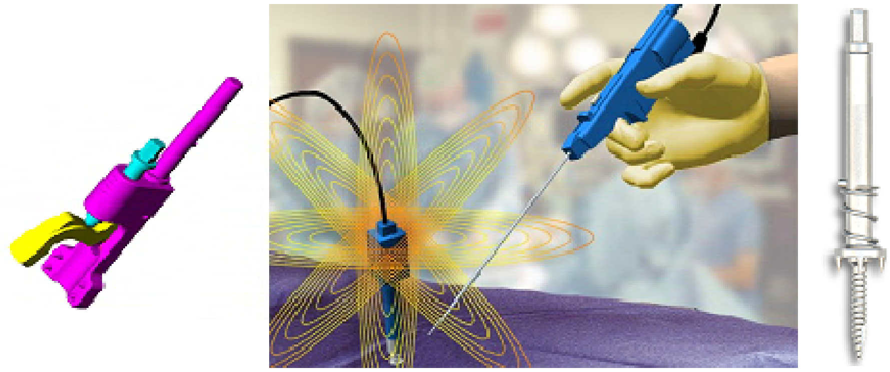

Figure 1.3 Illustrations showing bone clamp (left), transmitter generating the EM field (middle), and Caspar-style bone reference pin (right).

Kalfas, Murphy and colleagues first applied frameless stereotactic navigation to spinal surgery in the early 1990s[101,146] using CT data sets that later expanded to intraoperatively updateable and automatically registered C-arm fluoroscopic images. This eliminated some of the earlier challenges of accuracy, ease of use, and historic data sets. Welch et al.[220] reported their results using an articulated arm mounted directly to the head clamp (ISG Technologies, Elekta Instruments Inc., Atlanta, GA) for procedures of the craniocervical junction. These earlier methods helped the transition from cranial stereotaxis to spinal use.[60] Our navigation experiments utilize only a frameless tracking technology.

Surgical navigation systems show a surgeon, in real time, the precise position and orientation of the tip of the operating instrument(s) relative to the patient's anatomy on a display of the patient's imaged anatomy. To accomplish this, the patient's CT, MRI, or fluoroscopic images are combined with an instrument-tracking technology. The tracking technology must be able to accurately determine both the position and orientation of a freely moveable object located within the surgical volume with respect to a fixed reference.

Trackers currently used for surgical navigation platforms employ technologies based on mechanical arms with optical, sonic, and electromagnetic sensing. Each of these technologies has particular advantages and disadvantages, but all perform with acceptable accuracy and credibility as navigation devices within the surgical environment.

1.2.3 Optical Tracking Technology

Since the early 1990s, various image-guided systems entailing various software and hardware capabilities have surfaced to address various anatomical conditions; however, a typical system relies on preoperative CT imaging, specialized surgical instruments, a dynamic reference array (DRA), an electro-optical camera array, and a computer workstation (primary system interface). Light-emitting diodes (LEDs), also known as "active arrays," or reflective spheres, otherwise known as "passive arrays," are attached to the surgical instruments as well as the DRA and are monitored or tracked by the electro-optical camera array. The optical tracking digitizer measures the 3D locations of the arrays and the information is transferred to the computer workstation to produce a spatial orientation between the surgical and image anatomy (Figure 1.4).

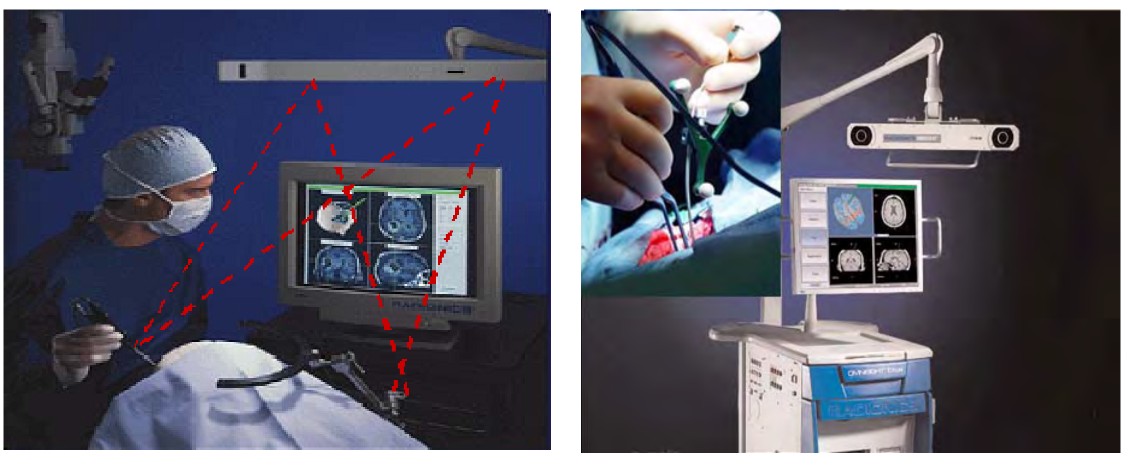

Courtesy of Integra NeuroSciences - Radionics

Figure 1.4 (A) Illustration showing optical camera and infrared LEDs communicating; (B) photograph showing optical spheres attached to a surgical tool.

1.2.4 Electromagnetic Tracking Technology

Electromagnetic six degrees-of-freedom (df) trackers, like optical infrared systems, provide three parameters of position (x, y, and z) using any convenient Cartesian coordinate system and three parameters of orientation (azimuth, elevation, roll angles) that completely describe the location and attitude of the moveable object. Most simply put, position parameters describe where the moveable object is in space, and orientation parameters describe which way it is pointing with respect to the fixed reference. The moveable object portion is referred to as a sensor and the fixed reference as a source.

Electromagnetic six-df tracking technology was invented and developed in the mid 1970s primarily for military use as a helmet-mounted sight or display in fighter aircraft. Both optical and electromagnetic technologies are applied for guidance of a pilot.[68,161] Optical systems employ infrared emitters on the helmet (or cockpit) and infrared detectors in the cockpit (or helmet) to measure the pilot's head position (Figure 1.5), but are limited by restricted fields of view and sensitivity to sunlight or other heat sources, which have correlations in a surgical environment: the ergonomic issues with the line-of-sight and optical infrared camera positioning.[35,139] Electromagnetic (EM) sensing designs use coils (in the helmet) placed in an alternating field (generated in the cockpit) to produce alternating electrical voltages based on the movement of the helmet in multiple axes. This technique requires precise magnetic mapping of the cockpit to account for ferrous and conductive materials in the seat, cockpit sills, and canopy to reduce angular errors in the measurement.[1,3,36] Similarly, in the surgical environment, the positioning of an electromagnetic reference sensor on the patient and in the surgeon’s hand instrument while maintaining surgical fields free of ferromagnetic distorters require distortion mapping to adjust the maximum performance of the EM technology to the surgical environment. One example is the distortion mapping of a C-arm fluoroscope for common intraoperative uses. We explored in previous experiments listed in the publications section and referenced in the Aims section the optimal surgical accuracy of tracker units, the environment with operating tables, and various surgical instruments for these situations.


Courtesy of M. Gunther, Vision Systems International, San Jose CA

Figure 1.5. Stock photograph showing a fighter pilot wearing a helmet that is tracked with an optical or electromagnetic system.

1.2.5 Electromagnetic Tracking Benefit

Kelly and Groes are credited in the early 1990s with the invention of electromagnetic stereotaxis.[109] Shortly after, electromagnetic tracking technology was modified for routine surgical use starting in ear, nose, and throat surgery (ENT) surgical navigation, primarily for endoscopic sinus surgery. Our previous company, Visualization Technology Inc, introduced the first electromagnetic commercial system for endoscopic sinus surgery. In the past, many medical researchers rejected EM tracker technology because it presented the problem of metallic sensitivity that could render EM trackers inaccurate when operating in severe metallic environments. However, EM technology provided a number of significant benefits necessary for successful operation within a surgical environment.

These benefits include the following:

- Frameless operation—that is, sensor measurements are made with respect to a fixed source attached to the patient's anatomy
- Nonshadowing—that is, absolute line of sight between the sensor and source is not required
- Six- degrees of freedom (df) outputs
- Speed
- Resolution
- Inherent accuracy

- Simple input/output (I/O) data communication
- Simplicity of calibration and use
- Simplicity of setup
- Safety
- Unique source and sensor architecture
- Ruggedness of the sensor and source hardware

1.2.6 Electromagnetic Tracking Disadvantages

The disadvantages of EM technology for use in surgical navigation include the following:

- Field distortion in severe metallic environments
- Deviations in the source and sensor field shapes
- Mathematically and computationally intensive

These issues of the magnetic field distortions in specific applications can be addressed in the development and engineering process by tuning the EM system to its environment and creating instruments that are compatible with this type of tracking technology. This provides a surgically accurate EM tracker system, which is used for endoscopic sinus surgery. The refined EM technology developed to address these disadvantages has allowed increased clinical usage of fluoroscopy-based electromagnetic tracking in many surgical fields including spine and orthopedic surgery. Current research for the future includes a micro-sensor and wireless electromagnetic tracking to improve the ergonomics of the system by providing increasingly user-friendly technology.

1.3 Detailed Description Of The EM System, Its Function, And Components

Electromagnetic systems use electromagnetic fields (EMFs) to determine the position and orientation of a remote object. The technology is based on generating low-frequency (10 to 20 kHz), near-field (quasi-static) magnetic field vectors from a single assembly of three stationary magnetic-dipole antennae (coil array) called a source or transmitter. The magnetic field vectors are detected with a single assembly of three remote sensing magnetic-dipole antennae (coil array) called a sensor or a receiver (Figure 1.6A). Each transmitter coil induces a voltage in each of the three sensor coils resulting in nine mutual inductances that are measured. (Figure 1.6B)

Figure 1.6(A) Electromagnetic transmitter; (B) electromagnetic receiver.

From these nine mutual inductances, the position and orientation of the sensor (receiving) antenna with respect to the source (transmitting) antenna are calculated. The calculated results are formatted into x, y, and z Cartesian coordinates for position (Figure 1.7) and ψ, θ, and ϕ (azimuth, elevation, and roll). Euler angles for orientation are sent to the host computer (Figure 1.8). The mathematical algorithm that computes the sensor position and orientation also simultaneously accounts for deviations from dipole field shapes or any nonconcentricity in the coil arrays and also corrects for errors due to the presence of field distorters that are fixed with respect to both the receiver and the transmitter.

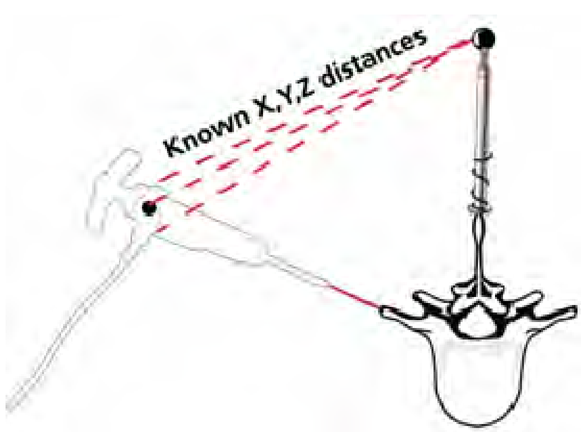

Figure 1.7 Transmitter attached to spine communicates with Receiver Surgical Instrument.

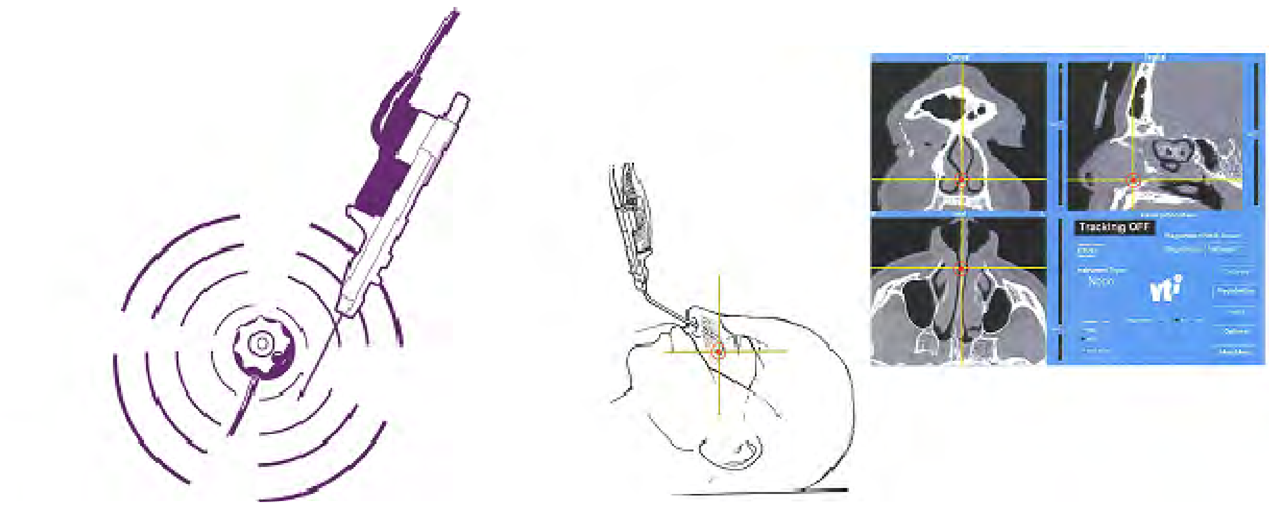

Figure 1.8 Illustration showing hand receiver with attached hand instrument communicating with the navigation workstation (left) and ENT sinus surgery transmitter attached to forehead via a headframe (right).

For spine and ENT, the electromagnetic navigation components are housed in a sterilizable tray that requires ethylene oxide (ETO) gas sterilization. The instrument components are stored in an autoclavable tray, and they consist of awls, probes, and taps, implant drivers, and a bone pin and clamp to secure the transmitter to the anatomy. The ENT sinus instruments, consisting mostly of aspirators, are singly packed, sterile instruments (Figure 1.9). With the ENT application, a single-use head reference frame is applied to the patient during preoperative CT scanning. After sedation or anesthesia for surgery, the headframe is placed back on the patient and the transmitter is then attached to the headframe. The surgeon uses one of the sterilely packed aspirators, which is calibrated to the receiver sensor, to register the patient's anatomy with the attached transmitter and headframe to the preoperative CT images, which are then displayed on the navigation screen (Figure 1.10).

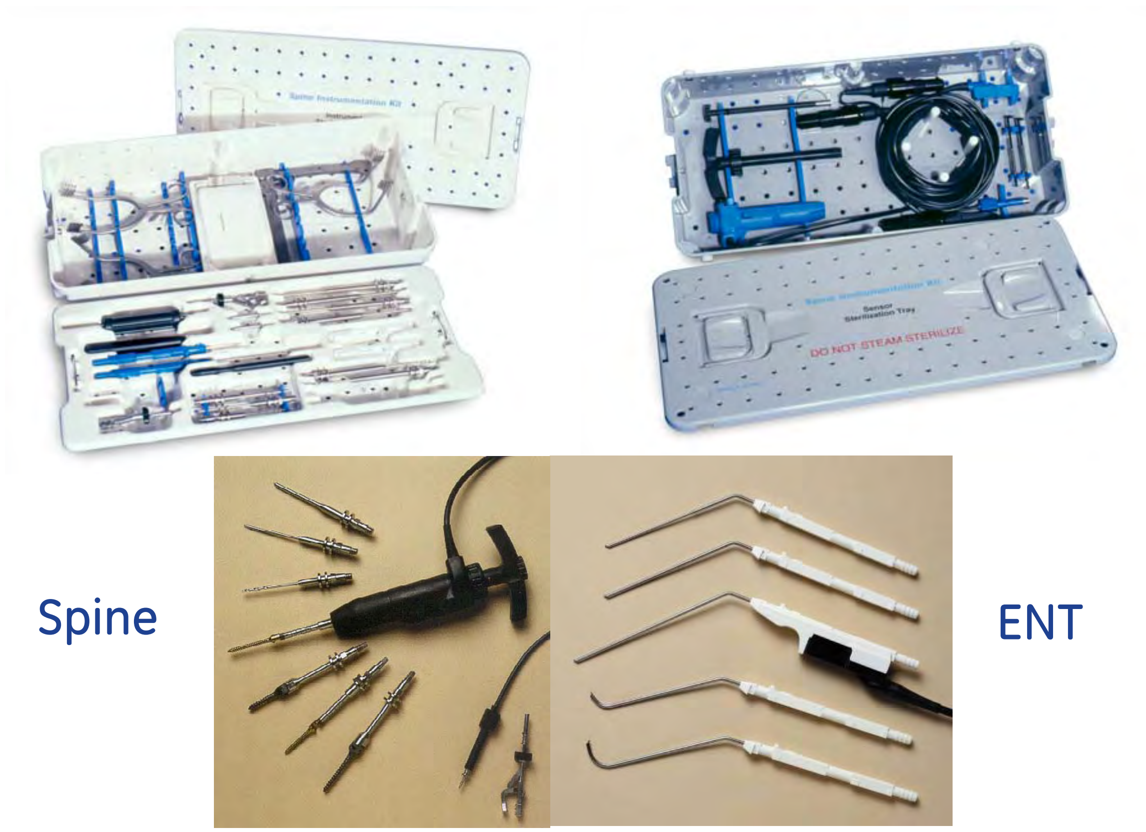

Figure 1.9 Photographs showing electromagnetic instruments for spinal and ENT applications.

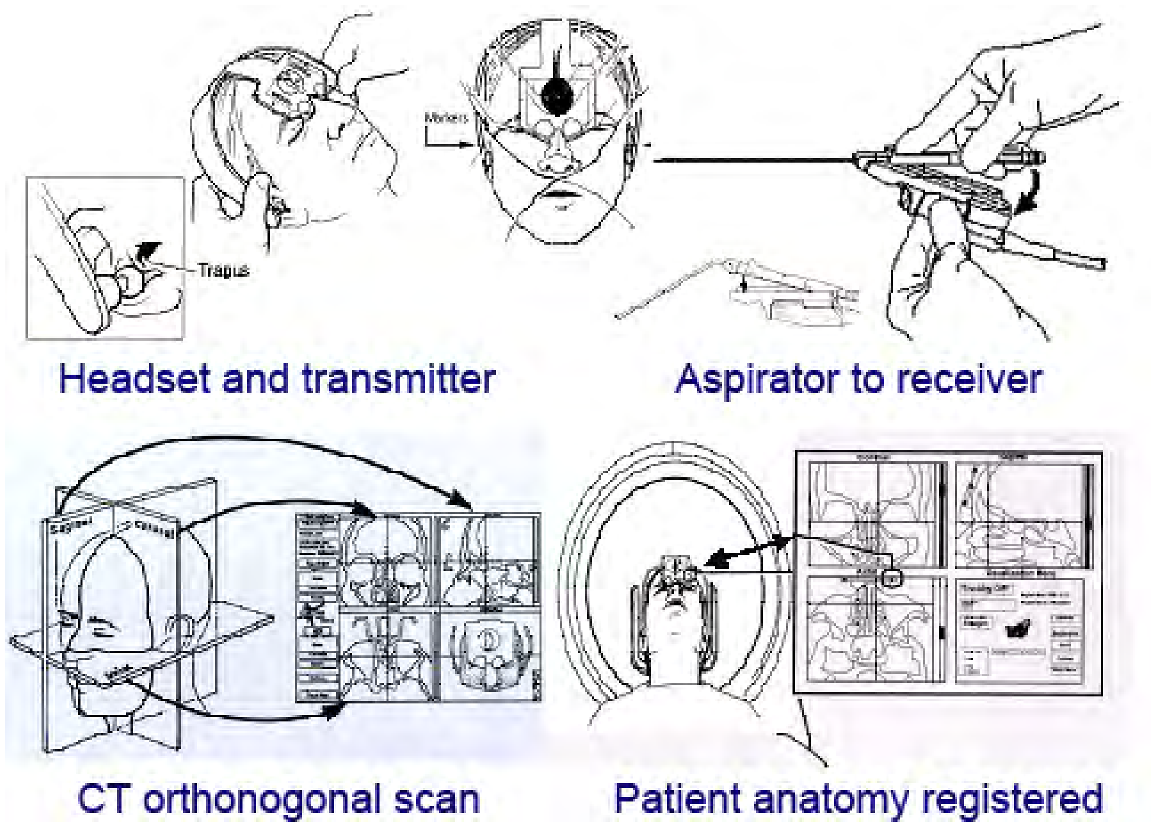

Figure 1.10 Illustration of registration of patient CT data sets and calibration of the instruments and preparation of sinus surgery instruments.

In the spinal application, a bone pin or a clamp is rigidly attached to the spinous process and a pin transmitter is then securely attached to the bone pin or clamp. The surgeon uses a C-arm fluoroscope with an image intensifier attached to a calibration grid to take the necessary AP/lateral or oblique views and saves them to the navigation workstation. At this stage, the surgeon will use either a manual or autocalibration method for measuring and setting the instrument tip-off sets. In manual calibration, the surgeon uses a pointer, for example, to manually calibrate the transmitter. For autocalibration of instruments, the surgeon selects the appropriate instrument and its corresponding screen icon, and factory calibration is used (Figure 1.11).

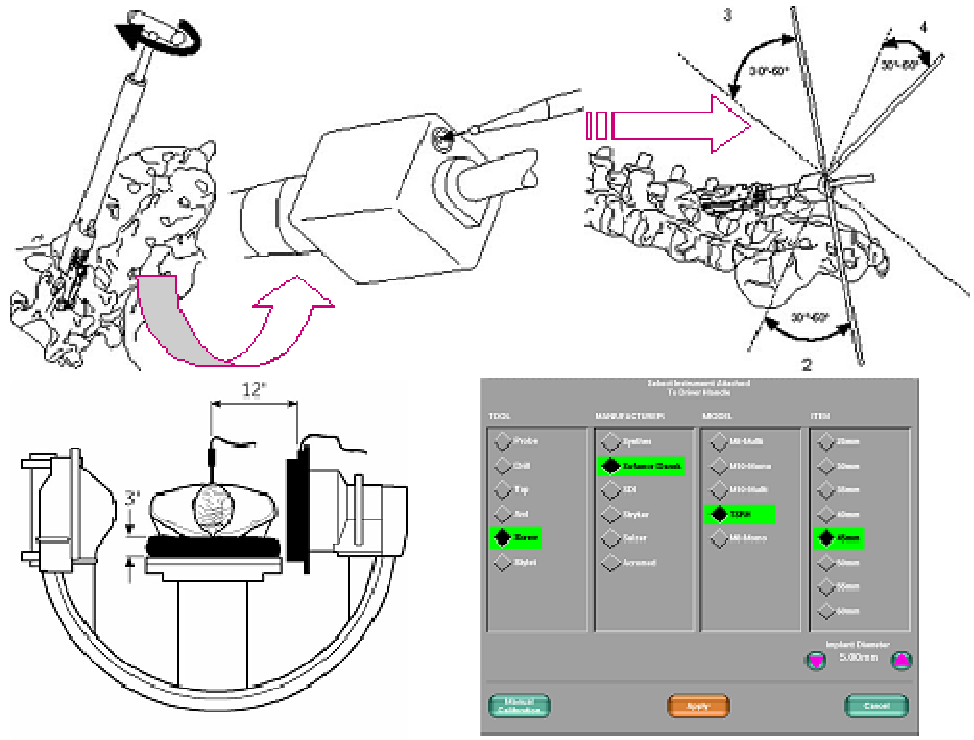

Figure 1.11 Illustration showing spine transmitter set-up and autocalibration screen.

1.3.1 Fundamental Physics

As touched upon earlier and at its most basic level, the system consists of two primary components: a source and a sensor. The source, or transmitter as it is commonly called, typically consists of three perpendicularly wound coils around a common core. Because of the perpendicularity of the three coils, the transmitter is also described as a three-axis source. Alternating electrical currents flowing through the coils produce a set of periodically time-varying magnetic fields (10 to 20 kHz). Varying the magnetic fields at these frequencies ensures that measurable voltages will be induced in the sensor coils over the working range of the tracker. It also ensures that the wavelengths of the fields are much greater than the distances separating source and sensor, thus simplifying the mathematics describing the behavior of the fields.

The generated magnetic fields also vary spatially with respect to the source coils. Along any straight line emanating radially from a source coil, the magnitude of the magnetic field falls off as the inverse cube of the distance ($1/\rho^3$)

from the coil. Thus, the fields are strongest nearest to the transmitter and fall off rapidly with increasing range (Figure 1.12). Additionally, the strength and direction of the magnetic field also varies tangentially at fixed distances from the source. It is this property of a mathematically computable spatial variation in magnetic field strength that is the underlying physical foundation of electromagnetic tracking systems.

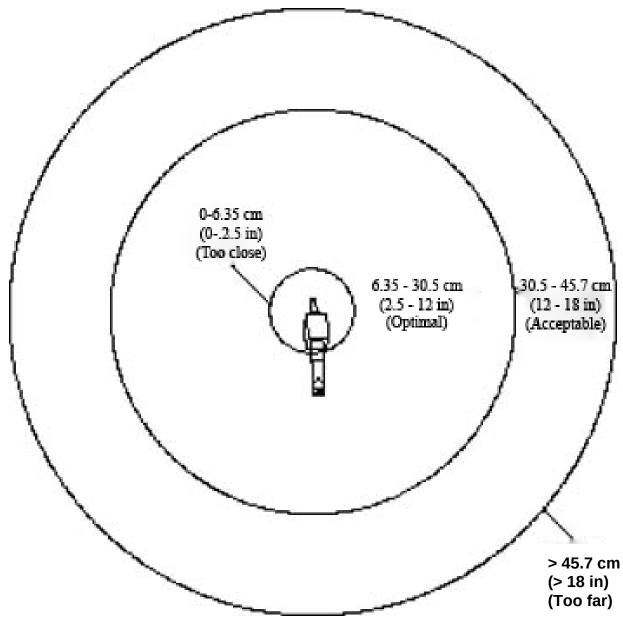

Figure 1.12 Illustration showing the range of the EMF strength from source to maximum distance of >50 cm.

The sensor also consists of three perpendicularly wound coils around a single bobbin. The sensor's three-axis coil geometry is precisely characterized after construction. The time-varying magnetic fields created by the source coils induce voltages in the sensor coils in accordance with Faraday's law of induction. The voltages are filtered and undergo digital signal processing to create a set of signals for each sensor–transmitter coil pair. The filtering and signal processing of the raw received signals reduces the effects of any interfering magnetic fields and noise. Ultimately, these signals are converted into the nine mutual inductances described previously.

There are three signal measurements for each transmitter coil (one measurement from each sensor coil). These three signals constitute a signal vector. At any sensor location in space, the values of the individual components of the signal vector depend on the alignment of the sensor relative to the transmitter.

Once the position of the sensor is known, computation of orientation is accomplished by determining the rotation matrix required to generate the measured signals. The base set for the rotation matrix is typically one of many Euler angle sequences or may be equally well described by quaternions. Regardless of the choice of basis, the orientation parameters are directly estimated from the rotation matrix.

1.3.2 System Configuration

In our development for a working tracking system, the implementation of the electromagnetic tracking system consists of an electronics unit powered by 50/60 Hz alternating-current mains supporting a single source (transmitter) and dual receivers (each receiver consisting of two sensors). The electronics unit returns each sensor's position and orientation information on demand to the tracker system's host computer over an RS232 serial data link at a rate of up to and including 115 K baud. The mechanical design of the receivers varies as a function of the surgical instruments to which they are attached. Similarly, transmitter mechanical configurations also vary as a function of mounting requirements depending on the particular application for which the system is used ENT cranial, axial-skeletal, and so forth.

1.3.3 Performance Characteristics

The unit's electromagnetic tracking system exhibits the following accuracy, speed, latency, and range performance characteristics:

- Position accuracy is 0.40-mm root mean square (RMS).

- Orientation accuracy is 0.25 degrees RMS.
- Speed is the maximum number of complete six-df updates per second and is a function of the number of sensors employed. The tracking system uses two sensors, and each sensor can output at a maximum rate of 33 Hz.

Latency is defined by the American National Standards Institute/Institute of electrical and electronic engineers (ANSI/IEEE) standard 100-1977 as the time elapsing between the application of a stimulus and the first indication of a response. To achieve real-time operation, tracking system latency must be minimal. The tracking system's data acquisition and computational time (latency) is 30 msec/s. The range of the tracking system is 50 to 450 mm + within a hemispherical field-of-regard (Figure 1.13).

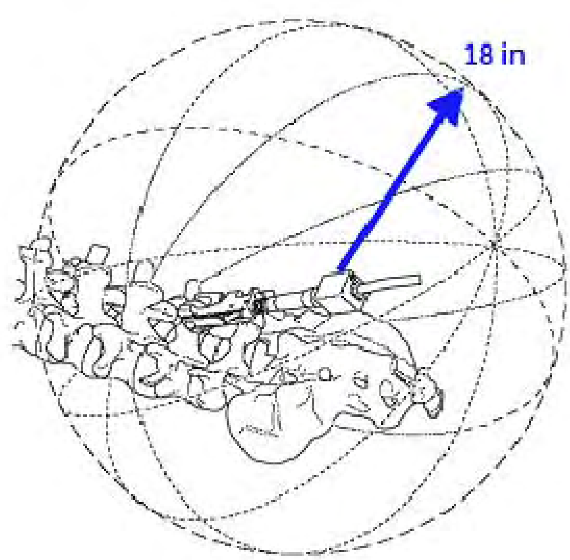

Figure 1.13 Illustration showing the maximum range from the transmitter attached to a spine of >50 cm (18 inches).

1.3.4 Safety

Medical instrumentation is subject to regulatory testing to verify compliance in the categories of emissions, immunity, and safety. The electromagnetic tracking system is no exception. We have tested it and it complies with the limits of EN60601-1 and EN60601-1-2 for electromagnetic radiation emissions and susceptibility, and the safety requirements of EN60601-1 (including UL2601-1 and CSA C22.2 NO 601.1-M90) and EN60601-1-1.

Radiation or field intensity produced by electromagnetic transmitters is an additional safety issue. The accompanying graph shows the calculated field intensity plotted over a 50-cm distance in both Teslas and Gauss. From a safety perspective, two points on this chart are significant. First, under typical operating conditions for the ENT application of the EM navigation (unit's) instrument, the tracking system's transmitter rests an average of 4 cm from the surface of the patient's skin, with slight variations occurring because of varying patient anatomy. Therefore, reading from the graph, a distance of 4 cm represents a field intensity of 0.12 Gauss. This value is approximately one third of the earth's magnetic field (0.30 Gauss). Second, the field intensity for the tracking system is more than a factor of three less than that specified in the Swedish MPR-2/SWEDAC and TCO-95 specifications. These specifications state that the magnetic field intensity for Band II (2 to 400 kHz) must be ≤25 nano-Tesla (nT) at a distance of 50 cm. The tracking system's calculated magnetic field intensity at 50 cm is 6.29 nT, which is only 25% of the allowable limit. Because the conversion factor between Tesla and Gauss is 10^4, the calculated magnetic field intensity at 50 cm is 6.29E-05 or 0.0629 milliGauss (Figure 1.14).

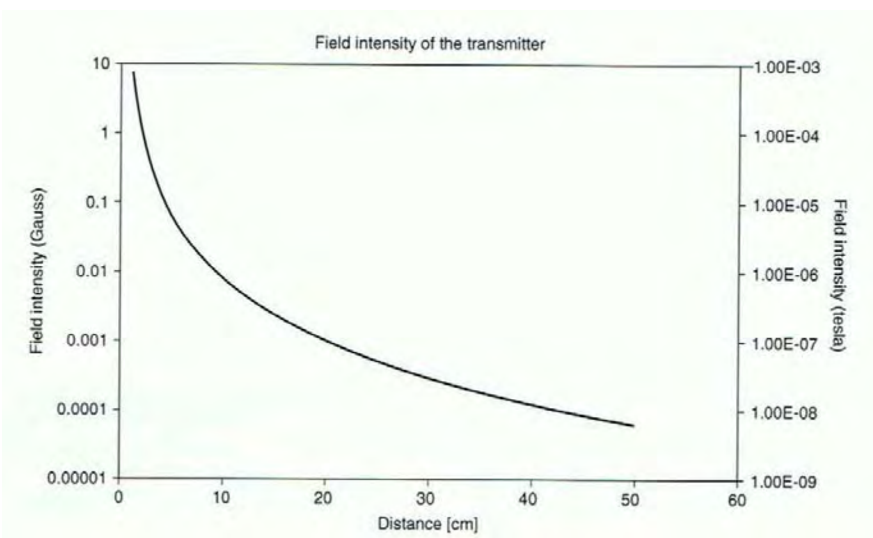

Figure 1.14 Calculated field intensity produced by electromagnetic transmitters.

Measured values of field intensity are in all cases below calculated values because measurement coupling is not ideal, thereby making the calculated values represent the worst-case condition. Because these values are well within the limits of the international specifications (MPR-2/SWEDAC and TOC 95), patient and surgeon safety is never compromised as a result of transmitter electromagnetic radiation.

1.4 Clinical Considerations

1.4.1 History

The electromagnetic tracking system has seen clinical usage since the introduction of the first commercial unit in 1996 for paranasal sinus surgery. We first used our surgical navigation platform containing the electromagnetic tracking system for functional endoscopic sinus surgery in 1996 and prior to any navigation technology or clinical group we know of. After roughly more than 200,000 navigation procedures to date, image guidance is fast approaching the worldwide standard of care for sinus diseases requiring endoscopic and functional endoscopic treatment. Our scientific and engineering development efforts resulted in other electromagnetic (EM) applications now used in the axial-skeletal spine, and cranial surgical fields. The latest navigation platform supports all of these applications using preoperative CT and MRI patient imaging data as well as intraoperative real-time C-arm fluoroscopy providing updated surgical navigation information.

The latest surgical tracking applications combine intraoperative C-arm fluoroscopic imaging with EM tracking technology. The fluoroscopic navigation application incorporates a calibration fixture containing calibration markers attached to a C-arm (ii) image intensifier (Figure 1.15), which corrects for the distorted cone-shaped x-ray beam created by C-arms and provides a means of tracking the position of the C-arm itself during image capture. Together, these functions provide a means of achieving accurate and instantaneous registration of the image to the anatomy (Figure 1.16).

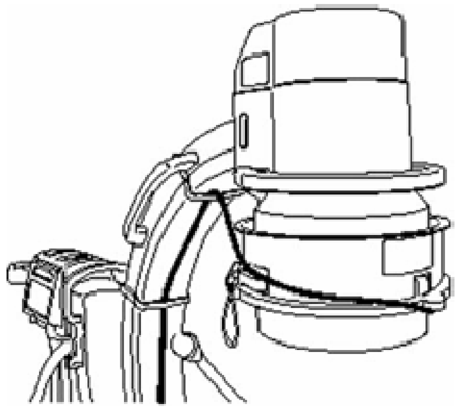

Figure 1.15 The calibration grid attached to the C-arm provides a mapping of the anatomy for the process of registration.

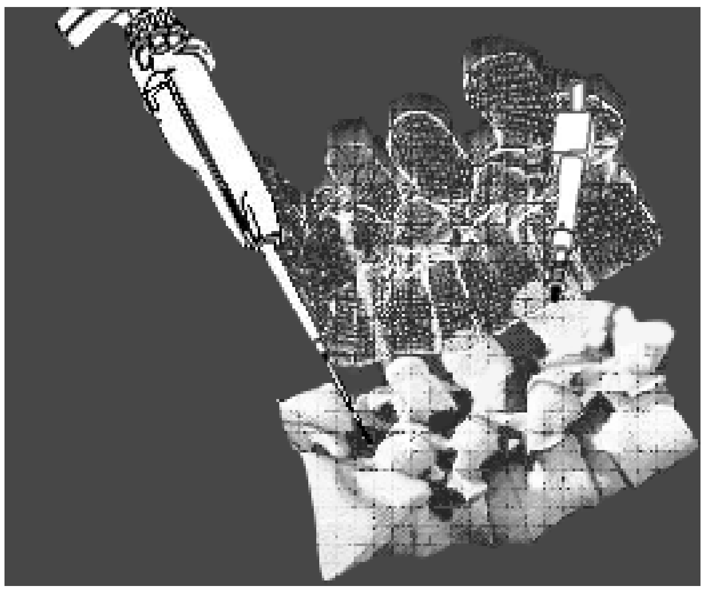

Figure 1.16 The process of registration super aligns the anatomical x-ray images to the patient's anatomy with submillimeter accuracy. Image also demonstrates a navigated spine handle (left) and an EM transmitter (right).

1.4.2 Field Distortion In Clinical Environments

Electromagnetic tracking field distortion occurs when a metal object is inserted into the transmitter's electromagnetic field (EMF). With induced current, the metal object or distorter will create its own magnetic field, which interferes with or distorts the transmitter's EMF. To maximize safety, the tracking system's receivers using mathematical algorithms detect field distortion due to metallic interference automatically. Our laboratory tests investigated conditions and detection devices to optimize the working environment for EM navigation. If a field induced distortion (FID) is detected, the surgeon is immediately notified, and system usage should be suspended until the source of the distortion is eliminated. We found that this is usually accomplished simply by relocating the distorting metal object or by changing the position of the tracking receiver.

When the offending metal object is removed from the operative field or 300-stainless steel, plastic, or titanium is used in the manufacture of retractors and surgical instruments, the issue is usually resolved. Positioning the patient on a radiolucent table with minimal ferrous framework is also helpful, but several tests have demonstrated that nearly all commercial operating tables are compatible with our navigation system or in worst case, the set-up can be slightly modified for maximum performance by applying an extra table pad to elevate the patient.

1.4.3 Sensor Instruments

We substantially improved the early limitations of EM-tracking technology with consistent software, manufacture and environmental verification and validations. Transmitters and receivers that are attached to the surgical anatomy and instruments are large and can interfere with one another in the confines of some surgical exposures, designs and workflows were modified to address this by organizing the cables within the operative field to a better ergonomic design and use. The improved physical characteristic of these sensors minimizes now the potential for dislodging or loosening of the transmitter from the anatomy, which may affect the accuracy of tracking. Recently working prototypes have been developed with smaller EM wireless transmitters and receivers with coils nearly 0.50 mm in diameter that we believe will eliminate the need of cables or wires connected to the surgical field in the future.

CHAPTER 2. AIMS AND HYPOTHESIS

Electromagnetic (EM) tracking systems have been successfully used for surgical navigation in ENT, cranial, and spine applications for several years. The EM system has also been used in surgical navigation applications. Our EM system has the benefit of not requiring a line of sight between devices; this makes it possible for it to expand into flexible instrument technology such as malleable needles, guidewires and catheters that can be navigated within the body.

In earlier investigations we split our experiments into two bench tests (located in the Appendix, page 126) to evaluate the technology for cadaver and human investigations. First, we evaluated various optical trackers in comparison to ours to assess individual static and dynamic performance characteristics. Second, we bench-tested the overall system accuracy in which the EM tracker performance was tested to ensure that the transmitter, receiver and tracker components are operating within our specifications. When we were satisfied, we proceeded with a series of different open and minimally invasive experimental investigations described in this Thesis.

In the first and second parts of our investigation, we built on our previously improved accuracy algorithm and combined it preclinically and then clinically in a feasibility experiment with a new 3D intraoperative fluoroscopic imaging method to enhance the real-time precision of endoscopic sinus surgery (ESS) and to compare differences in x-dose exposure between 3D fluoroscopy and CT. At two multi-center, high-volume tertiary care and academic hospitals, we applied and tested new software that allows the reconstruction of several 2D fluoroscopic images into a reconstructed CT-like volume intraoperatively for near real-time imaging and instrument navigation for the nasal cavity and paranasal sinuses. Our aim was to demonstrate that intraoperative updates of altering sinus anatomy during surgical dissection could be updated using a real-time 3D rotational fluoroscopic C-arm enhanced with improved software accuracy and that the image quality is sufficient to safely apply this method as an alternative opportunity to preoperative CT scans.

In the third part of our experimental investigations, we focused on the key component of enhancing a new surgical navigation technology using EM guidance for spinal applications by measuring and improving the performance of a new beta software algorithm we developed in comparison to our current system's available

software. We used two fully intact human cadaver torsos with a simulated OR set-up. Our aim was to use a fluoroscopically guided image platform with improved beta software called *Platinum* tracking to percutaneously place Kirshner wires (K-wires) into a navigated biopsy needle designed by (RVJ) and through pedicles in the regions of the thoracic and lumbar-sacral spine. We used the newer *Platinum* tracking software on one side of the spine and the current *Gold* tracking software on the contralateral segment of the same vertebrae to assess tracking accuracy and stability between these two different versions of tracking algorithms.

In our fourth preclinical investigation, we concentrated on spinal decompression and stabilization techniques in open thoracic pedicle screw fusion using EM–based fluoroscopic navigation. Our previous results show that the use of EMF image guidance for insertion of thoracic pedicle screws gives accuracy equal to that of conventional techniques while significantly decreasing the fluoroscopic time. Our aim was to compare the accuracy of EMF image-guided thoracic pedicle screw insertion to conventional techniques using anatomic landmarks and fluoroscopy and secondarily to measure insertion time and C-arm x-ray times.

In the fifth part of our experiments, we moved from open pedicle screw placements to a percutaneous approach to demonstrate the feasibility and safety of navigated bone biopsy needle designed by RVJ to place K-wires through the thoracic and lumbar-sacral pedicles in comparison to the standard free-hand fluoroscopy technique. Advances in technology have resulted in surgical techniques that can reduce surgical approach related trauma and morbidity as compared with standard open surgery. As a result of these technologic advances, minimally invasive and percutaneous procedures designed to treat various spinal conditions are rapidly growing in popularity. We integrated computer-assisted image-guided surgery with minimally invasive procedures to see whether we can provide an ideal environment for accurate and safe placement of a variety of future implants for both fusion and correction of deformities. Our aim was to demonstrate the safe and accurate placement of K-wires in a cadaver with a custom-navigated trocar to simulate the key initial operative steps of kyphoplasty in the treatment of vertebral compression fractures, transcutaneous insertion of a guidewire for percutaneous pedicel screw fusion and to measure the reduction of ionizing radiation to the operator.

In the sixth set of experiments, we continued with a minimally invasive approach built upon the previous cadaver study findings to assess the safe placement of specific transcutaneous spinal instrumentation and implants. Our aim was to build a prototype set of cannulated pedicle screw instruments and implants to evaluate the feasibility, accuracy, and time efficiency of an EM Navigation system compared with a conventional freehand and 2D fluoroscopic image-guided technique for percutaneous transpedicular instrument insertion. This experimental approach compared navigation to freehand implant placements side by side at the same vertebral segments with a standalone navigation platform and separate C-arm fluoroscope.

In our seventh experiment, we modified the previous percutaneous cadaver experiments by randomly assigned the levels rather than alternating the technique from side to side using a different set of instrumentation and measurement methods for ionizing radiation. A comparison by level in which one technique is performed bilaterally was thought to reduce the potential bias for a reduction in time and improved accuracy based on knowledge gained from placement of the first screw when placing the contralateral screw. Comparison by level is also more consistent with the manner in which some surgery is performed with sequential placement of screws bilaterally before moving to the next level. In addition, we tested different customized MIS instruments to demonstrate that these different brand instruments can be used with this type of EM navigation technology. We also measured ionizing radiation to the hands using special thermoluminescent dosimeter badges and rings. The growing trend of percutaneous spinal fusion techniques for decompression and stabilization in degenerative disc disease can be a challenging procedure with the loss of direct visualization of bony landmarks. This therefore creates a larger dependency on the application of fluoroscopic imaging that consequently increases the amount of ionizing radiation exposure to the patient and especially the cumulative exposure to x-rays to the surgeon and operating room staff. Our aim was to evaluate an integrated fluoroscopic and navigation platform, to measure the x-ray time and dose to the hands and thyroid between the navigation and freehand approaches of MIS implants. This study used a random level approach to the lumbar segments vs. the previous side-by-side approach at the same segmental levels and the only C-arm platform type of its class incorporated with navigation technology for a smaller footprint and better ergonomics.

The eighth investigation expanded the use of computer-assisted image guidance to a CT approach using 3D images to target the complex anatomy of the intervertebral disc space. A percutaneous approach to the intervertebral disc in the treatment of disease can be a challenging pathway to embark for the spinal surgeon in an effort to circumvent sensitive neurovascular tissues using a spinal trocar. Endoscopic and x-ray C-arm fluoroscopy provide visualization, but not in the transverse view. Our aim was to apply preoperative CT scans to provide axial images of the lumbar segments to demonstrate precise targeting when navigating Kambin's triangle with a tracked trocar and laser fiber and minimizing the need for repetitive C-arm fluoroscopy.

The ninth investigation included the use of a nonisocentric C-arm with software we created to generate a CT-like image of the spine with a series of 2D fluoroscopic images rotated around the vertebra to assess accuracy of percutaneous pedicle screw placement compared with placement by 2D fluoroscopic navigation and conventional non-navigated fluoroscopy. We used a human cadaver to place percutaneous pedicle screws first in the lumbar spine with the aim to test feasibility of prototype MIS instruments and to check the accuracy and x-ray times as compared with the conventional technique.

Our tenth final investigation transitioned to exploration of extremity-based fracture reduction in the field of orthopedics focusing on percutaneous approaches to femoral and intertrochanteric fractures in the pelvic region using EM surgical guidance. Approximately 300,000 hip fractures occur annually in the United States, the vast majority requiring operative stabilization. The technique for operative stabilization depends on the fracture pattern, but usually involves placement of one large compression hip screw (CHS) or three to four cannulated lag screws (CLS). Both procedures require frequent use of intraoperative fluoroscopy and image intensifier for placement of the guide wire, drilling and reaming, and insertion of the implant. Our aim was to evaluate the feasibility to use image-guidance and computer navigation to determine if it would significantly decrease the radiation exposure secondary to fluoroscopy use.

CHAPTER 3. SINUS SURGERY EXPERIMENT 1: PHANTOM INVESTIGATIONS

3.1 Introduction

Approximately six million people live with the pain of chronic sinusitis in the U.S., and about 32 million adults were diagnosed with some form of sinusitis in 2006 according to the Centers for Disease Control.[9,24,82] The region of the paranasal sinuses is one of the most complex regions in the body and therefore a difficult area to treat surgically. A thorough knowledge of all anatomical structures and their variations is key to performing proper sinus surgery and to avoiding adverse events. Complications with this type of surgery are usually due to lack of familiarity of the anatomical landmarks and the variations of anatomy in the paranasal sinuses during surgical dissection beyond the safe anatomical limits of the sinus. Surgical treatment can involve making incisions in the face, but a minimally invasive operation avoids this. In the past decades, there has been a major advance in the surgical treatment with a minimally invasive technique called endoscopic sinus surgery (ESS).

The era of modern endoscopy is believed to have begun in 1805 with the Italian-German physician Philip Bozzini, who developed a lighted tube known as a Lichtleiter to examine the urinary tract, rectum, and pharynx.[28] In 1853, Antoine Jean Desormeaux of France first coined the phrase “endoscope” for an instrument he made to examine the urinary tract and the bladder.[11,76,172] In the following century, use of this technology evolved from the optical fiber in the 1960s to the videoendoscope first used in gastric applications through the late 1970s. Endoscopic sinus surgery evolved from the early developments of Messerklinger and Stammberger in Graz, Austria and Wigand of Erlangen, Germany, which were reported at the Twelfth ORL World Congress in Budapest, Hungary, including those of Kennedy and colleagues in Philadelphia.[113,114,144,199,223]

ESS involves the use of an optical lighted tube called an endoscope to guide the rhinologists through the twisting sinus chambers. This 2D approach is limited by the need for the surgeon to mentally correlate a 3D anatomical CT image for guidance showing the location of vital anatomical structures beyond the view of the monocular endoscope and hand instruments, while trying to navigate by feel through the walnut-size paranasal cavities. The surgeon may be maneuvering instruments above the eye, near the olfactory bulb, the optic nerves, cavernous sinuses and the internal carotid arteries in close proximity to the sphenoid sinus where good visibility is a key safety factor. Through the introduction of image-guided sinus surgery over a decade ago, the surgeon has a 3D view from a preacquired patient CT scan to view the delicate anatomical areas. The intention of the navigation system is to provide greater exactness during surgery to better pinpoint the pathology and to treat it by restoring sinus function. Common procedures with navigation include surgical treatment of chronic sinusitis, nasal polyps, failed sinus surgery, chronic sinus headaches, congenital deformities and other sinus problems that require surgery or those at the skull base such as pituitary adenomas.

3.2 Computer-Assisted Sinus Navigation

CT is considered the gold standard for imaging the paranasal sinuses and is the only imaging modality to provide CT-reconstructed images for navigation using a specific CT scanning protocol for triplanar images and used for computer-aided endoscopic sinus surgery (CAES). The major limitation of CAES with the current technology is the inability of the surgeon to assess the surgically altered anatomy of the paranasal sinuses and skull base during surgery. This limitation exists because the surgeon is confined to performing CAES using a historic CT image that was acquired preoperatively. A second drawback of the use of CAES is the radiation dose experienced by the patient, which most experts believe is best to minimize (ALARP (as low as reasonably practicable) principle). CT scanning is an important and valuable technique in numerous situations to identify ailments in the head, chest, and abdomen. It is, however, sometimes regarded as overused in the United States, with approximately 62 million scans performed in 2006 up from 3 million in 1980. Medical exposure to radiation, mainly through CT scans, has replaced environmental radon as the dominant source of radiation exposure for the U.S. population.[4] Maintaining awareness of its potential overuse and effects may help to ensure caution is exercised in its application and may provide opportunities for alternate new solutions such as the use of intraoperative navigation systems.[29,150]

3.3 Aims

We investigated a new method for intraoperative 3D fluoroscopic imaging to enhance the precision of ESS. At our GE laboratories and two Cornell University multi-center high-volume tertiary care and academic hospitals in New York City, we applied new software that allowed the volumetric reconstruction of several 2D fluoroscopic images into a reconstructed CT-like volume intraoperatively for near real-time imaging and instrument navigation for the nasal cavity and paranasal sinuses. Our general focus was to demonstrate that intraoperative updates of altering sinus anatomy during surgical dissection could be updated using a real-time 3D rotational fluoroscopy method.

The application of preoperative CT scans used intraoperatively does not allow for intraoperative updates. Therefore we used our 9800 OEC C-arm to simulate real-time updates in ESS on phantoms in the laboratory. As my team and I had done several previous bench tests with human cadavers for simulated spine surgeries, we already had experience in the set-up and the feasibility of updating images with this method and acceptable image qualities in the spinal region. Now we wanted to measure the degrees of spin on a nonisocentric C-arm as well as the number of images and time necessary to reconstruct a CT-like image view of the paranasal sinuses. We also wanted to record the x-ray dose exposures from this system in comparison with those from a true CT scanner before using it in the human sinuses.

The radiation exposure using a C-arm fluoroscope in the head had not been measured previously in our experiments. Our larger aim was to measure and determine the radiation exposure using a C-arm fluoroscopic scan method to collect x-ray images for our electromagnetic navigation system and to compare these results with the x-ray radiation exposure during a CT scan for a stereotactic computer-assisted navigation procedure.

3.4 Materials And Methods

In our Boston laboratory, we conducted the following experimental tests to compare the x-ray dosage difference between a CT scan and a 3D rotational scan with a standard nonisocentric OEC/GE C-arm using a head phantom. A clean radiation badge was placed on the head phantom (Saw Bones, Inc., Seattle, WA), and five C-arm rotational scans were acquired with our OEC 9-inch fluoroscope (Figure 3.1). The TLD badge (Landauer, Inc., Glenwood, IL) was sent for reading. The total radiation was divided by 5 to get an average reading per C-arm rotational scan. A second clean radiation badge was placed on the head phantom and a CT scan was acquired with the protocol that is used for image-guided surgery.

The second sets of experiments were performed with the team in New York at the Cornell Presbyterian hospital where a radiation-measuring instrument was utilized to help determine the levels of ionizing radiation absorptions. The tools used included a Radiation Monitor (Radcal Corp., Monrovia, CA, Model 9010), a Signal Converter (Radcal Corp., Model 9060), a compact 6 cc ionization chamber (Radcal Corp., Model 10X5-6), which was check for proper calibration, and a 3.2 cc CT ion chamber (Radcal Corp., Model 10X5-10.3). These were used together with a headrest and clamp system (IntegraNeurosciences, Cincinnati, OH). The center reference line of the head phantom was aligned with that of the C-arm's arc rotation from left to the contralateral end point. This is important to maintain the center of the head phantom in the quasi-isocentric plane of the fluoroscopic beam. Since this fluoroscope is a nonisocentric model, it required that it be set up in a special mode. The C-arm was positioned at the head of the table and parallel to the floor. From our previous experiments in our Boston laboratory, we learned that the best way to mimic isocentricity with the goal of maintaining the x-ray beam on the centered target is to rotate the arc to a lateral view and parallel to the floor. From this position it could be driven into the target field (in this case, from the head of the table). In a clinical situation, this would require the anesthesia station to be moved to the side or to the foot of the table with extended air hoses.

From our original experiments; we also learned that the rotation of the C-arm could be bulky. In our first applications in Boston, we used an earlier C-arm model 9600 unit that was motorized. Here, a 9800 nonmotorized model was applied. Manual rotation of the C-arm from lateral to contralateral position is done under low-pulse continuous imaging mode. This was accomplished in two fashions: the first included the foot pedal and the second the manual button on the mainframe while a technician wearing a lead collar, apron, and glasses spun the C-arm. From these orbital actions, we started at a 0-degree marker and ended between 180 and 195 degrees. We learned that with these particular C-arm models, when approaching the 90-degree point of the rotation, a disturbance I termed a "sweep bump" would occur just before and after the 90-degree point. This action required that the user slow the C-arm rotation just before the midpoint and again as the midpoint was being exited. This slowing down to finesse through the sweep bump cost time in the overall spin cycle. We gauged the time to be between 30 and 35 seconds to complete a 190-degree spin. This sweep bump also caused concern initially for the image quality. We captured an image roughly every degree of a turn. The vibration from the bump caused the fluoroscopic reconstruction software to smear some images and diminished the image quality. Our solution was to create and place a metal and plastic buffer ring between the C-arm arc and the moment arm of the superstructure. This prevented the loose joint in the design of the C-arms from flexing into a sweep bump. We noticed in the second experiments in New York that the image quality and spin time improved. The centering of the head phantom in the radiation field with both lateral and anteroposterior (AP) fluoroscopic scout images was also essential. All fluoroscopic imaging used the C-arm's largest field of view, 9-inches (23 cm), with no additional manual collimation.

The head phantom for these radiation dose measurements (Nuclear Associates, Carle Place, NY, Model 76-414) is a standardized cylinder of polymethyl methacrylate (PMMA) with several tubular holes wide enough to accept a CT ion chamber. The central hole lies along the central line of the cylinder, and the four surface holes are centered 1cm from the surface of the cylinder and on opposite sides. It contains two electrodes, which enclose an air space, and the interaction of ionizing radiation with the air molecules causes the ejection of negatively charged electrons, leaving behind positively charged ions. During the radiation measurements, all holes other than the one containing the CT ion chamber were filled with acrylic plastic rods to ensure a consistent density of the cylinder. When a change of several hundred volts connected to the chamber's electrodes caused the electrons and ions to flow towards the positive and negative electrodes, it created a small electric current. This current is a measurement of the intensity of the radiation.

Figure 3.1 GE fluoroscopic C-arm with the head phantom in place.

Three fluoroscopic modes were used to measure the cumulative x-ray exposures: continuous fluoroscopy, continuous high-level fluoroscopy, and digital ciné at 15 pulses per second (pps). Data were recorded for a minimum of two scans in each mode, and all measurements were recorded with the CT ion chamber in the central and surface hole of the head phantom. The orbital spine of the C-arm started at just above the horizontal cross table line of the phantom and moved through a 190-degree spin in less time then previous experiments. The time was recorded at 21 seconds. For the recording in the surface hole of the head phantom, the CT ion chamber was placed in the most inferior hole because of the irradiation geometry, which makes this region the area of maximum surface exposure. After each scan, the user can enter the recoded data in the workstation to play back the digital fluoro-video. In this window, the user can scroll through the spin, frame by frame, to check for artifacts and areas of motion or sweep bumps. The software detects the poor images and ejects them in an effort to salvage image quality. It also counts the number of images captured and deleted.

To compare the exposure measurements with the radiation exposure from a CT scan, the data were converted from Roentgen to units of absorbed dose in milliGray (mGy) by multiplying by the conversion factor of 8.73.[138]

The acquired CT scans used for the electromagnetic navigation system were acquired on a GE Lightspeed® Plus CT scanner using a specific protocol. The typical scanning protocol for the Lightspeed requires a zero gantry angle, with a reconstruction matrix of 512 at an axial plane with a helical scan mode. The slice thickness is 1–1.25 mm, and the table interval mm/sec is 1.25 mm with a 0.9375 pitch. The field of view (FOV) is 25 cm. This test employed 120 kVp and 240 mA to produce approximately 60 adjacent 2.5-mm cuts in 40 seconds. The CT diagnostic imaging volume, which is a federally mandated measure of CT dose, is displayed directly on the control panel of the GE Lightspeed® Plus CT scanner and is measured in mGy.

3.5 Results

The preliminary experiments in our Boston laboratory demonstrated that, for each of the badges, the three reported radiation readings deep dose equivalent whole body, low dose equivalent, eye, and standard dose equivalent (DDE, LDE, SDE) were averaged into a single reading that is listed in the table below.

Image Mode	Average Dose x 5 (MREM)	Average Dose (MREM)
3D C-arm x 5	849	170
CT	N/A	7118

The ratio of the right-most columns in the above table is approximately 42, which indicates the factor of radiation difference between our 3D C-arm rotation and software method and CT. These results indicate that a CT scan of a phantom results in roughly 42 times higher radiation (as measured by a badge on the phantom) than with a conventional mobile C-arm rotational CT-like scan.

The New York Cornell raw and converted measurements of the maximum surface and central radiation exposure in the head phantom showed improvements over our preliminary sweep times and measured at 21 secs for an equivalent 190-degree nonisocentric C-arm sweep using identical fluoroscopic models. The scans are summarized in Table 3.1. The mean (±) standard deviation exposures ranged from a maximum central exposure of 0.895 ± 0.001 mGy in the continuous fluro mode to a maximum surface exposure of 10.7 ± 0.6 in the Digital Ciné mode.

Table 3.1 Surface and central radiation exposure measured using a standardized head phantom during a C-arm spin

Fluoroscopic Mode	**Surface Exposure in mR (mean ± std dev) (n=2)**	**Max Surface Exposure in mGy (mean ± std dev) (n=2)**	**Central Exposure in mR (mean ± std dev) (n=2)**	**Max Central Exposure in mGy (mean ± std dev) (n=2)**
Continuous Fluoro	217 ± 5	1.89 ± 0.04	102.5 ± 0.1	0.895 ± 0.001
High-Level Fluoro	427 ± 8	3.37 ± 0.07	176 ± 2	1.54 ± 0.02
Digital Ciné, 15pps	1229 ± 68	10.7 ± 0.6	473 ± 30	4.13 ± 0.26

Courtesy VJ. Anand - Otolaryngology - HNS, 2006 135: 409-412.[140]

The $CTDI_{vol}$ displayed on the GE Lightspeed® Plus CT scanner for the electromagnetic navigation CT protocol was 85.4 mGy at both the central and surface locations. The dose cylinder data show that the measured radiation of the maximum surface dose was more than twice that at the center of the head phantom during scanning in each of the three fluoroscopic modes. For a CT scan using the navigation system protocol, the central and surface radiation dose was recorded as 85.4 mGy. The maximum radiation dose measured in the head phantom using the Nav CT software protocol was a surface radiation dose during the Digital Ciné 15 pps. It was measured as 10.8 mGy. The Nav CT-software scan subjects the patient to substantially less radiation than the equivalent helical CT scan. In order to provide some scale of threshold examples for potential dose risks leading to injury against the recordings of the experimental readings, the threshold for production of skin injury (transient erythema) is approximately 2 Gy (2000mGy), whereas permanent epilation occurs at greater than 7 Gy (7000 mGy), and dermal necrosis and secondary ulceration occur at 18–20 Gy (18–20,000 mGy).[213] To reach the level of approximately 2 Gy (2000 mGy) the radiation exposure would require more than 1 hour of continuous fluoro in the Digital Ciné 15 pps mode.[2,13,194]

3.6 Discussion

New instruments and techniques in endoscopic sinus surgery provided great benefits for surgery of the small paranasal sinuses for diagnosis of sinonasal pathology through less invasive interventions with greater precision and improved functional outcomes. The treatment and visualization techniques continue to improve through even better understanding of the anatomy, better endoscopes and instruments, and now expanded options for visualization beyond 2D endoscopic soft tissue views using intraoperative 3D C-arm fluoroscopy. Conrad Roentgen's groundbreaking discovery of x-rays in November 1895, which was first mentioned in the Science magazine through a letter by Hugo Munsterberg in 1896 paved the way for x-ray fluorscopy,[145] . Shortly after, Thomas Edison an electrical engineer commercialized one of the first fluoroscopes, founded General Electric and introduced the incandescent light bulb in 1879, which later lead the way for lighted endoscopy.[79,145,151,175]

In our corporate laboratories in early 2000, we designed software that allows for the reconstruction of conventional C-arm images into axial views. This software was incorporated into our electromagnetic (EM) surgical navigation system and tested repeatedly for image quality originally with our motorized GE OEC 9600 C-arm. We tested phantom models, then stripped calf spines, and eventually intact human cadaveric specimens. Shortly after, in 2001, we converted to a newer-generation C-arm, experimenting with the OEC 9800, which was a nonmotorized version but provided a better generator and improved images. After multiple experiments for spinal and orthopedic extremity applications, we looked at the uses for sinus and craniofacial procedures. In sinus surgery, traditionally otorhinolaryngologists used coronal and, from time to time, axial CT scans obtained preoperatively viewed on an x-ray light box in the OR as a frame of reference. Our group originally at Visualization Technology Inc. in Boston, first introduced the navigational technology and methods in the development of electromagnetic stereotactic functional endoscopic sinus surgery with the aid of several rhinologists. This technology allowed rapid and accurate intraoperative localization during endoscopic sinus surgery using a preoperative protocol for specially formatted CT scans. The drawback here is that the use of historic CT scans does not allow for intraoperative updates to the surgical dissection and altering anatomy. In our experiments, we set out to prove that in bench tests, the use of a C-arm with special software could be safely applied and required less radiation in comparison to a CT. Today, novel volumetric systems designed to allow for a 360° rotation of a flat-panel detector and x-ray tube around the patient during a surgical procedure exist. These systems are mechanically designed to be isocentric C-arms with standard ii tubes or newer digital flat panel detectors transported in a “C” configuration into the operating suite.

The results of this investigation reveal that use of a conventional OEC 9800 C-arm mobile fluoroscope, integrated with our navigation software for acquiring 2D fluoroscopic x-ray images at approximately one-slice per degree over a minimum of 145 degrees to an approximate maximum rotation of 195-degrees, is feasible for reconstructing CT-like images with an electromagnetic navigation platform in CAES. This method exposes the patient to less radiation than the alternative preoperative CT scans for the conventional navigation methods performed to date.

CHAPTER 4. PARANASAL SINUS SURGERY EXPERIMENT 2: CLINICAL INVESTIGATION OF 3D SINUS FLUOROSCOPY

4.1 Introduction

Recent studies have suggested that CAES decreases the incidence of major complications in sinus surgery and allows for a more complete dissection.[66] Clinical cases include procedures such as anterior skull base, orbits, pituitary fossa, and selected sinonasal neoplasms.[48] Even with the recent advances, the endoscopic sinus procedure continues to depend on CT data sets acquired before surgery and can not be updated intraoperatively during a procedure. As a surgery is performed, various ethmoid cells are opened, disease is removed, and anatomical landmarks are frequently displaced from their preoperative locations, actively making a navigation system more vulnerable to the risk of inaccuracy. Intraoperative MR imaging is one option to overcome this shortcoming and has been described previously for use in sinus surgery but requires a high cost, specialized instruments to be compatible in strong magnetic field, and a dedicated staff.[64,90]

Fluoroscopy is used extensively in operating rooms, specifically for neurosurgical, orthopedic, and vascular procedures. Recently, the use of surgical navigation for computer image-guidance with C-arm fluoroscopy has become increasingly popular in both neurosurgery and orthopedic surgery, but the vast majority of x-ray images with these machines are 2-dimensional.[41,60,96,99] The latest innovation we worked on was to use the C-arm to obtain a series of images that can be reconstructed into CT-like images and then used for 3-dimensional navigation.[87,89,170] After our tests on phantom models and tests by others in cadaver models,[163] we undertook a clinical investigation of patients undergoing sinus surgery with the use of fluoroscopy for intraoperative C-arm imaging coupled with electromagnetic navigation.

4.2 Aims

Our aim was to demonstrate feasibility of near real-time image-guided sinus surgery using intraoperative fluoroscopic CT from a series of C-arm scans in a clinical setting. This clinical investigation was designed to determine whether it was possible to update images intraoperatively by using our software algorithm addition for CT reconstruction relying on regular C-arm fluoroscopy for our computer-assisted surgical navigation system in sinus surgery. The two aims in the investigation were 1) to produce CT-like images that would be adequate for the evaluation of sinus disease and surrounding anatomy and 2) to assess whether these images could be used for accurate navigation in computer-assisted surgical navigation in sinus surgery.

4.3 Materials And Methods

We initially conducted a gauge-test to follow up on our first preclinical experiments that used phantoms. In this gauge test we compared the x-ray dosage difference between a CT scan and the fluoroscopic CT software scan using a phantom.

A clean radiation dosimeter badge was placed on a phantom, and five fluoroscopic-CT scans were acquired. The total radiation was divided by 5 to get an average reading per Fluoroscopic CT scan. A second clean radiation badge was placed on the phantom, and a CT scan was acquired with the protocol that is used for image-guided surgery.

The radiation doses for the FluoroCT and CT were 170 and 7118 MREM, respectively; indicating the factor of radiation difference between Fluoroscopic CT and conventional CT is approximately 42. We concluded here that these results indicate that a CT scan of a phantom results in a factor of 42-higher radiation (as measured by a TLD dosimeter badge on the phantom) than a Fluoroscopic CT scan.

4.3.1 Clinical Investigation

Our clinical protocol was approved by the hospital's institutional review board. We also performed a trial run in a cadaver lab to assess a surgical environment to maximize performance of the clinical run. Fourteen consecutive patients undergoing image-guided surgery were recruited to participate in our investigational study. All the patients had a preoperative CT scan completed with our surgical navigation system image-guided protocol. These were loaded onto our electromagnetic navigation system preoperatively. The operating room set-up required the anesthesia station to be relocated to the side of the table in order for the C-arm to be placed at the head of the patient to allow 180-degree rotation from side to side (Figure 4.1).

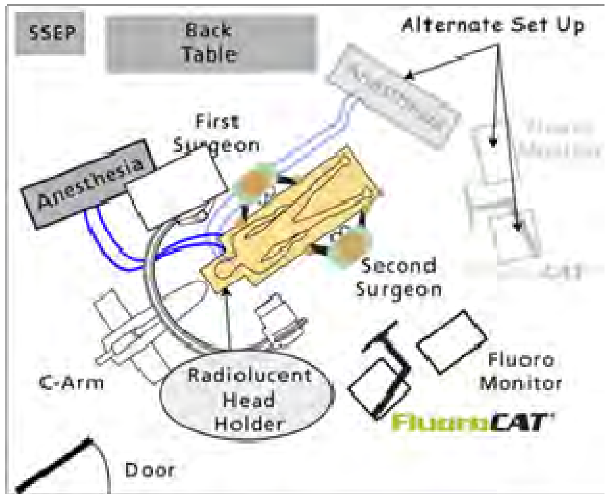

Figure 4.1 Illustration demonstrating the operating room set-up with C-arm at head of patient, anesthesia at the side of the patient, and the navigation unit with the endoscopic tower opposite the first surgeon.

All patients were positioned on an operating table that had been modified with a Plexiglas board to permit their head to extend past the end of the table or on a special diveboard-style cantilever table (Figure 4.2). This allowed for clearance of the C-arm to orbit around the patients head without interference from metal artifacts within the table such as metal rails.

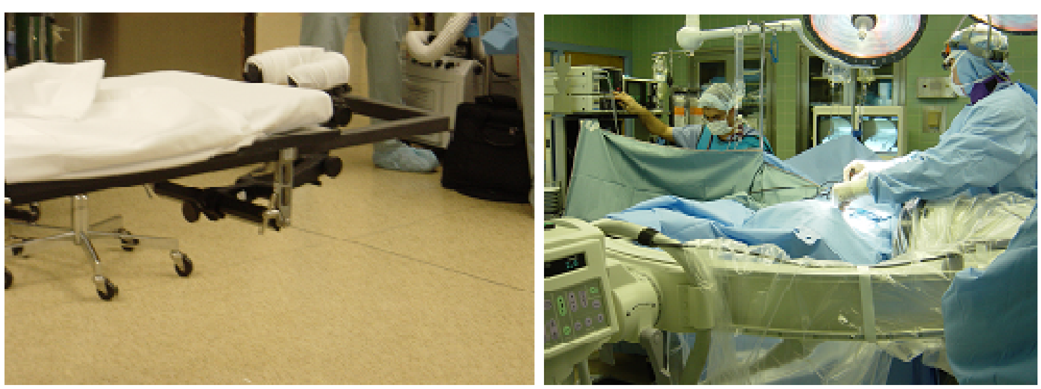

Figure 4.2 Special cantilever carbon fiber table designed by RVJ and C-arm set up for rotational spin around the head.

General anesthesia was used in all cases. The patient's headsets were modified (the headset provides for a rigid reference frame to capture and register x-ray images to the anatomy) preoperatively by gluing a special fluoroscopic reference transmitter to the back of the headset. Experienced ENT surgeons and staff facilitated the procedures. The nasal cavity was then decongested with cocaine. Each patient then had a series of preoperative fluoroscopic images obtained with a C-arm fluoroscope with a field of view of approximately 23 cm. This consisted of spinning the C-arm 190 degrees while the machine automatically took 190 images. The data acquired were then loaded onto our navigation platform using the fluoro-CT software program and reconstructed into CT-like images. The navigation instruments such as angled suction-aspirators, curettes, and shaver devices were then calibrated to measure their tip offsets in space. Using standard nasal anatomy including the bony/cartilaginous junction of the external nasal spine, the middle turbinate, and the anterior wall of the sphenoid sinus when visualized tested the accuracy of the system.[65] This was an estimated accuracy by comparing the instrument tip position on the navigation system with its actual location in the operative field. This method has been used in other studies looking at accuracy of image guidance in sinus surgery.[65,153] Standard CT images were then loaded to carry out the patients' surgery.

At the completion of the procedure, the nose was repacked with cocaine-soaked pledgets. The C-arm was then repositioned, and a second set of images was obtained after removal of the pledgets and extensive nasal suctioning. These were used in comparison to the preoperative CT and fluoroscopic images.

4.4 Results

4.4.1 Initial Patients

The fluoroscopic images were obtained from all patients by using the previously described methods. Variables became apparent during the patient studies that were not evident in our laboratory investigations. Initial images were deemed poor secondary to inadequate penetration and image scatter that we later improved. Several factors were noted to have an impact on the image qualities, including the presence of nasal packing, excess blood and/or nasal packing in the sinuses during image acquisition impairing image interpretations due to fluid, and extensive nasal polyposis that causes distortion of the images and making them inadequate for evaluation.

Other factors that affected the ability of the system to obtain good images included the weight of the patient on the modified operating table, the ability to rotate the C-arm in order to clear the patient and the operating table, the need to work around the drapes to change transmitters, and the interference of the CT transmitter affecting scanning and navigation. Based on these findings, we identified minor adjustments to significantly improve the quality of the scans. These adjustments included removing the CT reference transmitter before scanning the patient; placing the fluoroscopic reference transmitter closer to the C-arm to maintain full-range transmission throughout the C-arm rotation for image acquisition; using a brace to stabilize the C-arm, thus avoiding bumps during rotation; rigidly fixing the fluoroscopic reference transmitter to the headset with glue; and extensively decongesting and suctioning the nose before scanning to avoid artifacts. I designed and built a laser aimer for the navigation calibration grid attached to provide precise targeting for aligning the anatomical field of view.

4.4.2 Final Six Patients

The final six patients had images that were deemed adequate for evaluation of disease and delineation of anatomy and had similar navigation accuracy to the CT images (accuracy to less than 2 mm) (Figure 4.3). The bony anatomy was clearly shown on the preoperative images and extent of disease easily detected. These images were still determined to be inferior to standard CT images, particularly in the axial plane. Postoperatively, on all but one of the last six patients, blood was seen as an air-fluid level in the images. This was particularly true in the maxillary sinus. The patient with the best postoperative images was a patient with a large mucoceles, that when opened showed aeration of the frontal sinus not seen preoperatively. Our investigation led us to hypothesize that extensive predominance of soft tissue and fluid densities may alter the rendering of air-bone interfaces on the images. We also considered the possibility that inappropriate acquisition settings may have led to some distortions or limitations of our reconstruction software. This hypothesis would also explain why our best-image resolution was achieved in a largely pneumatized anatomy with little bleeding and no polyposis after opening a large mucocele. Furthermore, it may also be an explanation for the rapid and rather easy dissemination of fluoroscopic reconstruction in such fields as orthopedics and spine surgery that will be investigated in this Thesis, in which the vast majority of anatomic structures involved are bony and therefore potential artifacts caused by blood and soft tissue are minimal in these regions.

Figure 4.3 Fluoro CT reconstructions of the sinuses in three views with a virtual trajectory that replicates the aspirator seen in the endoscopic view.

4.5 Discussion

Intraoperative application of 3D C-arm fluoroscopy may be useful in the future for cases where complete resection is necessary. This could be helpful in particular situations for removal of both benign and malignant nasal tumors that are more so being done endoscopically. There could be a role for this type of technology in the bony tumors such as ossifying fibromas, osteomas, and clival chordomas. With improvement in the soft tissue definition, we believe that this 3D software used with C-arm fluoroscopy would also help in resections of inverting papillomas, angiofibromas, and some malignant nasal tumors. The potential exists also for 3D fluoroscopy to be helpful in endoscopic skull-base surgery and specifically in pituitary surgeries in which subtotal resection is sometimes performed secondary to inadequate visualization of the tumor. As the practice of endoscopic skull base surgery continues to advance, the use of 3D fluoroscopy could possibly play a role in assisting in complete removal of other tumors such as esthesioneuroblastomas, meningiomas, and craniopharyngiomas. With any of these procedures, it may be estimated that between one and four fluoroscopic scans may be used depending on the location of the lesion and the amount of residual disease.

A recent study[163] using cadavers determined with a similar fluoroscopic CT navigation device that it was able to produce high-quality images using an enhanced graphic resolution of bony and soft tissue structures, but the cadavers used were free of sinus disease and not subject to bleeding. Furthermore, this study did not include any evaluation of accuracy. Because our previous experiments determined that each scan produces only approximately 12% of the radiation of a standard image-guided sinus CT (consistent with a study that of a device similar to ours that calculated a radiation dose of 1 mGy per scan or about 10% of the radiation of a diagnostic CT scan).[163] If the use of fluoroscopy can improve outcomes or decrease the incidence of postoperative CT scans and revision surgery, then the additional amount of radiation, time required, and economics can be legitimized.

4.5.1 Conclusion

We concluded that fluoroscopic near real-time CT-like computer-assisted sinus navigation is feasible. We note that improvements need to be made to increase image quality, and adjustments are necessary to make the system use more intuitive to manage better the workflow. Additional modifications need to be completed to allow integration with a C-arm fluoroscopic, and software additions need to be developed to enable the use of the standard image navigation tools and electromagnetic transmitters. Prospective case-controlled studies must be designed to determine the benefits and indications of intraoperatively updating images that are suitable for ear, nose and throat and skull base navigation procedures.

CHAPTER 5. NAVIGATION FOR SPINE SURGERY: SPINE CADAVER EXPERIMENTS FOR TWO NAVIGATION TRACKING ALGORITHMS

5.1 General Introduction

The goal of spinal fusion surgery is to achieve strong and stable fixation, a feature critical in achieving bony arthrodesis. Pedicle screw fixation is the most effective and widely used form of internal fixation having been generally demonstrated to be biomechanically advantageous and with better fusion rates than other posterior column stabilization constructs, [30,69,121,186,231,234] where in the anterior column a larger surface area can provide a higher fusion rate with ventral expandable cages and ventral plate synthesis.

Spinal instrumentation (probes, taps, pedicle feelers, and implant drivers) often involves the application of screws or other devices into anatomic regions not exposed to the surgeon. The use requires great attention and care to avoid neurovascular injury. To minimize risk and to avoid vital neurovascular structures (Figure 5.1), surgeons frequently use intraoperative fluoroscopy in addition to their knowledge of 3D anatomy . Fluoroscopic imaging is considered the standard of care for many clinical procedures since 1977.[192] C-arm technology brings new capabilities to the operating room that are enabling surgeons to perform their jobs with more accuracy and precision than ever before. Physicians and other health care providers have used fluoroscopy systems for various diagnostic, surgical, and interventional[141,147] procedures for visualization during clinical applications. These devices perform three key functions: 1) they visualize the anatomy beyond a surgical exposure; 2) they guide instruments relative to anatomy; and 3) they update anatomical features and instrument positions during and after an intervention. With the growing popularity of minimally invasive surgeries, C-arms (also known as radiographic/fluoroscopic units) are becoming less of a luxury in the O.R. and more of a necessity.

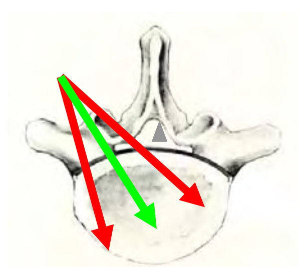

Figure 5.1 Drawing depicting approaches through the pedicle that result in medial inferior/lateral breaches (red arrows). Green arrow illustrates ideal trajectory.

5.1.1 Pitfalls Of X-Ray Use

The use of intraoperative fluoroscopy for placement of pedicle screws or other modes of internal fixation has some drawbacks that have resulted in prolonged fluoroscopic time and radiation exposure to the surgical personnel and patient. Many authors, including Rampersaud et al., [165] have shown that positioning, distance from the tube, and mode of fluroscopy used can significantly affect radiation exposure to various parts of the body, such as the hands (most at risk)[165,184] and other body regions for both the patient and the surgeon, especially if he or she is standing on the same side as the source of the beam.[108,143] Slomczykowski et al. found that the total patient dose was greater with a preoperative CT scan than with intraoperative biplanar fluoroscopy.[196]

To minimize radiation exposure and improve the surgeon’s orientation to unexposed anatomy,[100] we applied image guidance based on existing technology and principles used in stereotactic neurosurgery[176] and added our new technology of electromagnetic tracking instead of the conventional optical electric camera-based technology. The two main issues relevant to current surgical navigation systems we investigated were data acquisition (CT vs. fluoroscopy) and tracking of surgical instruments. We focused first on the 2D approaches to spinal navigation and then expanded to 3-dimensional approaches (Figure 5.2).

Figure 5.2 (Left) Navigation screen demonstrating correlation between implants and screwdriver to the virtual instrument line. (Right) CT-like view of a pedicle screw placement.

5.1.2 Malpositioned Pedicle Screws

In spine surgery, the published incidence of misplaced pedicle screws using conventional techniques ranges from 3 to 55%.[39,54,55,74,124,133,152,187,201,203,210,217] Surgical navigation systems must provide accurate and rapid feedback to the surgeon in real-time to allow minute adjustments to be made as the spine is being instrumented. Rampersaud et al.[166] defined the accuracy requirements of an image-guided navigation system based on available data concerning pedicle morphometry. Maximum permissible tolerance ranged from 0 mm and 0 degrees at T5, to 3.8 mm and 12.7 degrees at L5. Kalfas states that lumbar pedicle fixation will tolerate a 2-mm error.[100] In addition, the system should not interfere with the surgeon or surgical field in such a way that the instrumentation becomes either too cumbersome or limits movement and access to the pertinent anatomy.

5.2 Aims

In response to these concerns and requirements and in an attempt to merge real-time tracking with up-to-date spinal anatomy imaging, we applied and investigated an electromagnetic field (EMF)-image-guided navigation system that utilizes an EMF to track surgical instruments coupled with intraoperative fluoroscopy to obtain the virtual anatomic images. We investigated system accuracy and report the findings.

In this experiment, we undertook cadaveric comparison testing between two software algorithms for spinal tracking that we developed with our software engineers. We used the resources of a cadaver laboratory affiliated with the St. Louis Medical University, where we set out to evaluate our new prototype version of tracking software we called *Platinum Accuracy*. The prototype was tested for accuracy against the current version of software used on our EM navigation platform. This current tracking algorithm is called *Gold Accuracy.* In a statistically balanced experiment using human cadavera and a simulated surgical environment, we aimed to measure the differences in accuracy and stability between the two tracking algorithms we developed (*Gold* vs. *Platinum*).

5.3 Materials And Methods

Two fresh-frozen human cadavers were used for the test and were noted to have good bone quality and no deformity. The specimens were thawed approximately 24 hours prior to use at slightly above room temperature.

Each specimen was placed on a radiolucent surgical table in a prone position with all but the thoracolumbar regions of the exposed back draped. A 9-inch (23cm) surgical C-arm image-intensifier (ii) (OEC 9900) was positioned at the tableside to capture x-ray images for the electromagnetic (EM) surgical navigation standalone platform (running both software versions, *Gold* vs. *Platinum*). The EM navigation unit has a 20-inch (51-cm) touchscreen monitor for the x-ray images and juxtaposed navigation features (i.e., virtual instrument trajectories) (Figure 5.3).

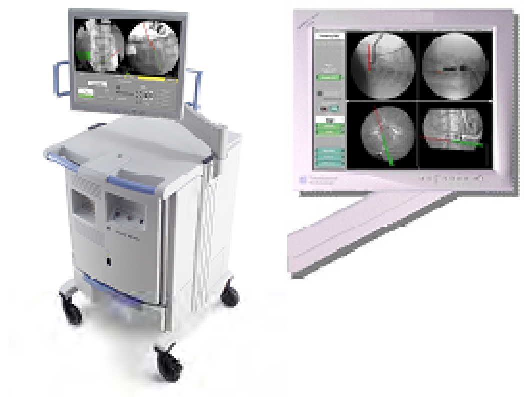

Figure 5.3 Electromagnetic stand-alone Surgical Navigation System with 51-cm LCD touch-screen monitor.

5.3.1 Set-Up

The C-arm workstation was plugged into the navigation platform via a 9-foot (3-meter) coaxial video cable from the video-out plug in the back of the x-ray workstation and into the video-input plug of the navigation unit. The satisfactory x-ray images of the spine were saved into the navigation unit via a frame grabber (Figure 5.4, right). An electromagnetic reference dynamic frame (RDF) was attached to the spinous processes of the thoracic and lumbar levels (Figure 5.4, left) . This was accomplished by a small 1-cm stab incision followed by blunt finger dissection to the appropriate thoracic and lumbar spinous processes to attach the reference transmitter. A 2-mm Casper-like bone pin was driven securely into the plateau of the spinous processes (we measured them to be between 5 and 8mm in diameter) and checked each for a rigid purchase placement (Figure 5.4, center). If the pins are loose, the navigation tracking can be off by several centimeters, therefore it is essential they are anchored solidly into the bone and checked intermittently for solid bone purchase. The EM transmitter was then applied to this, and the process of image acquisition and registration was done. The basic spine kit was then prepared with instruments calibrated for use (Figure 5.5).

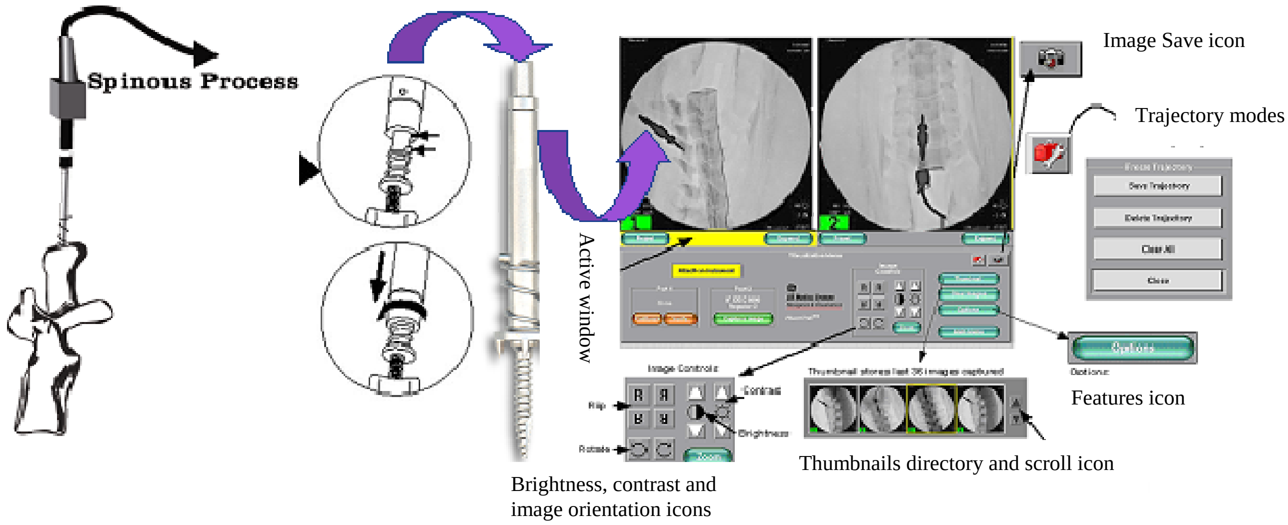

Figure 5.4 Transmitter attached via a Casper bone pin to spinous process and the Nav screen image features displayed.

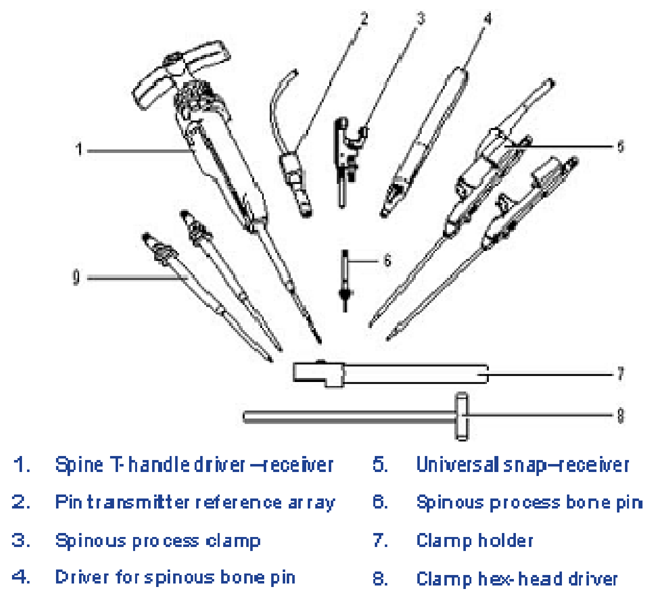

Figure 5.5 Illustration of the basic spine kit.

5.3.2 Experimental Protocol

We next performed the step of instrument calibration and verification with an orthopaedic surgeon's assistance by navigating a bone biopsy needle designed by RVJ also known as the Nav trocar, transcutaneously through each pedicle between the thoracic and lumbar spine levels. The *Gold* and *Platinum* software modes were alternated such that each vertebra was operated in both modes: one mode/side. The surgeon was unaware of the mode he's operating in. The spine was divided into three segments, each with 3 vertebrae (the EM transmitter is affixed on the spinous process of the middle vertebra) (Figure 5.6). In each segment, the mode was switched once (Gold ↔ Platinum), and the NAV access Needle was recalibrated after each mode switch. AP and lateral images were used for navigation. For each pedicle, accuracy verification was measured at the entry point (AP, lateral) and at the vertebral body exit point (lateral) yielding 3 accuracy numbers (Figure 5.7A). Control shots were taken to further assess placement accuracy between the two modes (Figure 5.7B, 5.8). In addition, the surgeon noted whether he would use the placed K-wires on a real patient (YES/NO) and assessed the helpfulness of the system (LOW/MED/HIGH).

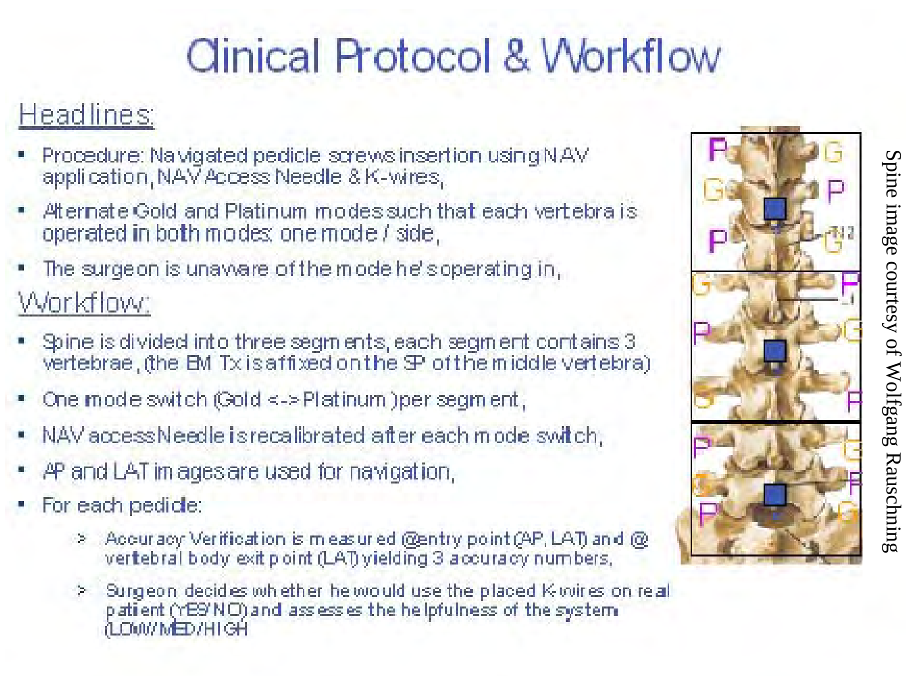

Figure 5.6 Pre-clinical method.

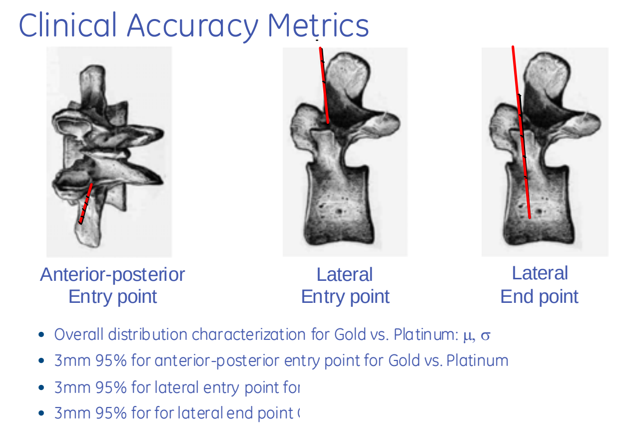

A

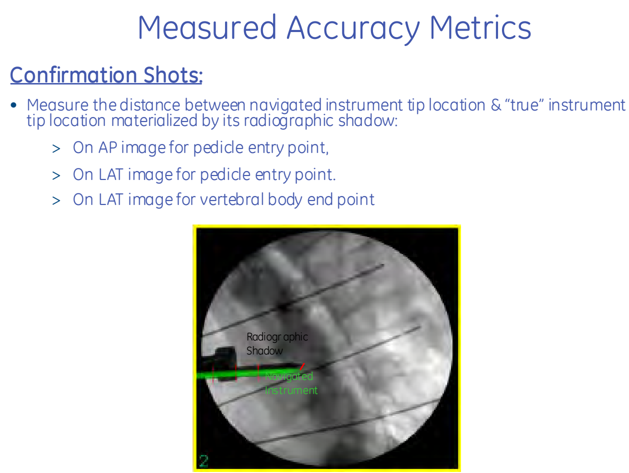

B

Figure 5.7 (A) Pre-clinical accuracy metrics. (B) Control shots used to measure precision.

After each bone biopsy needle (Nav trocar) was safely through each pedicle and into each vertebral body, the needle was removed, leaving a 3.2-mm trocar work channel for the K-wire placement step simulating a MIS Kyphoplasty or cannulated pedicle screw procedure relying solely on navigational guidance. Three accuracy measurements were performed on each navigated pedicle: pedicle entry point on an anterior/posterior image, pedicle entry point on a lateral image, and vertebral body final point on a lateral image.

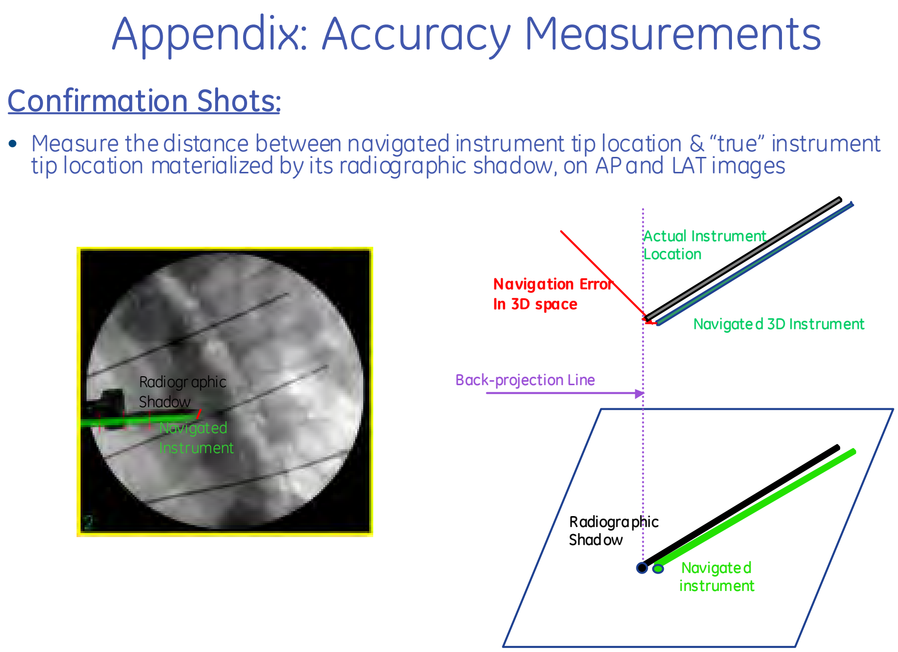

Figure 5.8 Method used to calculate positional difference of Gold and Platinum modes.

5.4 Results

The surgeon successfully navigated 34/36 pedicles on two cadavers in the lower thoracic and lumbar-sacral spine between T10-S1. The surgeon accepted 100% of the placements with the *Platinum* tracking software (17/17) vs. 88% (15/17) with the *Gold* tracking software. One of the *Gold* failures can be linked to multiple issues: a) system inaccuracy of 3.9 mm, 2) usage of the system in the frontier of the "too close to transmitter" area (as detected by the navigation system, meaning that the receiver-sensor in the surgeon's hand was too close to the transmitter reference frame in the spinous process, which creates distortion in the EM-field within a 7.5-cm proximity to each other), and 3) navigating on a collapsed vertebral body. The other failure was due to the surgeon's inability to drill the ideal pilot hole in the bony structure with the available instrument.

The surgeon ranked the navigation system highly useful for 100% of the pedicles navigated with *Platinum* (17/17) vs. 94% (16/17) considered highly useful and 6% considered somehow useful (1/17) with *Gold*. The user never ranked the system low.

On the average, the *Platinum* configuration was 40% more accurate than *Gold* (combining all the measurements, mean and standard deviations that are [1.87, 1.00] mm for *Gold* and [1.12, 0.78] mm for *Platinum*).

The Platinum system resulted in better placement of the K-wires. The three critical to quality (CTQ) measurements were: 1) Entry point, posterior image (mm, 95%ile): 1.50 *Platinum* vs. 2.94 *Gold*; 2) Entry point, lateral image (mm, 95%ile): 3.14 *Platinum* vs. 3.18 *Gold*; and: 3) vertebra body point, lateral image (mm, 95%ile): 2.36 *Platinum* vs. 3.42 *Gold* (Figure 5.9).

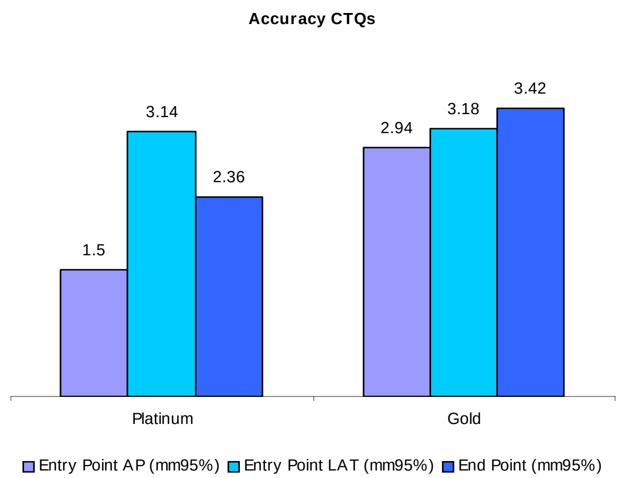

Figure 5.9 Bar graph showing accuracy critical to quality.

5.5 Discussion

Our results were in line with what was expected, based on our engineering tests (Figure 5.10). The surgeon ranked the navigation highly useful in nearly all of the wires placed. The surgeon indicated the medium useful ranking was due to interpretation issues of the 2D image (parallax), not navigation accuracy. The surgeon acknowledged that an axial view would have avoided the issue. We explore the use of axial views later in the following experiments.

Metric	Platinum	Gold
Acceptance of K-wires placement (YES/NO)	100%	88%
System Helpfullness		
Low	0%	0%
Med	0%	6%
High	100%	94%
Overall average error (mm)	1.12	1.87
Overall standard deviation (mm)	0.78	1.00
95% @Pedicle Entry Point AP (mm)	1.5	2.94
95% @ Pedicle Entry Point LAT (mm)	3.14	3.18
95% @ Vertebral Body End Point (mm)	2.36	3.42

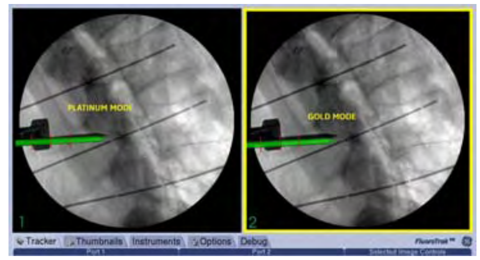

Same Fluoroscopic image calibrated
and registered in Platinum then Gold modes

Figure 5.10 Summary of results of studies comparing Platinum and Gold systems and sample data images from both systems.

The *Platinum* system was systematically better than *Gold* and passed the 3-mm 95th percentile requirement except on the lateral entry point where error conditions like “C-arm too far”/“Caltarget Field Induced distortion” or “transmitter too-close” warnings made data collection problematic. These results need to be further investigated.

Our cadaver experiments confirmed the magnitude of the improvement that *Platinum*-tracking software brings over the current *Gold*-tracking software (~40%). As expected, higher inaccuracies were measured in the clinical simulated environment than in the engineering test bench, thus bringing the *Platinum* system slightly out of our intended use specifications. The fact that the surgeon relies solely on navigation and that the accuracy measurements are taken at the farthest range possible make this study a worst-case scenario for the accuracy measurement, and a "before mitigation" study with respect to the usage of the control shots prescribed by the system labeling. This study was intended to stress the system to investigate how *Platinum*-tracking software can perform in a defined clinical environment, not to verify or validate *Platinum*-tracking software. Thus, in the rest of this Thesis, we investigate further with the current *Gold*-tracking software to evaluate how the clinical environment impacts accuracy and how we may improve the system robustness and inaccuracy detectability to avoid such out of specification cases and further improve the overall precision, reliability, and ease of use of our technology.

CHAPTER 6. SPINE EXPERIMENT 2: CADAVER OPEN THORACIC INVESTIGATIONS

6.1 Introduction

Since Roy-Camille introduced pedicle screw fixation in the late 1950s, it has been a widely used technique for the stabilization of the spine to address conditions such as trauma and deformity and for treatment of the degenerative spine.[178] Because of the inability to visualize the pedicle during pedicle drilling and actual screw placement, one of the main problems facing the surgeon is perforation of the vertebral wall.[179] Such a perforation can lead to potential problems such as dysesthesia, paraparesis, or paraplegia.[200] Current techniques such as mechanical probing, electromyography (EMG), somatosensory evoked potentials (SSEPs), spinal cord monitoring, and image-guided C-arm fluoroscopy have aided in both the optimal placement of pedicle screws and the avoidance of potential harmful complications. However, as noted earlier, the pedicle procedures do have drawbacks such as inaccurate placements of screws, long x-ray dose times, and parallax. The use of computer-assisted navigation helps to alleviate these concerns in the hands of the trained spine surgeon.

The advent of image-guided surgery has helped to decrease the need for continuous or repeated radiographic images in spinal surgery. The current standard for image-guided spinal surgery uses optical technology for tracking of instruments and the patient's anatomy. Many studies have shown that this technology is very accurate, and in many instances can improve on the accuracy of pedicle screw placement in the thoracic spine when compared with conventional fluoroscopy.[10,16,116,119,203]

Although it is commonly known that optical systems are associated with line-of-sight issues, there are no specific studies in the literature describing it as a major technical problem with existing systems. In a previous study, we introduced an EMF technology in tracking and navigating spinal anatomy for placement of lumbar pedicle screws.[188] EMF tracking was developed as an alternative to optical tracking to avoid this potential problem and we investigate its uses in spine surgery. We found that accuracy[188] was improved over the conventional technique for the application of lumbar pedicle screws. Some setbacks with the use of this technology in our early learning curve phases was the increased time for pedicle screw insertion, and distortion of the EM field by any substance that can carry a current (i.e., 400 series stainless steel instruments).[188] We improved these shortcomings in later experiments. In the meantime, our current design uses low or non-ferrous material such as 300 series stainless steel, titanium, and plastic instruments including retractors (Figure 6.1). In addition to standard OR tables, the popular Jackson table, which is made of a carbon-fiber type of tubing, is also a good option in maximizing the performance of our electromagnetic system.

Jackson table courtesy of MizuhOSI, Union City, CA

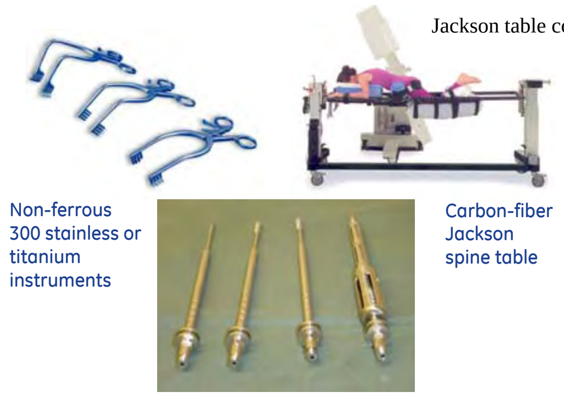

Figure 6.1 Retractors and spinal instruments are composed of low-ferrous stainless steel or titanium to maximize the performance of the EM field, and performance is further enhanced by the use of a carbon-fiber operating table.

6.2 Aims

The purpose of this investigation was to compare EMF tracking and conventional fluoroscopy in the placement of thoracic pedicle screws in a human cadaveric model. Accuracy, fluoroscopic exposure time, and screw insertion time were evaluated.

6.3 Methods And Materials

At the Syracuse University School of Medicine in the Department of Anatomy, I organized the use of four fresh-frozen human cadavers that were thawed and randomly allocated into one of two groups. None of the specimens had significant deformity as a result of scoliosis, spondylolisthesis, or fracture in the thoracic region. The posterior aspect of the thoracic spine was exposed to allow localization of landmarks for placement of thoracic pedicle screws and performance of an intertransverse fusion. We applied screws bilaterally at each level from T1 to T12 in all specimens. An awl was used to perforate the posterior cortex, and then a blunt pedicle finder was used to locate the pedicle. Five-millimeter USS pedicle screws (Universal Spine System, Synthes, Paoli, PA) were used in all cases.

6.3.1 Fluoroscopic Method

In the cadavers in Group one, thoracic pedicle screws were inserted with conventional fluoroscopic (OEC 9800 image intensifier, GE/OEC, Salt Lake City, UT; Figure 6.2) technique using AP, lateral, and oblique views as necessary. There were two specimens in this group, and two screws were inserted at each thoracic level for a total of 48 screws.

Figure 6.2 Photograph showing the navigation system integrated into a C-arm workstation (left) with navigation screen. (Right) Nine-inch C-arm fluoroscope with attached calibration grid for navigation.

6.3.2 Navigation Method

In the cadavers in Group two, thoracic pedicle screws were inserted using the EMF-based image guidance system alone. This system uses intraoperatively acquired AP and lateral fluoroscopic images to navigate the spinal anatomy (Figure 6.3). There were two specimens in this group, and two screws were placed at each level for a total of 48 screws (Figure 6.4). The technical aspects of using EMF navigation have been outlined previously.[188] The set-up for navigation included the rigid placement of a bone pin or clamp to each spinous process. To these, a dynamic reference frame is attached (in this case, our electromagnetic transmitter to the bone pin). We moved the transmitter to each bone pin or clamp and updated our C-arm x-ray images as we did at previous levels in our earlier experiments for the lumbar spine.[182] After the transmitter was securely placed at each level with saved images, our spine T-handle was used with various attachments (awl, bone probe, and implant driver) after they were calibrated for each tip offset. The next step was to choose an anatomical point or a rigid fiducial such as the bone pin or clamp visualized in the x-ray image for use as a verification point to return periodically throughout the procedure to assess accuracy and drift. The virtual instruments were then displayed on our 20-inch touch-screen navigation monitor superimposed over the previously acquired and saved C-arm x-ray images (Figure 6.5). The C-arm image intensifier (ii) has a calibration grid attached to it that was mapped to the specific 9-inch ii to eliminate distortion from the large metal bulk that would otherwise interfere with the electromagnetic tracking capability of our navigation system. The calibration grid also has a sensor built into it that allows the navigation unit to track its 3D position in space. The transmitter attached to the spinous process is used to track the C-arm's position. The tracking range here is also 18 inches, or approximately 46 cm, distance.

Figure 6.3 C-arm use in our cadaver laboratory studies acquiring AP and lateral oblique images.

Figure 6.4 (A) Photograph demonstrates RVJ and team implanting the navigated pedicle screws. (B) Photograph showing navigated Synthes USS screw targeting the pedicle entry point.

Figure 6.5 (A) Photograph demonstrating a cadaver with attached transmitter and navigated pedicle screws. (B) Photograph showing the navigation spine holder with the AP and lateral navigated X-ray views in the background.

Our navigation system operates within a defined range for electromagnetic tracking. This is defined as tracked instruments within a radius of 18 inches, or 45.7 cm, from the transmitter (Figure 1.13 p.18).

6.3.3 Procedural Workflow

The time to insert thoracic pedicle screws, as well as the total image-intensification exposure time, was recorded for each specimen in each group. In addition, the time required for set-up of the image-guided navigation system (placement of transmitter) as well as time for the computer to capture an appropriate image for navigation was recorded in group two. This was later factored into pedicle screw insertion time for this group.

Once all pedicle screws were placed, we dissected all the specimens' en bloc. We then dissected individual levels to assess the accuracy of screw placement (Figures 6.6 and 6.7). We noted the number of cortical perforations for each specimen and level. In addition, the direction and extent of perforation (in mm) was measured with a flexible ruler and noted. Any perforation that was through the medial or inferior aspect of the pedicle or the anterior cortex of the vertebral body was termed a critical perforation, implying that neurovascular structures were potentially at risk. A lateral perforation with the screw between the rib and pedicle was not considered a critical perforation as long as no screw thread was exposed outside of pedicle or rib.[23]

Figure 6.6 Photograph showing RVJ and team harvesting the vertebrae (left); the thoracolumbar vertebrae with implanted pedicle screws (right).

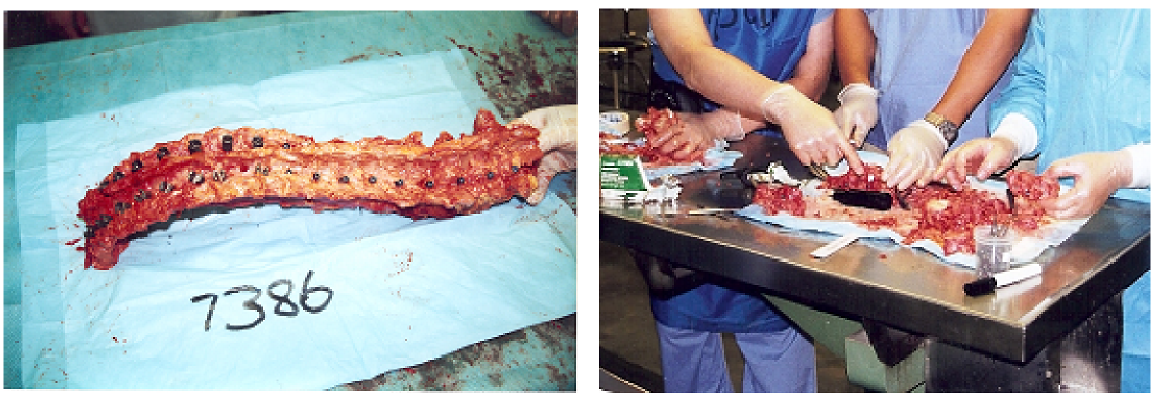

(A) (B)

Figure 6.7 Left image (A) demonstrates a completely harvested thoracolumbar spine with implanted pedicle screws. Right image (B) shows meticulous dissection of the vertebral segments for inspection by RVJ and team.

We then analyzed the data to compare accuracy, insertion time, and fluoroscopic time between each of the groups. Statistical analysis was performed using one-way ANOVA and chi squared analysis. Data was considered significant at $p<0.05$.

6.4 Results

We placed a total of 48 screws in each of groups one and two (Figure 6.8). The average insertion time per pedicle screw differed significantly between the two groups (Table 6.1). Group 1 averaged 261 seconds per pedicle screw and group 2 averaged 179 seconds per pedicle screw (p=0.04). However, when image acquisition and set-up time (i.e., application of bone pin and transmitter) was factored in, insertion time averaged 293 seconds per pedicle screw for group 2. This difference was no longer statistically significant.

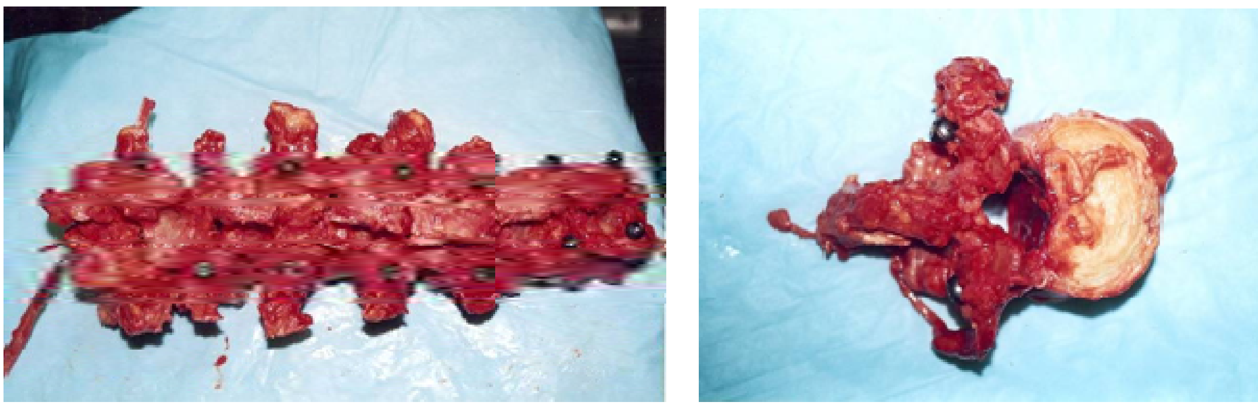

(A) (B)

Figure 6.8 (A) Close-up photograph showing pedicle screw placements in a thoracolumbar specimen. (B) Axial view of a thoracic segment.

Table 6.1 Thoracic pedicle screw insertion

Variable	**Group 1: Fluoro**	**Group 2: IGS**	**P Value**
"Safe" screws 1	43 (90%)	44 (92%)	NS
"Accurate" screws 2	26 (54%)	28 (58%)	NS
Critical perforations 3	5 (10%)	4 (8%)	NS
Mean perforation	2.36 mm	1.71 mm	(p=0.055)
Insertion time / screw	261 seconds	179 seconds	(p=0.007)
Set-up + Capture time / screw	n/a	114 seconds	
Total Insertion time / screw	261 seconds	293 seconds	(NS)
Total fluoro time used	270 seconds	162 seconds	(p=0.045)
Mean fluoro time / screw	5.9 seconds	3.6 seconds	(p=0.084)

1. Safe screw = perforation less than 5 mm ***and*** only lateral or superior cortex, or between rib head and pedicle.
2. Accurate screw = no perforation through any cortex.
3. Critical perforation = medial or inferior pedicle cortex, anterior vertebral cortex

IGS = image-guided surgery

6.4.1 Total Fluoroscopy

Total fluoroscopic time for group 1 was 270 seconds, and for group 2 it was 162 seconds. The average amount of fluoroscopic time per pedicle screw was 5.9 seconds for group 1, and 3.6 seconds for group 2. This difference was statistically significant (p=0.04). We anticipated higher fluoroscopic times as we placed a reference transmitter at each level and acquired new AP and lateral images. Our next studies will demonstrate how we learned from this study and lowered the overall need for x-ray use.

6.4.2 Accuracy

The accuracy of groups one and two were 90 and 92%, respectively. This difference was not statistically significant. This was due in part to the more difficult anatomy. This results in greater focus on multiple fluoroscopic views as this area of the spine can tend to be smaller and more challenging to the surgeon's general comfort level compared with the lumbar spine where the tendency to rely less on intraoperative C-arm fluoroscopy and more on general feel when EM navigation was used.

In addition, when a misplaced pedicle screw occurred, the degree of misplacement was reduced with the EM navigation. Critical perforations were seen in 10% in group 1 and 8% in group 2. This difference was not statistically significant. The average extent of break through or perforation was 2.36 mm for group 1 and 1.71 mm for group 2 (p=0.055).

6.5 Discussion

6.5.1 Thoracic Considerations

Many spine surgeons are familiar with the application and technique for placement of lumbar pedicle screws. In quality bone, it is an extremely powerful method of segmental fixation in the spine for many spinal deformities.[72,132], There are an increasing number of reports in the literature regarding the safety and efficacy of this technique applied in the thoracic spine.[23,133,167] Advantages over conventional laminar and pedicle hook fixation include not violating the canal and having a sounder mechanical construct with superior control of the spine for achieving and maintaining correction of deformity.[83,204,227] However, highly variable pedicle anatomy coupled with the proximity of vital neurological, vascular, and pulmonary structures makes the application of this fixation technique in the thoracic spine less inviting to the casual spine surgeon.[46,166,230] Thus, accurate localization of pedicle anatomy is key in avoiding complications, and many techniques have been devised to aid in optimizing screw placement. The more recent of these include aiming devices and computer navigation with image-guidance using either preoperative CT scans or intraoperative fluoroscopy.[10,12,16,116,119,203]

6.5.2 Thoracic Imaging Concerns

As in the lumbar spine, the issues are accurate placement in a timely fashion with minimal exposure of the surgeon and patient to fluoroscopic radiation. Although this technique is technically more demanding, attention to detail, preoperative imaging, and thorough knowledge of anatomical structures have resulted in safe placement of thoracic pedicle screws in a high percentage of patients.[23,83,167] The current concern with thoracic pedicle screws apart from safe placement, however continues to be the excessive use of fluoroscopy, which is often more than that required for lumbar pedicle screw placement.

Thus, with the concerns of accurate placement in difficult hidden anatomy and excessive radiation exposure to patient and OR personnel, computer navigated spinal surgery is gaining popularity.

6.5.3 Optical Navigation Results In The Thoracic Spine

Initial in-vitro studies using optical tracking and preoperative CT scans provided the benchmark for computer navigated thoracic pedicle screw placement. Assaker et al. showed that the accuracy was equal for computer-assisted and conventional fluoroscopic technique (97.5 and 95%, respectively).[16] Because of time required to perform surface matching, however, insertion time per pedicle screw was much longer with image guidance (13 minutes vs. 4 minutes). Kothe et al. showed that computer-generated images (virtual images) represented “reality” (in this case, radiographs) with remarkable accuracy (± 1–2 mm). None of the 54 screws breached the pedicle cortex.[119] Kim et al. further validated this technology with additional cadaver work that produced a 7.5% major perforation rate (neurovascular structures potentially at risk). They also highlighted the significant learning curve involved in using computer navigation that other reports have touched on.[116]

6.5.4 Clinical Reports Of Optical Navigation

Clinical reports of using optical image guidance for placement of thoracic pedicle screws with preoperative CT scan data also show encouraging results. Arand et al. reported an 80% accuracy rate (completely within the pedicle) for image-guided spine surgery (IGSS).[12] No malpositioned screws resulted in any neurovascular complications [2].

Youkolis et al. demonstrated an 8.5% cortical penetration rate in 224 thoracic screws placed with IGSS. Only 2.2% were felt to be structurally significant, however, and no neurovascular complications were encountered in any of the misplacements.[230]

One clinical report involves using EMF tracking coupled with preoperative CT scan data. Amiot et al. compared a prospectively followed group of patients treated with IGSS (294 screws) to a historical cohort of patients treated with conventional fluoroscopic technique (544 screws). They found that accuracy improved from 85% to 95% with IGSS, and that the extent of perforation was much less with IGSS (no screws > 2 mm out with IGSS, 15 screws > 2 mm out with fluoro).[10]

6.5.5 EM Validation

Our investigation validates two technologies in an in-vitro setting of thoracic pedicle screw placement: EMF tracking with image guidance and intraoperatively obtained fluoroscopic data to create the virtual imagery. Navigated IGSS placement of thoracic pedicle screws had an accuracy of 58% (completely within pedicle), but 92% of screws were considered safely positioned (no neurovascular structures at risk). This is in agreement with reports of other existing image-guidance systems and conventional fluoroscopic technique. We were also able to demonstrate a significant reduction (40% less with IGSS) in the amount of radiation exposure related to C-arm fluoroscope utilization time.

As with other navigation tracking technologies, inherent technical problems exist with EMF IGSS. Although surface matching with preoperative CT data is not required, extra time is incurred with setting up of the system, placing the transmitter, and acquiring images that are suitable for computer navigation. We later decreased this extra time through improved technology features and better learning curves. In this initial thoracic investigation, total time to insert pedicle screws was the same for IGSS and the standard fluoroscopic technique and x-ray exposure time was less.

6.5.6 Conclusion

Navigated EMF tracking technology coupled with intraoperative fluoroscopic imaging provides an alternative to optical tracking for placement of thoracic pedicle screws. We have demonstrated the potential for accurate insertion of thoracic pedicle screws with a substantial reduction in radiation exposure without increasing operative time. Our experiments showed that EM navigation for computer-assisted pedicle screw insertion improves accuracy, diminishes degree of misplacement, and reduces radiation exposure when compared with standard C-arm fluoroscopic technique.

These benefits of EM navigation from initial studies come at the cost of increased insertion time per screw as a result of increased set-up and image time, although the insertion time per screw is quicker in our experience. The total operative time per groups with all factors was similar. In recent software upgrades and the numerous preclinical experiments to follow in this document and clinical encounters with routine use, the set-up time has been reduced. Reductions were noted by the combination of improved tools for transmitter registration, software, and workflow (e.g., clamp vs. bone pins, improved image capture times, factory-calibrated instruments). Additions of implant screwdrivers and taps are expected to further erode x-dose times and overall operative times as noted in the following chapters.

CHAPTER 7. SPINE EXPERIMENT 3: MINIMALLY INVASIVE SPINAL SURGERY CADAVER INVESTIGATIONS

7.1 General Introduction To MIS Spinal Surgery

Minimally invasive spinal surgery is one of the fastest growing realms of spinal surgery. The goal of minimally invasive spine surgery is to achieve surgical outcomes that can be comparable with those of conventional open surgery, while minimizing the risk of iatrogenic injury that may be incurred during the exposure process. These muscle-sparring techniques often used endoscopy and muscle-splitting retractor systems to obtain access to the spinal column, while incurring minimal damage to the paraspinal musculature and limiting retraction-related injuries like muscle denervation.

7.1.1 Modern Imaging Technologies

These new approach techniques were fueled also by the revolution of new technologies in the medical device industry for implantables made of enhanced and new materials. Lumbar disc disease has been treated using chemonucleolysis, percutaneous discectomy, laser discectomy (investigated in this Thesis), intradiscal thermoablation, and minimally invasive microdiscectomy techniques. The initial use of thoracoscopy for thoracic discs and tumor biopsies has expanded to include deformity correction, sympathectomy, vertebrectomy with reconstruction and instrumentation, and resection of paraspinal neurogenic tumors.

7.1.2 Applications In Spine

Throughout the past decade, laparoscopic techniques, such as those used for appendectomy or cholecystectomy by general surgeons, have evolved for use in procedures performed by spinal surgeons for anterior lumbar discectomy and fusion. Laparoscopic techniques have also been used in other regions of the spine for cervical transoral procedures, video-assisted thoracic procedures, anterior, posterior lumbar interbody fusions, and newer transverse and extreme-lateral lumbar interbody fusions (TLIF and XLIF). The earliest mini-access and fiberoptic approach techniques were initially researched in Hungary by Jako et al. using a Jakoscope®, a mini-retractor–endoscope with fiber-optic lighting.[95] Motion preservation devices and biologics also are paving ways for MIS in spine surgery to treat among things disc herniations, compression fractures, degenerative disc disease, and other chronic and debilitating back pain. However, the safe and effective use of MIS surgery techniques with current and new instruments is beset with several technical challenges, including the limited tactile feedback, 2D video image quality of 3D complex spinal anatomy, and fine manual dexterity needed to manipulate instruments through small working channels. Although the aim of these techniques is to preserve the normal anatomical function and structures of the spine while treating spinal pathology, surgeons face a steep learning curve.

7.1.3 Value Proposition

In order for surgeons to safely perform MIS procedures, they must appreciate correct surgical orientation and pertinent surgical anatomy. This perhaps represents the steepest learning curve since MIS approaches expose only a small portion of the spine and require a thorough understanding of 3D anatomy of the spinal column. As use of these newer techniques spreads into the elective younger patient demographics seeking techniques with good cosmesis and less soft tissue trauma in older patients, the new instrumentation and procedures will continue to revolutionize the spinal field.[7,52,59,62,157,158,177,180,185,232]

As less invassive spinal interventions expand, the reliance on accuracy, imaging, and the effort to minimize ionizing radiation becomes more critical. Therefore, one of the additional achievements in the last decade for MIS spine has been the introduction of stereotactic computer-assisted image guidance systems that have been adapted to help define surgical orientation as well as pertinent surgical anatomy by elaborating on various dimensions of preoperative and intraoperative surgical planning. From a practical point of view, surgical navigation can facilitate pedicle screw placement through enhanced localization and implant placement accuracy and minimal intraoperative x-ray times while assisting in the determination in the extent of surgical dissection.

Nevertheless, in order for image-guidance technology to be used frequently in MIS surgery, a number of practical and technical obstacles need to be addressed, including anatomically relevant accuracy, instrument compatibility, ease of use, reduced or equivalent operative time, and reduction in x-ray exposure.

7.2 Trans-Pedicular Percutaneous Guide-Wire Placement

7.2.1 General Background

Minimally invasive spinal procedures have been developed to reduce morbidity from injury to the back muscles and soft tissues that can occur with open fusion procedures. This reduction in soft tissue manipulation can reduce postoperative pain enough to allow some instrumented fusions to be performed as outpatient procedures. By eliminating the exposure of adjacent spine segments, there may also be a reduction in adjacent-level disease. Other less complex noninstrumented procedures now considered in the U.S. as an outpatient procedure is kyphoplasty and vertebroplasty to treat vertebral compression fractures.

7.2.2 Fluoroscopic Concerns

All MIS cases require the use of fluoroscopic images to guide the accurate placement of pedicle screws or needles for injections or aspirations. The repetitive change in fluoroscope position for AP and lateral images creates the potential for contamination of the sterile field. Surgeons must wear lead aprons for protection from the ionizing radiation and this has a negative effect on ergonomics and does not completely eliminate surgeon exposure.

7.2.3 EM Benefit

As described above in section 1.4.3 EM Tracking Benefit, electromagnetic navigation with fluoroscopic images allows the tracking of instruments for placement of pedicle screws or needle trocars for cement augmentation by referencing intraoperative images to a transmitter mounted to the patient's spine. The transmitter creates an EMF around the region of interest that can be registered by a receiver mounted into a variety of surgical instruments.

Vertebroplasty and kyphoplasty are examples of minimally invasive vertebral augmentation procedures in which a filler material is percutaneously injected into a vertebral body for the treatment of vertebral compression fractures associated with osteoporosis, malignant conditions, hemangiomas, and osteonecrosis.[26,70,85,104,117,122] In vertebroplasty, the filler (PMMA) is injected directly into the bone through a needle trocar that is preferably a 13-11 gauge Jamshidi or Murphy needle and can range between 10-15g. In kyphoplasty these trocars are typically 17- or 18-gauge and used to place a flexible Kirshner guide-wire for a larger cannulated trocar and sleeve to follow over. Removing the K-wire and cannulated trocar with the tubular sleeve in place, creates a working channel for a balloon tamp inflation (Figure 7.1).[71,103,127,218] With the kyphoplasty balloon technique the filler is then injected through the Kyphon tube into a vertebral body bone cavity created by inflation of a balloon tamp usually bi-laterally and transpedicularly. Each method involves the injection of PMMA cement. The goals of treatment include circumventing the sensitive neurovascular structures with precision placement of the trocar and guide wire, avoiding cement leakage, and achieving pain relief, fracture stabilization, potential restoration of vertebral height, and strengthening of the vertebral body to reduce the risk of a future fracture at the same level.[19-22,70,85,104,117,122]

Figure 7.1 Photo demonstrating the navigated RVJ trocar transpedicularly into the vertebral body.

7.2.4 Aims

In this cadaver investigation we explored the navigated placements of trocars and K-wires for Kyphoplasty and percutaneous pedicle fusion procedures. At the time, there was no record of percutaneous transpedicular needle insertion in the thoracolumbosacral spine using an electromagnetic navigation tracking system. Determining the feasibility of using this technique was necessary to determine whether this technology would enhance the standard intraoperative fluoroscopic information for localization of the pedicle entry point and trajectory. Our aim was to conduct a preclinical study to assess the accuracy and time efficiency (placement and fluoroscopy) of using an EM tracking navigational technique versus a conventional fluoroscopically guided technique to place a navigated trocar and K-wire**.**

7.3 Materials And Methods

At Harvard Medical School affiliate laboratories and in collaboration with G. Weber of the Pecs Department of Experimental Surgery, I organized and obtained four fresh-frozen human cadavers and randomly allocated (two in each group) to be instrumented using fluoroscopy-based EM navigation (EM group) or fluoroscopy alone (Fluoroscopy Group). The specimens were screened to eliminate significant deformity such as scoliosis, spondylolisthesis, or ante mortem fracture. Experienced spine surgeons performed all K-wire insertions. K-wires were applied bilaterally at each level from T10 to S1 in two specimens (one in each group) and T8 to S1 in two specimens (one in each group) for a total of 80 wire placements (40 levels, 2 bilateral wires per level) (Figure 7.2).

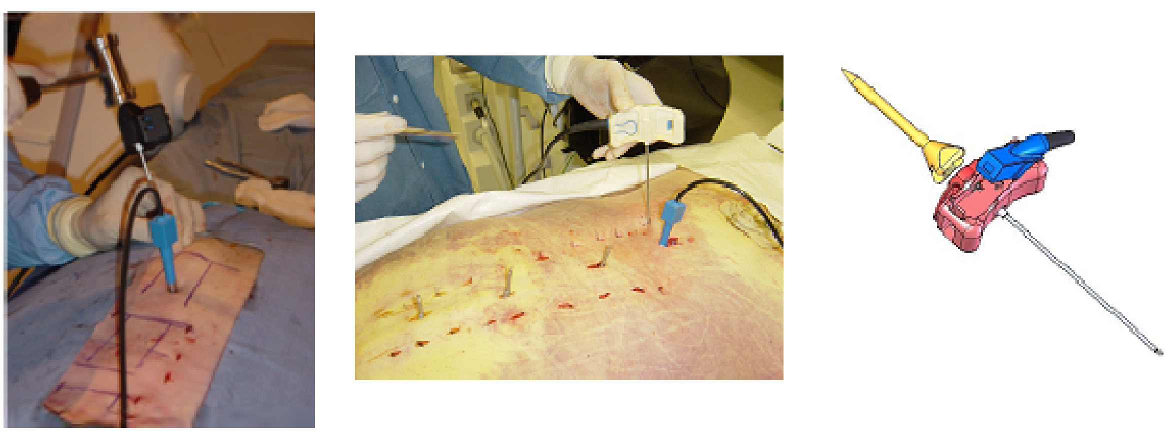

Figure 7.2 Picture demonstrating insertion of the navigated RVJ trocar between the thoracic and lumbar levels.

7.3.1 Fluoroscopy Group

In the Fluoroscopy Group, the K-wires were inserted via conventional biplanar fluoroscopic technique using a C-arm image intensifier (GE Healthcare). Multiple anteroposterior and lateral fluoroscopic views were used to localize the pedicle at each level, followed by insertion of a newly designed 18-gauge, 3-inch (15.2-cm) bone biopsy needle through the pedicle and into the vertebral body. We used a mallet to penetrate the cortical and cancellous bone.

7.3.2 EM Group

The EM-based navigation system required additional steps. A small cuboidal transmitter was attached rigidly to a spinous process via a bone clamp or threaded pin through a separate stab wound. The transmitter produces three orthogonal EM fields that surround the surgical anatomy). This defines the “surgical volume,” or space within the EM field where accurate tracking is permitted. The strength of an EM signal diminishes exponentially as the device moves away from the source. To maintain accurate tracking within a stable EM field, tracked objects must be within a radius of 18 inches, or 45.7 cm, from the transmitter. As discussed above, the computer alerts the operator of field distortion during the procedure.

7.3.3 Experimental Workflow

We obtained anterior-posterior (AP) and lateral views of the spinal segment to be navigated with a C-arm image intensifier outfitted with a calibration grid much the same as that used by optical tracking/fluoroscopic systems. The image-intensifier calibration grid contains a receiver that interacts with the EM field surrounding the anatomy, thus permitting the navigational computer to localize the imaged anatomy in 3D space relative to the image intensifier. To initiate tracking, the instrument with an attached receiver is calibrated to the EM transmitter to accurately localize the tip of the instrument. Each time a new instrument is chosen, it must be re-calibrated as discussed above. Tracking of instruments and screw placement is now possible through the interaction of the receiver in the instrument handle and the three orthogonal EM field set up by the transmitter, with real-time AP and lateral images being displayed simultaneously. We repeated this step for each transmitter location with storage of image sets for later use. Based on our earlier experiments showing accurate navigation for the immediately adjacent vertebral levels, the transmitters were placed three vertebral segments apart. The typical montage would be T11, L2, and L5.

7.3.4 Navigation Needle Trocar

RVJ designed and patented an 18-gauge bone biopsy needle six inches in length with a handle designed to hold the EM receiver to cannulate the pedicles. This is also known as the Nav trocar. In the set-up, only stored AP and lateral images from initial transmitter placement were used, and updated images were only checked at the end to determine K-wire depth (Figure 7.3).

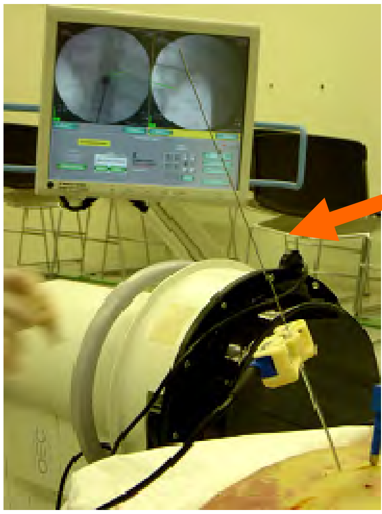

Figure 7.3 Navigated RVJ trocar placed transpedicularly into the vertebral body creating the work channel for the K-wire placement.

We used CT imaging as the reference standard for wire trajectory and location. All K-wires were trimmed, and the spines were then harvested as a single en bloc segment and the torsos were checked for vascular perforations. The specimens underwent multidetector CT imaging (GE Healthcare) of the instrumented volume. Small isotropic voxels (0.75 mm) were created for multiplanar reconstructions. Multiplanar reformatted (MPR) images were constructed in the coronal and sagittal projections using the standard reconstruction algorithm. Axial images were generated using both the standard and high spatial frequency (bone algorithm) in 2.5-mm contiguous sections. An experienced spine radiologist (JAC), who was masked to the method of placement, interpreted the CT images in a structured fashion by individual levels.

7.3.5 Statistical Analysis

For each specimen the percentage insertion and set-up time was ascertained. We defined the percentage insertion by number of needles inserted divided by the attempted number of pedicles. The set-up time was defined as beginning when initial localization images were taken and lasting until the first RVJ Nav trocar (bone biopsy needle) was placed through the skin.

For each level (both sides aggregated) of each specimen, we recorded measurements for total for both placement and fluoroscopy time. Placement time was defined as the total insertion time required for both K-wires at a particular level. Fluoroscopy time was defined as the total exposure time (radiation dose) used at a particular level. Placement time and fluoroscopy time were compared between the two groups using a t-test.

For each side and level of each specimen, the following measurements were tabulated based on the CT imaging: pedicle cortical penetration, vertebral body cortical penetration, critical cortical breach, facet joint violation, and comparison to an idealized trajectory. Pedicle cortical penetration was recorded as a dichotomous variable (Yes/No) and characterized by location (medial, lateral, cephalad, caudal) and distance outside the cortex (amount measured in mm). Vertebral body cortical breach was recorded as a dichotomous variable (Yes/No) and characterized by location (anterior, medial, lateral, cephalad [disc], caudal [disc]) and distance outside the cortex (amount measured in mm). A "critical" cortical breach was defined as encroachment or compression on the neural elements and recorded as a dichotomous variable (Yes/No). Any perforation that was through the medial or inferior aspect of the pedicle or the anterior cortex of the vertebral body was termed a critical perforation, implying that neurovascular structures were potentially at risk. Facet joint violation was defined as transgression of the articulation by the wire and recorded as a dichotomous variable (Yes/No). Comparison to an idealized trajectory was performed. The “ideal trajectory” was considered to be a convergence of the wires at the ventral aspect of the vertebral body in addition to staying within the pedicle. This was graded on a 4-point scale as follows: Ideal (grade 0), minimally displaced by 1–3 mm (grade 1), moderately displaced by greater than 3 mm but less then 5 mm (grade 2), and markedly displaced by greater than 5 mm (grade 3). Comparison between these dichotomous variables was performed using a chi square test.

Descriptive statistics were calculated for all variables. Comparison between continuous variables (time measurements) dichotomous variables was performed using a t-test. Comparison between dichotomous variables (cortical perforations) was performed using a chi square test. Statistical analysis was performed using a computer software program (StatCrunch 4.0, http://www.statcrunch.com/). The results were considered statistically significant when $P \leq .05$.

7.4 Results

Our EM technique had an average set-up time of 575 seconds. The Fluoroscopy technique had an average set-up time of 218 seconds. The average placement time per level in the EM group average time was 381 seconds (range 90–780 seconds). The average placement time per level in the Fluoroscopy group was 579 seconds (range 258–960 seconds). This difference was significant (p=0.005, t-test). For Fluoroscopy Time, the average time per level in the EM group was 11 seconds (range 1–53), while in the Fluoroscopy group, the average time per level was 48 seconds (range 15–86). This difference was significant (p<0.0001, t-test).

The number of successful K-wire placements, pedicle breaches, vertebral body breaches, and facet joint transgressions did not differ significantly between groups (Table 7.1). There were no critical cortical breaches in either of our groups. There was a significant difference between idealized trajectories (p = 0.04, chi-square) but not for the entire distribution of trajectories (p= 0.17, chi square test for trend).

Table 7.1 Comparison of EM group to fluoroscopy group

	EM Group	**Fluoroscopy Group**
Average Setup Time (min)	9.6	3.6
Average Placement Time Per Level (min)	6.3	9.7
Average Fluoroscopy Time Per Level (min)	0.18	0.80
Number of Successful K-wire Placements	40/40	40/40
Percentage of Pedicle Breaches (%)	10.0	15.0
Percentage of Vertebral Body Breaches (%)	0.03	0.0
Percentage of Facet Joint Breaches (%)	15.0	12.5
Ideal Trajectories (%)	62.5	40
Minimally Displaced Trajectories (%)	22.5	27.5
Moderately Displaced Trajectories (%)	10.0	25.0
Markedly Displaced Trajectories (%)	5.0	7.5

7.5 Discussion

Minimally invasive surgical procedures have been designed to decrease approach-related soft tissue damage associated with open surgical techniques. These techniques have been advocated to shorten hospitalization, speed the return to normal activities, minimize muscle wasting, and reduce the need for opioid medication while attempting to retain the effectiveness of open approaches. Soft tissue dissection and muscle retraction during surgery has been shown to do short-term damage and to affect long-term, degenerative changes[105,107] , which increase the patient's susceptibility to reinjury.[73] Recovery from open spinal surgery may expose the patient to prolonged opioid analgesia and can pose a significant risk of initiating, or exacerbating, addiction in a patient during the postoperative phase.[159] It has also been shown that the trauma incurred in open spinal surgery often necessitates a long recovery time, which can be linked to an extended loss of productivity.[51]

The ability to insert surgical implants percutaneously into the spine was initially demonstrated by Magerl but the technique involved external connectors and rods that were cumbersome and created a potential for infection. The key in minimally invasive surgical fusion procedures was the development of novel techniques and instrumentation that allow for the subfascial insertion, connection, and manipulation of pedicle screws and connecting rods through small skin portals. The first MIS pedicle screw system was described by Foley[59], and now there are several systems available from various manufacturers.

All minimally invasive procedures are dependent on fluoroscopic guidance to safely target the spine and to verify the position of instruments and implants. This process requires the manipulation of a portable fluoroscope around the sterile operative field, which can be a potential source for infection. The use of an intraoperative fluoroscope also requires the use of protective devices and aprons to minimize exposure to ionizing radiation, which can have a negative effect on ergonomics in the operating room suite.

Current IGS platforms for spine surgery incorporate either optical or EM technology. Both technologies require the application of a patient reference to create a coordinate system around the patient's anatomy and to allow navigation of instruments based on intraoperative fluoroscopic images. The advantage of the EM system is the elimination of optical line-of-sight issues and the potential of tracking flexible or deflectable devices.[35,61,139] By using nonferromagnetic instruments (i.e., 300 grade stainless steel or titanium) and carbon fiber OR tables, potential distortion of the EM field can be eliminated, eliminating the primary limitation of the technology. The ability to create axial tomographic images intraoperatively with a fluoroscope is advancing steadily and will further enhance the ability to navigate safely in the spine.

The initial publication on the use of EM tracking for placement of pedicle screws in the thoracic, lumbar, and sacral spine compared image-guidance using EM tracking coupled with a preoperative CT imaging data and surface registration to a historical cohort who had pedicle screws placed in standard fashion using anatomic landmarks and fluoroscopy. The author found that EM IGS had an accuracy (completely within the pedicle) of 95% compared with 85% using standard technique. Seven percent of conventional technique patients required reoperation for misplaced pedicle screws, whereas none required reoperation in the computer-assisted group. Preoperative CT images, however, have been shown to have a higher radiation dose as compared with standard fluoroscopy.[196], and there are potential problems with registration of the images at the time of surgery.

Another investigation using fluoroscopic-based IGS found that fluoroscopy time and insertion time per screw were not improved using an EM-tracking IGS system for lumbar instrumentation,[182] but the same investigators noted a significant reduction in fluoroscopic time and exposure for the thoracic spine.[183] We extended this work into a percutaneous MIS paradigm, and our results similarly showed a significant reduction in x-ray exposure time with only a negligible overall time penalty for both the thoracic and lumbar spine.

Some of the technical challenges for IGS include improving intraoperative imaging, fusion of images from multiple modalities, the visualization of oblique paths, percutaneous spine tracking, mechanical instrument guidance, and creating software architectures for technology integration.[47] Certain anatomic regions remain challenging such as the cervicothoracic junction because of the overlap of the shoulder girdle and upper thoracic spine.

The surgical navigation system used in our experiments integrates C-arm fluoroscopy with electromagnetic tracking technology. It features automatic registration of the fluoroscopic image to the patient's anatomy, making system set-up and use easy and relatively fast. Through the development of MagneticIntelligence™ (a proprietary algorithm), the system automatically detects and compensates for metal in the field, resulting in improved clinical accuracy and reliability. The C-arm fluoroscope is removed from the operative field after image acquisition, making the operating environment less encumbered. The calibration fixture attaches easily to C-arm image intensifier, enabling use with larger patients without image degradation. The EM transmitter attaches to bony anatomy, typically the spinous process, allowing surgical freedom in operative area and eliminating line-of-sight issues common with optical systems.[35,61,139] Because of the elimination of the need for repetitive imaging, the patient, OR staff, and surgeon receive lower doses of ionizing radiation.

The results of this preliminary investigation must be viewed within the context of the experimental design. The sample size for specimens and number of needles inserted was adequate. The placement of K-wires rather than the actual pedicle screws eliminates additional steps that involve larger implants, which create additional opportunities for implant misplacement. Although in this investigation the operator was an experienced spine surgeon with considerable experience in percutaneous screw placement and kyphoplasty, operator inexperience could be an issue.

Based on this pilot investigation, I am encouraged to pursue future avenues of research using this EM navigation system. For surgical applications, we want to confirm these results using a larger sample size and more challenging spine levels for instrumentation, and to identify the incremental benefit for various levels of operators (trainee, fellow, etc.). Currently, the system can only be used to track relatively large-bore (gauge) needles. As technical improvements occur, the ability to track a wider variety of instruments facilitates the application to other types of percutaneous procedures.

7.5.1 Conclusions

This experimental study demonstrates that an EM navigation system can assist the spine surgeon in percutaneous transpedicular procedures by providing high-accuracy K-wire placement with a significant reduction of fluoroscopy time and safe positioning in relation to neuron-vascular tissues. The overall placement time per vertebral level also improved with the EM technique with a negligible increase in set-up time. The next experiments to test the feasibility and expand the use into applications that can benefit from high accuracy and reduction in x-ray fluoroscopy times are the new trends in percutaneous instrumentation for pedicle fusion procedures.

CHAPTER 8. SPINE EXPERIMENT 5: PERCUTANEOUS PEDICLE SCREWS INSERTED IN CADAVERS USING TWO METHODS PER LEVEL

8.1 Introduction

Recently published research has focused on methodologies for ensuring precise and efficient percutaneous pedicle screw fixation. Wiesner et al. demonstrated a pedicle screw misplacement rate of 6.6% among 408 percutaneously placed screws in 54 patients.[221] Of the 27 misplaced screws, only one screw-related nerve root injury was reported.[84] In a study comparing conventional pedicle screw fixation using anatomic landmarks with computer-assisted screw fixation using an optoelectronic navigation system, Laine et al. found a significant difference in pedicle perforation rate (13.4% conventional vs. 4.6% computer-assisted, p = 0.006).[123] Several other groups have used optical tracking systems that use dynamic reference frames to provide real-time 3D guidance in pedicle screw placement.[27,116] As described previously, we found similar rates of screw misplacement in the thoracic spine in cadavers between EM IGS and conventional anatomical/fluoroscopic guidance.[183] EMF tracking, as an alternative to optical tracking, significantly reduced mean screw insertion time (179 vs. 261 sec, p = 0.007) and mean total fluoroscopy time (162 vs. 261 sec, p = 0.045).[183] As such, EMF tracking technology, which, unlike optical imaging, does not depend upon continuous line-of-sight registration,[35,61,139] and represents an important development in the advance of image-guided complex spine surgery.

8.2 Aim

While our previous navigation experimental studies demonstrated the utility of EM-navigational guidance in the open thoracic and lumbar spine and percutaneous needle-trocar placement, its use in the minimally invasive transpedicular placement of lumbar pedicle screws has yet to be tested. Therefore, the aim of my cadaveric study was to evaluate further the surgical precision and efficiency of an electromagnetic field (EMF) navigation system in percutaneous lumbar pedicle screw insertion compared with conventional fluoroscopic image-guidance using a customized set of MIS instruments. The intent was to prove the feasibility of using longer MIS instruments within the tracking range limitations of the EM navigation field and to show that the material change and workflow steps would continue to perform with the required accuracy in pedicle screw implantation with a reduction in x-ray dose.

8.3 Materials And Methods

I included five human cadaveric specimens in this study. The specimens were prescreened to eliminate significant deformity such as fracture, scoliosis, or spondylolisthesis. The specimens were each placed on a Jackson carbon fiber table ideal for spine surgery due to its hollow tabletop design and radioluceny in the prone position for posterior access. Each cadaver was subject to screw placements from L1 to S1 (inclusive); K-wires were applied bilaterally at each level. For comparative analysis, screws were placed on one side of each cadaver using conventional fluoroscopic technique alone and on the opposite side using the EM-based navigational system (Figure 8.1).

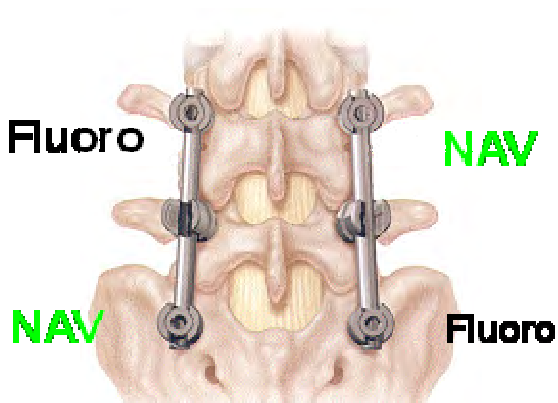

Figure 8.1 Drawing showing the alternate side method of placement at each segmental level.

8.3.1 Set-Up

For the conventional fluoroscopy group, K-wires were inserted via a Jamshidi needle using multiple AP and lateral views to localize the pedicle at each level. For the EM group (EM), a custom designed minimally invasive instrumentation kit was created by RVJ and used for these experiments (Figure 8.2). In this EM group, K-wires were inserted using the EM Navigation system. An EM transmitter was attached rigidly to a spinous process to produce three orthogonal EM fields encompassing the anatomical field. AP and lateral views of each target spinal segment were obtained using the image intensifier outfitted with a receiver-outfitted calibration grid that interacts with the EM surgical field. Surgical instruments that require tracking were each fitted with an EM receiver and calibrated to the EM transmitter. With calibration, instruments could be tracked in real time simultaneously on AP lateral and oblique image displays (Figure 8.3).

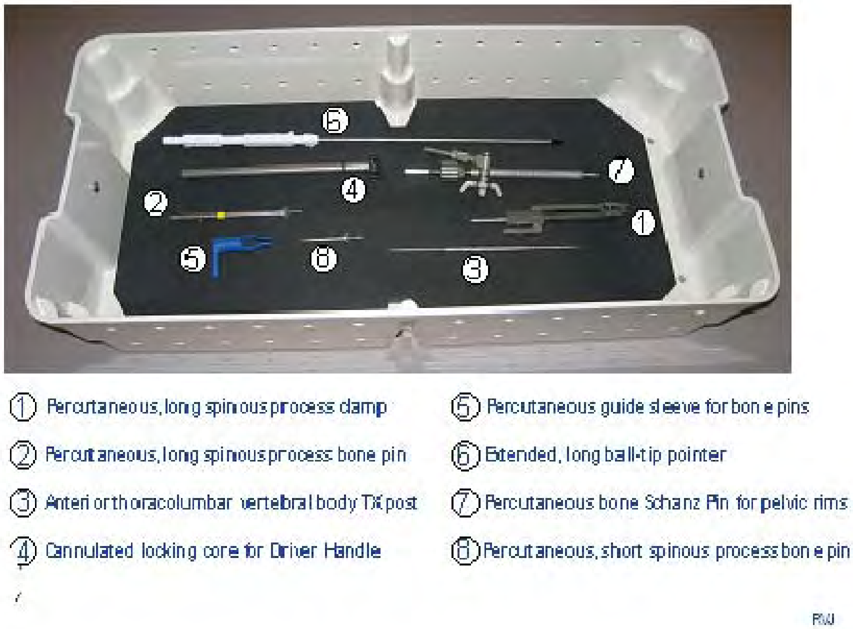

Figure 8.2 Custom MIS Navigation Spine Kit designed and built by RVJ.

Figure 8.3 Correlating the Depuy J&J cannulated MIS Viper pedicle screws with the navigation tracker.

Using this tracking method on the EM-side and ‘free-hand’ fluoroscopic placement on the control side, a navigated NAV Access Needle™ (Jamshidi style) designed by RVJ was placed, and a custom cannulated NAV Spine T-handle built by RVJ with custom-attached Taps (J&J - Depuy Spine) were used (Figure 8.4) Finally, Depuy Spine Expedium style (Viper) cannulated lumbar pedicle screws were placed using custom screwdrivers together with a intervertebral body implant driver navigated by electromagnetic tracking technology (Figure 8.5).

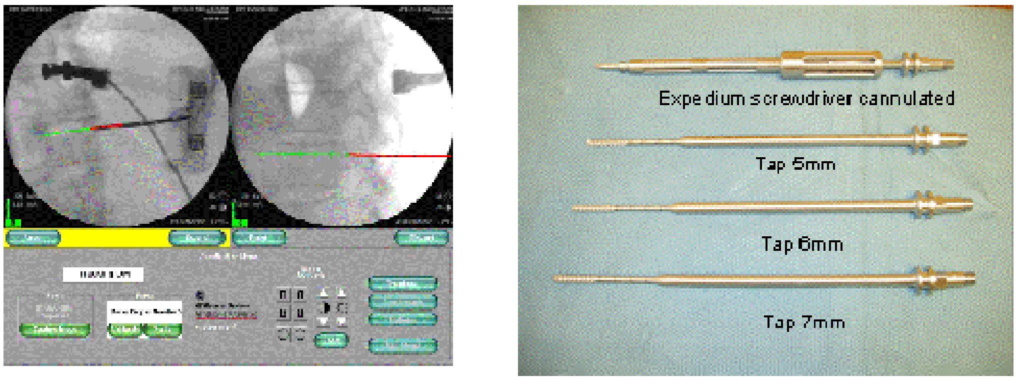

Figure 8.4 (Left) Virtual trajectory of the Nav trocar superimposed over the X-ray image. (Right) Cannulated MIS instruments co-designed by RVJ and J&J - Depuy Spine.

Figure 8.5 Navigation screen shot demonstrating the percutaneous placement of a navigated intervertebral body PEEK® spacer cage with a posterior tension band pedicle screw and rods.

8.3.2 Experimental Analysis

We conducted an intracadaveric analysis to compare EM-navigational guidance to conventional fluoroscopy with a radiologist blinded to the protocol. Intraoperative variables for analysis included total fluoroscopic time and mean fluoroscopic side per screw by dividing the number of screws placed and taking approximately 3 AP shots and 3 lateral shots per specimen in order to place the 12 screws. Each specimen underwent a postoperative CT with reconstructions by an independent, blinded radiologist to rate screw placement for pedicle breach, defined at penetration through the cortical edge of the pedicle breach, vertebral body breach, and critical breach. The ideal trajectory was defined as screw placement precision toward medial ventral aspect of the vertebral body such that bilateral screws would converge while remaining entirely within the pedicles. The trajectory was rated accordingly: 0 (ideal), 1 (1–3mm off ideal), 2 (>3 but < 5 mm off ideal), 3 (≥5mm off ideal). In comparing trajectories, overall number of pedicle breaches, vertebrae breaches, and critical breaches were evaluated for EM-guidance compared with conventional fluoroscopy. Additionally, lumbar spine segment (L1-L5) breaches were evaluated in a separate comparison to specifically study the breach rates for lumbar pedicle screw placement.

Statistical analysis was conducted using Wilcoxon Matched-Pairs Signed-Ranks Tests for total fluoroscopy time, mean fluoroscopy time/screw, and trajectory. Fisher Exact tests were used to compare rates of pedicle breach, vertebrae breach, and critical breach. P-value < 0.05 was considered significant.

8.4 Results

Overall, the average total fluoroscopy times/specimen were 383.3 ± 255.6 sec for CF and 160.5 ± 79.6 sec for EM, which was an insignificant difference. The overall mean fluoroscopy time per screw was 58.9 ± 44.7 sec for CF and 27.4 ± 13.5 sec for EM (p = 0.0003). Data for total fluoroscopy time was excluded for one specimen (Spine 5); L1 was not instrumented in Spine 5 due to a previous kyphoplasty, and S1 was not instrumented due to an abnormal anatomic relationship with the pelvis that confounded screw placement. As such, a total fluoroscopy time for that specimen would be confounded by the exclusion of two levels.

Trajectory and breach were analyzed on postoperative CT. The difference in the mean trajectory rating was 1.1 ± 1.1 for CF and 1.4 ± 0.2 for EM, which was not significant. The number and distribution of breaches are demonstrated in (Figure 8.6). The overall breach rate is shown in (Table 8.1). Overall, the EM screws demonstrated 3 more pedicle breaches, but 3 fewer critical breaches than the CF screws (not significant). (Figure 8.7) summarizes the results for lumbar pedicle screw placements (L1-L5). When lumbar screws were evaluated alone, EM-guided screws demonstrated one more vertebrae breach, but 6 fewer critical breaches (p = 0.02).

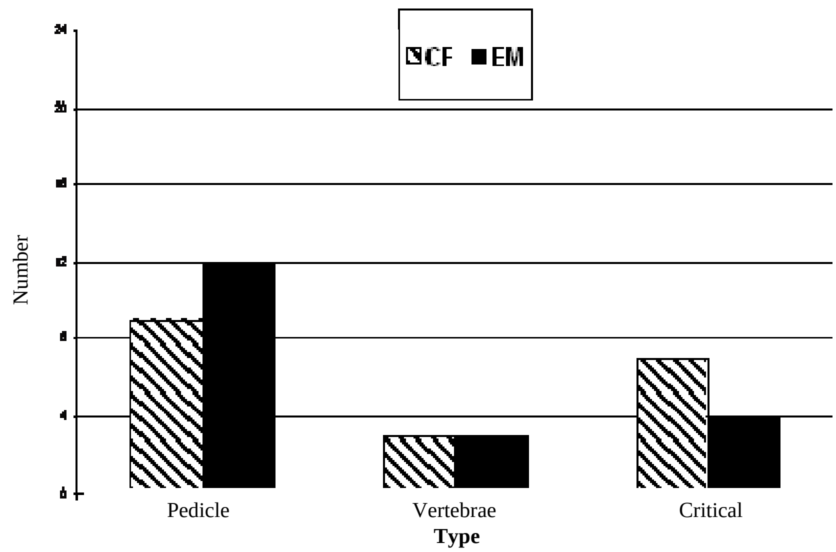

Figure 8.6 Distribution of all breaches.

Table 8.1 Rates of breach by type for Conventional Fluoroscopy (CF) versus Electromagnetic Guidance (EM)

	Overall Breach Rate (%)		Lumbar Breach Rate (%)	
Breach Type	CF	EM	CF	EM
Pedicle	32.1	42.8	33.3	33.3
Vertebrae	10.7	10.7	8.3	12.5
Critical	25	14.2	25	0

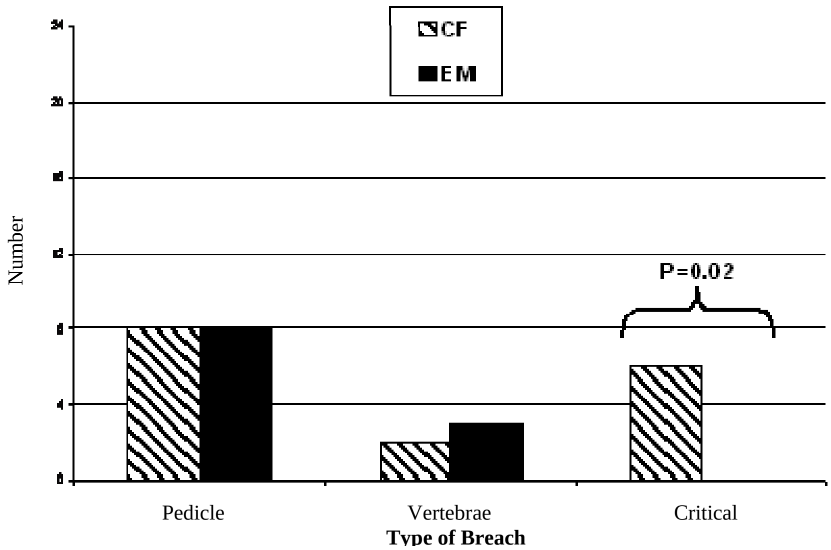

Figure 8.7 Distribution of breaches in the lumbar spine.

8.5 Discussion

While limited to five cadavers, our investigational study demonstrated significant reduction in fluoroscopy time spent per level from L1 to S1 and a reduction in critical breaches in the lumbar spine (L1-L5). These results demonstrate that EM guidance may provide some benefit in the placement of percutaneous pedicle screws in the lumbar spine. Although an ideal analysis would compare patients in a randomized fashion, our cadaveric study provides a strong foundation for such future studies. In large spinal fusions, reduction of operative time remains an important goal; reduction in operative time may reduce blood loss, anesthesia time, and complication rate. As such, tools that demonstrably reduce operative time are essential in spinal surgery. While the absolute reduction per screw may be relatively small, multiple time differentials result in a significantly dissimilar overall operative time in large spine fusion cases. These results in the lumbar spine mirror comparable results from other studies in the thoracic spine.[183] As such, EM navigational guidance tools for pedicle screw placement show a distinct advantage in the thoracolumbar spine. Another advantage is that the initial radiographs for EM navigation can be taken with the OR personnel protecting themselves by either stepping behind a lead screen or leaving the room, thus limiting personnel exposure. During CF placement of pedicle screws, this is not possible.

8.5.1 Reports Of Earlier Experiments

There has been extensive recent interest in stereotactic computer-assisted navigation for spine surgery, especially as minimally invasive fusion techniques require real-time imaging feedback. While minimally-invasive procedures such as percutaneous pedicle screw fixation have been shown to be safe and reliable, they demand an effective imaging tool to accurately predict target trajectory for screw placement.[222] Early versions of optical tracking real-time spine imaging demonstrated a thoracic pedicle cortex breach rate of 19.2%, compared with the thoracic pedicle breach rate of 8% published in cadaveric studies of EMF tracking in the thoracic spine.[116,183] Similarly, published experience with real-time tracking for percutaneous pedicle screw placement in the lumbar spine has been encouraging. In a study of patients with previous fusion undergoing new instrumentation, Lim et al. found only 4.1% of 122 pedicle screws placed in the lumbar spine using frameless stereotaxy for guidance to have unintended cortical violations on follow-up after.[134] While our pedicle breach rates for conventional fluoroscopy and EM navigational guidance were at equipoise, there were significantly fewer critical breaches among EM navigational guided screws. As such, EM-guidance may be an important tool to make percutaneous screw placement in the lumbar spine not only more efficient but also more precise.

While our investigational study demonstrates important findings regarding the use of EM-navigational guidance in lumbar fusion techniques, it represents a limited examination in a small-scale cadaveric model. Thus, our investigational study provides a foundation upon which to base a clinical examination of this subject.

8.5.2 Conclusions

Minimally invasive spine fusion in the lumbosacral region requires an accurate real-time imaging modality for screw trajectory guidance. EM navigational systems provide safe and effective tools for intraoperative guidance. Our cadaveric study suggests the EM navigational guidance may be more efficient and safer than the conventional fluoroscopic technique. Further preclinical and clinical studies are needed to further elucidate these differences, and this investigational study provides a foundation and justification for such research.

CHAPTER 9. SPINE EXPERIMENT 6: PERCUTANEOUS SCREWS INSERTED IN CADAVERS USING TWO METHODS BY RANDOM LEVELS

9.1 Introduction

9.1.1 Standard Approaches

Pedicle screw fixation is the most effective and widely used form of internal fixation and provides superior biomechanical strength when compared with wiring or hook-based constructs for creation of a stable environment for bony fusion.[30,69,121,186,234] Standard methods of pedicle screw instrumentation require significant exposure of the posterior bony elements of the spine to provide landmarks from which to guide the placement of instrumentation. Such exposure is associated with significant amounts of blood loss,[98] as well as paraspinal muscular injury, which has been associated with postoperative back pain.[105,106] Even with wide exposure, however, accurate placement of pedicle screws remains difficult and is largely a blind procedure after penetration of the bony cortex is accomplished. Acceptable trajectory after this point depends on tactile feedback, knowledge of anatomic relations, and 2D fluoroscopic imaging, which can be time consuming and is associated with significant radiation exposure.[165] Open pedicle screw placement is associated with a cortical breach rate in excess of 30%.[74,118,125] The accuracy of placement of pedicle screws has been shown to be improved with the use of frameless stereotaxic image guidance in most[16,17,118,125] but not all studies.[84] Overall adoption of image-guided surgical techniques has been limited to date amid concerns of increased operative time and complexity of the technology.[16]

9.1.2 MIS Observations

Recently, there has been developing interest in minimally invasive techniques of spinal stabilization. These techniques offer a less traumatic approach resulting in less damage to the surrounding musculature, decreased blood loss, and decreased recovery time.[91,97,115] These characteristics may eventually translate into improved long-term results, with decreased muscle denervation, atrophy, and pain.[171] Accurate minimally invasive pedicle screw placement is complicated, however, by the obscuration of normal anatomical landmarks. Errors in placement are therefore a primary concern, with one study reporting almost 10% of patients needing revision surgery.[171] Additionally, the technique depends heavily on fluoroscopic guidance, which can result in significant levels of radiation exposure to both the surgeon and assistant.[165] An efficient image-guided navigation system that allows accurate pedicle screw placement and a reduction in the amount of fluoroscopic time would therefore to be of value.

Various methodologies have been devised to increase the accuracy of screw placement, including the use of articulated manipulators,[5]Doppler ultrasound, [37,101] isocentric fluoroscopic 3-dimensional imaging techniques,[6,164] robotics,[131,209] and computer-aided fluoroscopic techniques.[41,60,160,168] This latter technique has been the subject of most investigation and has been shown in various reports to aid in the accurate placement of pedicle screws.[41,60,160,168] Widespread adoption with earlier systems using optical technology has been low due to increased time for set-up, extension of operative time.[7] A particular advantage of an EMF navigation system over more widely available optical-based systems is the elimination of cumbersome optical array receivers. Furthermore, line-of-sight issues can interfere with the normal flow of the operative procedure.[35,61,139] The trade-off for this flexibility is the limited size of the EMF field (18-inch diameter or 46 cm) (Fig. 1.13 p.18) relative to larger patients and the need to eliminate ferromagnetic devices and instruments that can create distortion within the EMF field.

9.1.3 Aims

In our eighth experiment, we repeated the previous percutaneous cadaver experiments but randomly assigned the levels rather than alternating the technique from side to side. A comparison by level in which one technique is performed bilaterally was thought to reduce the potential bias for a reduction in time and improved accuracy based on knowledge gained from placement of the first screw when placing the contralateral screw. Comparison by level is also more consistent with the manner in which surgery is performed with sequential placement of screws bilaterally before moving to the next level. In addition, we tested different customized MIS instruments of which some were designed and built by me to demonstrate that these different brand instruments can be used with this type of EM navigation technology. We also measured ionizing radiation to the hands using special thermoluminescent dosimeter badges and rings (Figure 9.1).

Figure 9.1 Thermoluminescent -TLD collar Badges at the thyroid and TLD finger rings one each for fluoroscopy and for navigation comparisons.

9.2 Materials And Methods

9.2.1 Preparation

For this experiment I organized eight fresh-frozen human cadavers with intact spines from at least T8 to the sacrum with colleagues from the Texas Back Institute and the University of Los Angeles. The spines were prescreened for osseous vertebral pathological conditions, including evidence of tumor infiltration, traumatic disruption, or past surgical intervention. All thoracic, abdominal, and pelvic structures were left intact to mimic fluoroscopic imaging clarity typical for the operating room. The cadavers were placed in the prone position on a radiolucent table and localizing images were obtained.

A C-arm fluoroscope with an integrated navigation system (navigation unit built into the C-arm as one platform) was used for fluoroscopic imaging.. Our latest navigation software allows for the simultaneous tracking of two surgical instruments. Two operative stations were used to compare two different minimally invasive pedicle screw systems that had been modified for use in an EMF environment: the Paramount system (Innovative Spinal Technologies, Mansfield, MA) and the Pathfinder system (Abbott Spine now Zimmer Spine, Austin, TX). Titanium screw extenders for each system built to avoid interference within the EMF field that would be expected from the normal 400 series ferromagnetic stainless steel extender instruments. A special bone biopsy needle known as the Nav Access Needle or Nav trocar designed by RVJ, which provides stable attachment of an EMF receiver-sensor, was used for Kirschner wire (K-wire) placement. A minimally invasive bone pin or spinous process clamp was used for stable fixation of the EMF dynamic reference transmitter to the spinous process. Accuracy for adjacent level vertebrae had been determined in our previous studies for k-wire placement and initial MIS screws and, as a result, the typical montage for transmitter placement was on the spinous processes of T11, L2, and L5. For two cadavers, T8 was also used for placement of the EMF transmitter.

9.2.2 Operative Procedure

Our four attending spinal surgeons with experience in minimally invasive spine surgery worked in pairs on each cadaver. Each cadaver was randomly assigned to implantation with either the Pathfinder custom MIS-Nav implant system or the custom Paramount pedicle screw system. Comparison of EMF navigation (Nav) with standard fluoroscopic imaging (Fluoro) was performed based on screw placement per level. A comparison by level, in which one technique is performed bilaterally, was thought to reduce a potential bias for a reduction in time and improved accuracy based on knowledge gained from placement of the first screw when placing the contralateral screw. A comparison by level is also more consistent with the manner in which surgery is performed with sequential placement of screws bilaterally before moving to the next level. The entire procedural steps are shown in (Figure 9.2).

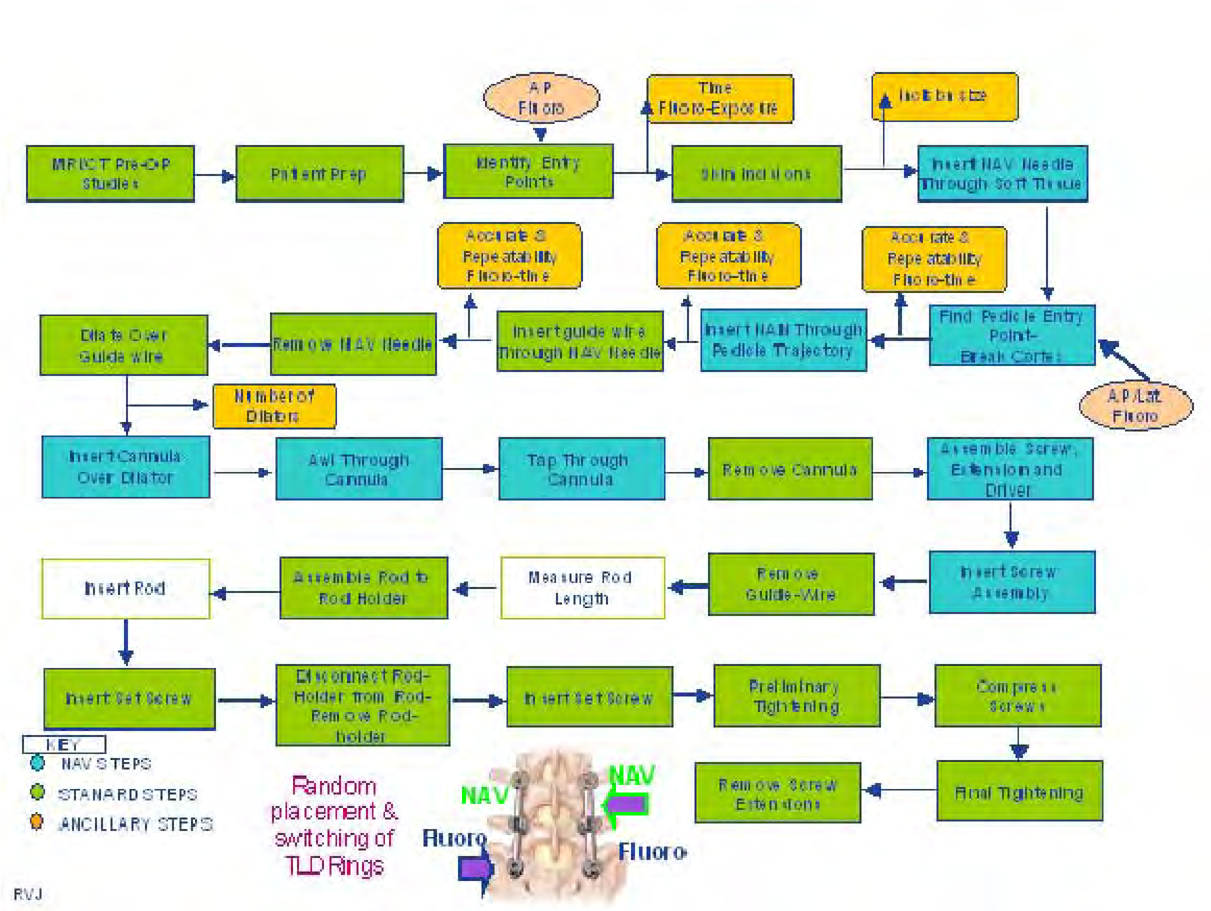

Figure 9.2 Workflow chart demonstrating intervals between navigation and conventional pedicle fusion steps.

The S1 level was allocated to either the Nav or Fluoro group on an alternate basis to ensure the numbers for this level were even between groups. All other levels were randomly allocated starting at L5 and moving upward based on a coin flip. The EMF transmitter was placed on the spinous processes of the levels noted above, and images centered on the vertebral body being instrumented were saved in both the anteroposterior (AP) and lateral views. K-wires were then placed percutaneously by using the 18-gauge (15-cm) Nav Access Needle mounted with the EMF receiver for the Nav vertebral levels and a standard conventional 18-gauge 6-inch (15-cm) Jamshidi needle for the Fluoro vertebral levels with live AP and lateral fluoroscopic images. With either pedicle screw system, a series of custom titanium dilators (Figure 9.3) were then used to place a plastic tubular retractor through which the custom MIS awl, tap, and finally the virtual navigation screw and extenders were placed as shown on the navigation control screen shots from each system brand of Zimmer (Austin, Texas-USA) or Innovative Spinal Technology (Mansfield, MA-USA) (Figure 9.4). In the Nav group, these were all placed using the specially designed EMF T-handle to accept the K-wires through a hollow core, which attaches to the individual instruments and allows real-time biplanar visualization of the trajectory and progress of the awl, tap, and screw. We used the standard fluoroscopic technique in the Fluoro group. Once inserted, our screw extenders were removed without rod placement and the screws were left in place for subsequent CT scan evaluation.

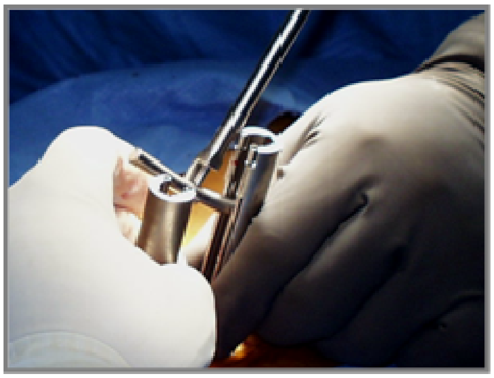

Courtesy of Abbott Spine, San Antonio, TX

Figure 9.3 Low-ferrous titanium dilator sleeves are used with the navigation system through which the percutaneous rod insertion technique is accomplished.

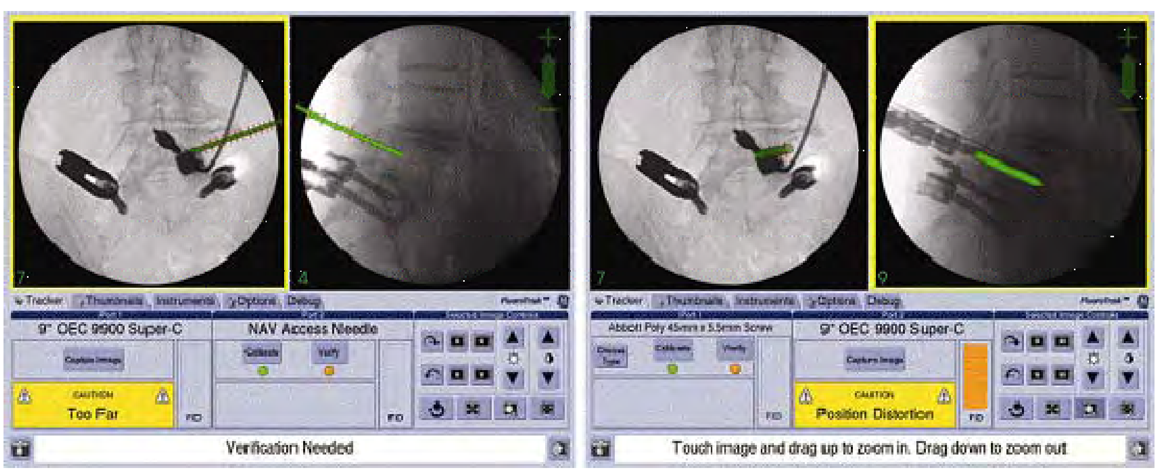

Figure 9.4 Fluoroscopic navigation screen shot demonstrating the navigated instruments in AP and Lateral views of the lumbar spine. The left images demonstrate navigated percutaneous instrument cannulation of pedicles. The x-ray images at the right demonstrate the navigated pedicle screw insertion and correlation with x-ray to access immediate accuracy and the EM field induced detector (FID) activated.

9.2.3 Outcome Measures

Intraoperative measured variables included set-up time, insertion time, fluoroscopy time, and radiation exposure as detected by hand and ring thermoluminescent dosimeter badges. Insertion time measurements included set-up and initial image capture time for both Nav and fluoro groups. Post-procedural CT scans were performed on each specimen and each screw was assessed for pedicle breach, vertebral breach, critical breach, and ideal trajectory. The ideal trajectory is considered to be a convergence of the pedicle screws at the ventral aspect of the vertebral body that stays within the pedicle. We used this 4-point scale below for grading:

Grade 0 (Ideal) – accurate screw with no perforation through any cortex

Grade 1 (Minimally displaced) – safe screw with perforation of <3 mm

Grade 2 (Moderately displaced) – displaced by ≥3 mm but ≤5 mm

Grade 3 (Critical perforation) – displaced by >5mm

The accuracy of each technique over each spinal zone (thoracic, lumbar, and sacral) was statistically analyzed using a chi-square test with p= 0.05 considered significant.

9.3 Results

In total, we placed 122 pedicle screws, 62 under fluoroscopic guidance and 60 under EMF guidance. Seventy-eight of these were lumbar pedicle screws, 28 were thoracic, and 16 were sacral.

Accuracy of placement over all segments, as assessed by pedicle and vertebral body breaches, was better in the EMF group than in the fluoro group, but this difference was not statistically significant: Pedicle breaches were seen in 17% of EMF-placed screws and 29% of fluoroscopically placed screws (p=0.12) while vertebral body breaches were seen in 1.7% of the EMF-placed screws and 4.8% of the fluoroscopically placed screws (p=0.33). Accuracy of placement of lumbar pedicle screws was significantly improved with the use of EMF (16.2% pedicle breach vs. 42.5% with fluoroscopic; p=0.01), but there was no significant decrease in cortical breaches with the use of EMF in the thoracic or sacral regions.

Ideal trajectories were achieved more often with EMF guidance over all spinal segments (62.7% vs. 40%; p=0.01). This effect was most pronounced in the lumbar segments, where 64.9% of screws placed with EMF guidance achieved ideal trajectory versus 40% placed with fluoroscopy (p=0.03). There was no significant difference between the two techniques over other segments.

Our insertions times, including set-up time, between the two techniques did not significantly differ overall for the two groups (923 seconds with EMF vs. 952 seconds with NAV; p=0.6911), and this was also true for any spinal segment that we analyzed separately. Radiation time, however, was significantly reduced over all segments (5 seconds with EMF vs. 22 seconds with Fluoro; p<0.0001). Highly significant reductions in radiation time were seen over all spinal segments upon individual analysis.

Total body and hand radiation doses experienced by the operating surgeons were decreased with the use of EMF, although these results were just less than significant (13.8 vs. 20.2 mrem, p=0.073 and 15.0 vs. 37.5 mrem, p=0.058, for body and hand, respectively). Of note, all surgeons tended to take a step away from the fluoroscope during image acquisition for both the Nav and Fluoro groups, and this is a reflection of their experience using fluoroscopy.

9.4 Discussion

Minimally invasive approaches to the spine place heavy demands on x-ray image guidance. Traditional fluoroscopic guidance is suboptimal for many of these approaches as it requires frequent rotation of the fluoroscope for biplanar views and exposes the surgeon, patient, and staff to potentially harmful amounts of radiation. Stereotactic computer-guided navigation technology promises to lessen the radiation burden and provide real-time biplanar views but has not yet been widely adopted, primarily because of concerns regarding ease of use and additional operating time and cost. The results of this study demonstrate that surgical EMF navigation significantly increases the overall accuracy of pedicle screw placement compared with fluoroscopic navigation over the treated levels (T8-S1). Subgroup analysis revealed a highly significant increase in accuracy in the lumbar spine. This is particularly notable since it is sometimes thought that guidance is unnecessary in this region given the larger pedicle size, increased margin for error, and more consistent anatomy.[16,17] Significant gains in accuracy with guidance in the lumbar spine have been demonstrated in a recent, large meta-analysis.[118] Navigational guidance should, therefore, be considered a valuable tool, even in the lumbar region, and this effect should be magnified when dealing with revision surgery or deformity.

9.4.1 Cortical Breach Measurement Methods

Accuracy of pedicle screw placement in this experimental study was measured by assessment of cortical breach in both the pedicle and vertebral body as well as by subjective assessment of ideal trajectory. Cortical breach has been the most commonly used measure in determining pedicle screw accuracy,[118] but there is significant variability in the definition of these findings in the literature, making comparisons between series difficult. Kosmopoulous and Schizas[118] reported on the use of 35 different methods of assessment in their meta-analysis and noted that approximately 50% of studies making claims about the accuracy of placement did not clearly define how accuracy was assessed. Even when cortical breach is used as a parameter, considerable variation exists between studies. Some authors have reported only a cortical breach of >2 mm and others reported only on the direction of breach.[118,171] The assessment of cortical breach is straightforward on post-procedural CT scans and should represent a minimum-reporting requirement to serve as a basis for comparison between studies. The amount and direction of breach are secondary measures that may have significance in relation to the potential of neural injury.[187]

9.4.2 Workflow Times

Time for insertion with the EMF technique did not vary from that of the standard fluoroscopically guided technique in the current study. This result is underscored by the fact that the version of the navigation system in this study was new to all participating surgeons. Thus, all were at the start of the learning curve and even faster operating times could be expected with further familiarity with the navigation system. Although increased speed has not been shown in other studies, this can be a reasonably expected byproduct of navigation because manipulation of a fluoroscope during surgery can be time consuming, especially in minimally invasive surgeries that require AP and lateral imaging for each level. Elimination of the required movement of the fluoroscope around the operative field should also reduce the potential for contamination of the operative field and concern for infection. Additionally, simultaneous viewing of both AP and lateral projections can help facilitate the placement of percutaneous screws.

9.4.3 Additional Outcome Measures

An additional outcome measure in this experimental study was total fluoroscopic time and total radiation exposure. Although the reduction in fluoroscopic time with EMF was highly significant, the reduction in radiation exposure did not quite achieve statistical significance. This is likely due to each operator's habit to back away from the fluoroscope with each exposure, which may provide some protection to the surgeon. Total fluoroscopic time and radiation exposure are directly related and any reduction in exposure time should be significant for the patient and the operating room staff. These exposure times were not evaluated in the study. This finding holds special implications for the spine surgeon, as radiation exposure in spinal surgery has been demonstrated to be 10–12 times that of other musculoskeletal surgeries and has the potential to exceed recommended yearly allowances.[165] Factors unique to spine surgery that may contribute to increased exposure include the increased penetrating beam energy requirements to image the spine adequately,[136] increased proximity of the surgeon's hands to the field (which may be exacerbated by the need to maintain alignment of instrumentation), increased Compton scatter at the beam entry site, and the frequent necessity of having either the surgeon or assistant standing next to the beam generator.[165] Furthermore, poor technique in which the hands are directly irradiated can dramatically increase exposure to as high as 4000 mrem/min (recommended yearly hand allowance is 50,000 mrem).[143] While the consequences of chronic radiation exposure are, as yet, unknown, the increasing exposure beyond recommended limits is certainly a cause for concern.

9.4.4 Conclusions

The use of Stereotactic computer-assisted EMF navigation for the insertion of pedicle screw instrumentation was found to increase overall accuracy without any demonstrable change in surgical time. A significant reduction in fluoroscopic time was also noted in the EMF navigation group and we believe this should be an important factor in considering the adoption of this technology for spinal instrumentation cases.

CHAPTER 10. SPINE EXPERIMENT 7: NAVIGATED 3D FLUORO VERSUS 2D NAVIGATED FLUORO VERSUS NON-NAVIGATED FLUORO

10.1 Introduction

Minimally invasive techniques for pedicle screw insertion have recently been advanced with the potential advantage of minimizing morbidity of paraspinal muscle denervation and devascularization as seen with open techniques. Conventional fluoroscopy is a familiar technology to surgeons but has limitations of radiation exposure to patient and staff and need to reposition the fluoroscope repeatedly to obtain adequate image guidance. Optical-based virtual fluoroscopy provides virtual images of the spine based on “captured” fluoroscopic images. Potential disadvantages of this technology are increased registration time associated with line-of-sight technology and the absence of CT images, which provide coronal and axial images of the spine.[35,61,139] We experimented with a new technology we created that generates a virtual CT scan from images captured on a fluoroscope axially rotated around the patient at the time of surgery.

10.2 Aims

We set out to perform an in vitro assessment of our EM-based computerized fluoroscopy system, which creates a virtual CT scan image for a minimally invasive surgical technique used for pedicle fixation using special software we developed. We compared the speed, accuracy, and radiation exposure to conventional fluoroscopy and assessed the image quality of the reconstructed CT-like orthogonal images. We wanted also to see how triplanar axial spinal views can improve the placement of pedicle screws over our previous biplane experiments in the spine.

10.3 Materials And Methods

At the Cedars Sinai University Hospital in Los Angeles, forty-eight pedicles (T11-S1) in three intact unenbalmed human cadavers were randomly assigned to undergo paired percutaneous pedicle instrumentation using a lighted dilating bivalved endoscopic assembly (based of the Jakoscope concepts first applied in spine by Howard-Jako in

1992) via conventional fluoroscopy, virtual fluoroscopy, or our 3D C-arm fluoroscopy method (Figure 10.1). After attaching our EM transmitter to the spinous process, fluoroscopic images were obtained, calibrated, and saved. Paired insertions of two adjacent pedicle screws for a single-level fusion were compared side to side from T11 to S1 using the three imaging techniques. Side-to-side comparisons were made between standard fluoroscopic technique on one side and either virtual fluoroscopy or the 3D fluoroscopy technique on the other side (Figure 10.2). Operative time from skin incision to completion of pedicle screw insertion was measured as well as fluoroscopic time. The 3D fluoroscopy images were also obtained after pedicle insertion and compared with virtual CT images. The specimens were subsequently checked for accuracy by comparing dissecting specimens under 2X magnification to evaluate for pedicle wall perforation.

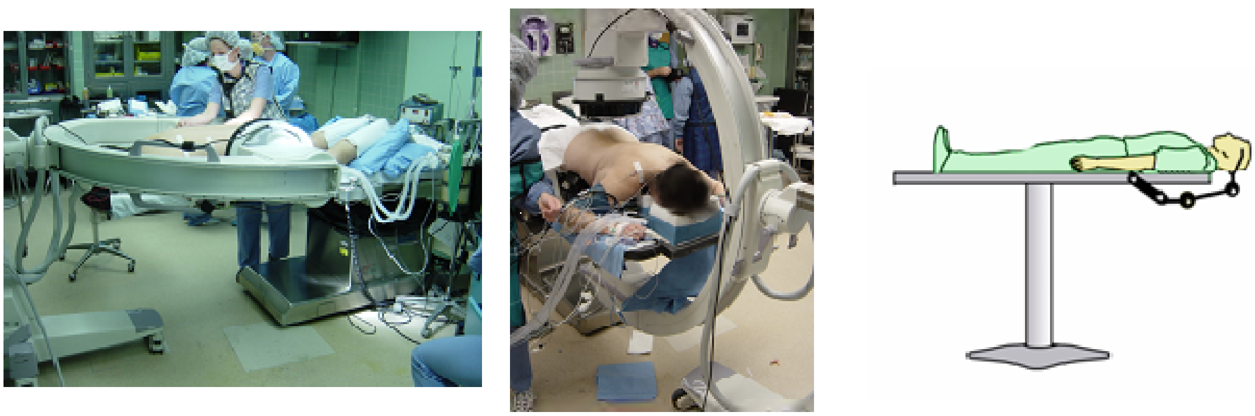

Figure 10.1 Demonstration of the C-arm set-up for 190-degree rotation from lateral to contralateral position using a cantilevered table.

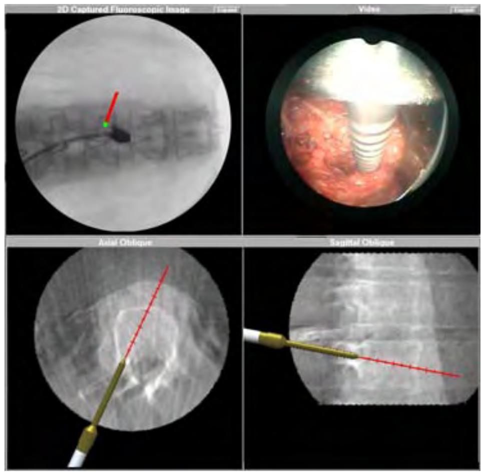

Figure 10.2 A navigation screenshot of the 3D C-arm demonstrating axial, sagittal and the anteroposterior views of the virtual pedicle screw placement correlated with the endoscopic view.

10.4 Results

The operative time using standard fluoroscopy was 40 minutes (30–65 minutes); virtual fluoroscopy was 35 minutes (15–66 minutes), and 3D fluoroscopy was 38 minutes (29–50 minutes). Radiation time was 90 seconds (36 seconds–3 minutes) for standard fluoroscopy, 11 seconds (2–30 seconds) for virtual fluoroscopy, and 30 seconds for the 3D fluoroscopy group (Table 10.1). The 3D fluoroscopy group takes 30 seconds to sweep through a 180-degree arc and takes approximately 90–120 seconds to render reconstructed axial, sagittal, and coronal images, down from the original 3–4 minutes with our version 1.0 algorithm. The poor images due to image scatter from vibration or artifacts are automatically ejected by the computer's 3D image quality software. This time was not counted toward the operating time, as this would occur while the patient was being anatomically prepared for surgery. The 3D fluoroscopy had to be recalibrated once during our experiments as a result of a loosening transmitter pin from the osteoporotic spinous process. We had the option to use transmitter clamp for the spinous process, but wanted to keep the incision length to a minimum. The mean trajectory angle difference between virtual and fluoroscopic displayed probes was 3.1 degrees ± 0.9 degrees. The mean probe tip error was 0.99 ± 0.55. There were no pedicle wall perforations using standard fluoroscopy, the 2D fluoroscopic navigation, or the 3D fluoroscopic navigation (Figure 10.3).

Table 10.1 Operative time for standard fluoroscopy and virtual fluoroscopy.

Image Mode	Time (min)	Fluoro Time
Straight Fluoro	40 min range (30-65)	1:30 range (:36-3:00)
Virtual Fluoro	35 min range 15-66	11 secs rnage (2-30 secs)
FluoroCT	38 min range (29-50)	30 secs range (2-3 min rendering)

Accuracy was verified in all groups. Radiation time was significantly longer in fluoroscopy group. FluoroCT appears to add accuracy regarding the medial wall.

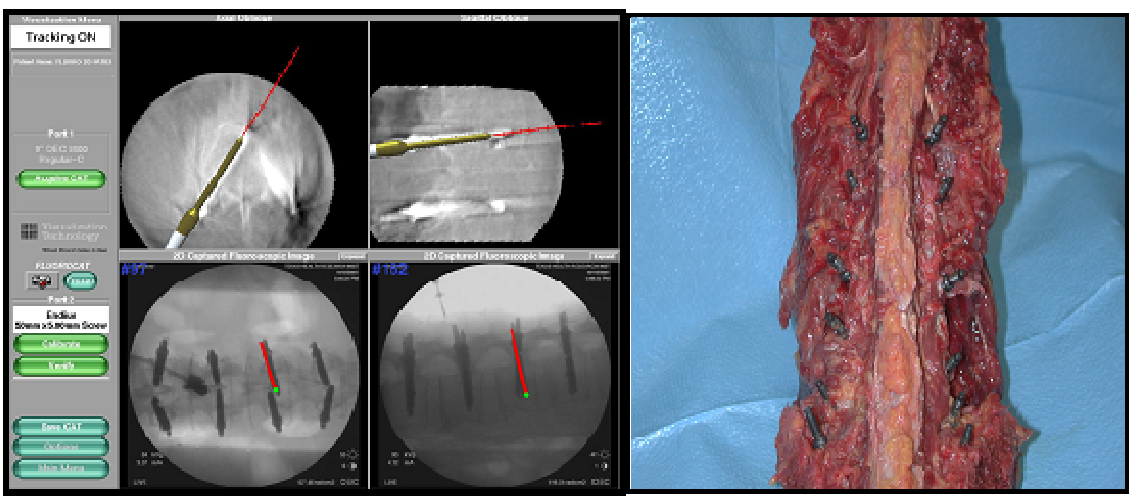

Figure 10.3 Accuracy verification of the virtual instrument lines correlated with the implanted pedicle screws (left). RVJ harvested the lumbar spine with the implanted pedicle screws (right).

10.5 Discussion

This experiment evaluated electromagnetic 2D virtual fluoroscopic navigation and 3D fluoroscopic navigation scans for pedicle screw insertion. This technique differed from optical based virtual fluoroscopy published by Foley et al.[60]

10.5.1 Conclusion

We observed excellent correlation between 2D virtual fluoroscopic navigation, 3D fluoroscopic navigation, and conventional fluoroscopy. The EM-based navigational technique associated with percutaneous pedicle instrumentation of the thoracolumbar spine appears to be associated with a significantly decreased amount of radiation exposure compared with conventional fluoroscopy.

CHAPTER 11. SPINE EXPERIMENT 8: STEREOTACTIC CT SURGICAL NAVIGATION EXPERIMENTS FOR LASER DISCECTOMY

11.1 Introduction

Surgical application of lasers was first developed in the larynx. Jako first applied a pulsed neodymium (Nd):glass laser (1064 nm) in 1965 and then used the carbon dioxide continuous wave (CW) laser (10.6 nm) in 1966 (Figure 11.1) on cancerous human laryngeal specimens before developing the field of laser microsurgery for clinical applications in patients.[93,94,20240,41,80]. In the 1970s, the continuous-wave Nd:YAG (neodymium-doped yttrium aluminium garnet) laser (1064 nm), which allowed the use of quartz fiber waveguides for delivery, became available. In 1986, Choy proposed applying the Nd:YAG laser for coagulating intervertebral disc hernias.[42-45]. Choy and Ascher began the clinical application of the new concept of minimally invasive laser treatment of disc pathology.[14,15]

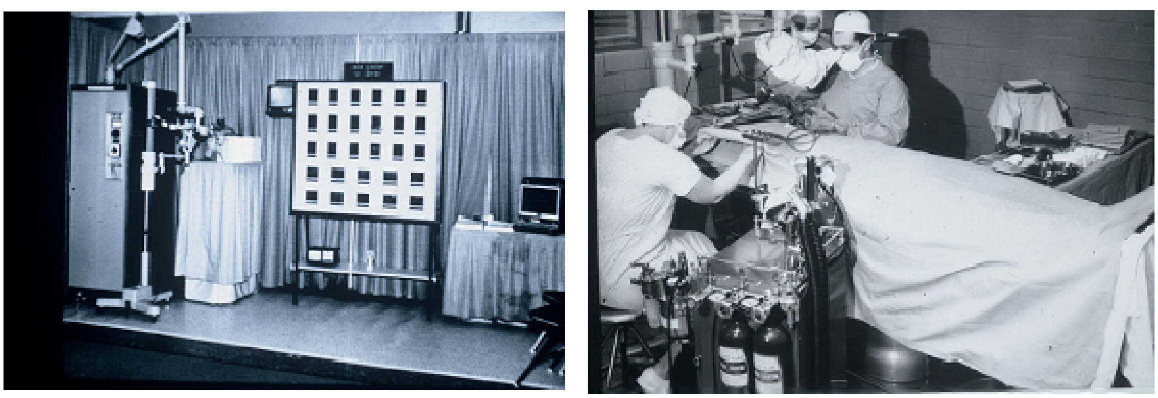

Figure 11.1 First laser surgery exhibit and microscopic operation of the soft tissues by G. Jako in the 1960s.

During the past two decades, numerous minimally invasive surgical techniques combined with different wavelengths of lasers have been used worldwide for total or partial removal of disc disease. Experimentally and clinically, the Excimer, KTP 532, Nd YAG,[42-45] Holmium YAG, Erbium YAG, and $C0_2$ [32-34,38,49,81,126,148,169,193,225,228,229] lasers have been used in laser surgery, but these lasers are rather cumbersome and expensive. Therefore, in recent years, innovations and technical developments of high-output infrared diode lasers at different wavelengths have come to the forefront of lasers in medicine. These infrared wavelengths can also be delivered through quartz fiber waveguides.

In this preclinical study, we used the high-output Biolitec (Jena-Germany) clinical diode laser apparatus at 980-nm wavelength. Laser evaporation is used for decompression of the disc pressure by coagulation and evaporation of disc nucleus material. To deliver the laser radiation, a laser fiber is inserted through a thin trocar into the disc with the assistance of x-ray imaging. Pre- and intraoperative localization with a C-arm image intensifier is routine and popular, but the exposure of both patients and staff to radiation each time a new x-ray view is required is a disadvantage and the use of the C-arm may be a time-consuming and potential aseptic concern when moving between new angles for x-ray viewing. Because of these and other limitations associated with x-ray imaging, the use of stereotactic computer-assisted surgical navigation offers an alternative. It presents preoperative images to the surgeon that can be used for multiplanar, 3D tracking, which has been demonstrated to increase safety in a variety of spinal procedures in preclinical and clinical studies. In addition, surgical navigation on preoperative 3D images may provide a more accurate and expedited placement of the special spinal trocar by minimizing the neurovascular injury and complications from a prolonged complex procedure.[75,86] Finally, surgical navigation can minimize ionizing radiation exposure from intraoperative C-arm fluoroscopy.[182,212]

11.2 Aims

Our goal was to demonstrate the use of computer navigation to track the 980-nm solid-state diode laser beam delivered through fiber optics for transcutaneous laser discectomy. The secondary goal was to improve the placement of a custom-navigated spinal trocar through the critical triangular zone of vessels and nerves into the intervertebral space for debulking of disc material with greater precision of preferably 2 mm or less.

11.3 Materials And Methods

11.3.1 Cadaver Material

Two ex-vivo porcine lumbar spines were obtained and used according to the policies of the University of Kaposvar Medical Center’s Institutional Review Board. The fresh specimens were from two 80-kg swine and were prepared with intact soft tissues, paraspinous muscles, and skin. The porcine spine has six lumbar vertebrae; we experimented on six intervertebral discs for each of the two specimens for a total of 12 discs.

11.3.2 Laser

High-intensity, small-size clinical laser equipment with fiberoptic guides manufactured by Biolitec AG (Jena, Germany) was used for this study. The Ceralas D 25 model delivers up to 25 W of laser power. Its wavelength is 980±10 nm, which is close to the wavelength of the Nd:YAG, and its water absorption is also similar. The manufacturer provides 200-, 400-, and 600-µm diameter quartz fiber waveguides. For the delivery we used the 400-µm guide. The fiber was inserted into a custom-made 17-gauge, 300 series stainless steel trocar (laser fiber tube) designed by the authors (Figure 11.2). This was subsequently introduced into the navigation trocar (Nav Trocar) designed by the author (RVJ) and integrated with an electromagnetic (EM) tracking receiver[212] The laser fiber trocar tube has a side connector, which is attached to an aspirator to eliminate evaporation plumes produced by the laser irradiation.

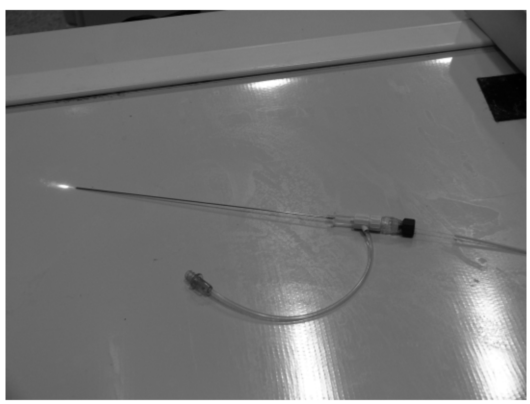

Figure 11.2 Photograph showing laser trocar and fiber, which is illuminated with a red pilot beam.

.

11.3.3 Surgical Navigation Equipment And Instrumentation Method

We used a computer-assisted surgical navigation system with its accessories. This system uses the preoperative computer tomographic (CT) scan and EM tracking technology to provide positional feedback of an instrument's location and orientation within a given anatomy (Figure 11.3).

Each swine specimen was placed into a plastic basket in the prone position and scanned using both CT and magnetic resonance (MR) imaging to obtain the preoperative scans for registration.

Figure 11.3 Left palate demonstrates the pre-operative CT and the right palate demonstrates pre-operative and post-operative MR assessment of the intervertibral discs.

The navigation computer compiles the anatomical image data from the CT scan through an Ethernet connection between the CT suite and the operating room and renders three orthogonal planes (axial, sagittal, and coronal views), as well as a 3D reconstructed model of the spinal segments and an optional endoscopic view.

To align the x-ray images to the specimen, the process of registration matches the preoperative CT image data (virtual) to the physical space occupied by a specimen or patient during surgery. The accurate registration (i.e.,, alignment or matching) of these two data sets subsequently allows localization of the surgical instruments within the operative space. Two methods for this registration exist. One includes a manual and invasive method, which requires anatomical points to be localized directly from the exposed spine. The second method, used in our experiment, includes external markers automatically detected on the CT that are affixed to the spine surface region and used for autoregistration. These can be bone-anchored markers or radiopaque intact-skin-affixed fiducials placed before CT imaging and used until registration is complete. A percutaneously mounted (EM) transmitter affixed directly to the spinous process[53,181,191] was used for this study to maintain registration accuracy by compensating for movement of the spine (Fig. 11.4).

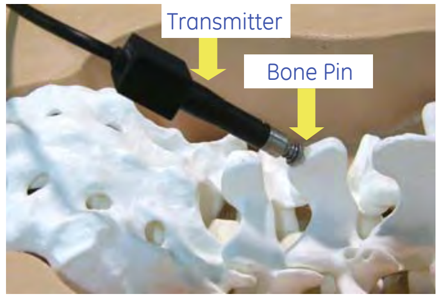

Figure 11.4 Photograph demonstrating the placement of the EM transmitter to the spinous process via a 2mm Caspar-style bone pin.

Recently, a new autoregistration system is improving speed and ease of use by facilitating the employment of an intraoperative C-arm and algorithm to register the CT images. Once the process of registration is completed, the navigation instruments are calibrated and verified so that surgical navigation can begin. The tracked surgical position of an instrument is then correlated on a 20" interactive flat-panel monitor with four visual quadrants that depict the preoperative CT scan images in three dimensions, including a displayed reconstructed 3D model of the spine. Any of the four visual quadrants can also be substituted with a spinal endoscopic view in procedures using an optical telescope.

The EM tracking system uses a radiofrequency EM transmitter and an EM receiver. It relies on detecting the EM field at the receiver relative to the transmitter. It responds to variations within the detected EM field caused by movement of an instrument or the patient.[63] The system consists of an anatomically placed reference transmitter percutaneously affixed to the spinous process by a 2-mm bone pin and a receiver placed on the surgical instrument, or in this case integrated with the Nav Trocar.[31,56,63] The sensors provide positional (X, Y, Z) information, which correlates the movement of the Nav Trocar to the preoperative CT images displayed on the interactive monitor.[31] The Nav Trocar is calibrated to show the tip position with respect to the CT images. The processing unit determines the surgical instrument's location relative to the surgical anatomy and displays on measured crosshairs a linear trajectory of the instrument in triplanar views, providing anatomical orientation to critical neurovascular structures.

Preoperative CT radiologic evaluation of the two porcine lumbar spines showed a narrower than human, but still accessible, disc approximately 3 mm in thickness. Access techniques to the lumbar discs with radiographic landmarks have been well described in previous publications.[102] In this study, the intact fresh specimens were positioned prone on a low-ferrous radiolucent surgical table. Using the CT data on the navigation screen in preoperative planning mode, the target and entry points were plotted by placing a digital marker or seed at both the surgical entry point (specimen CT skin surface) and the target end point (CT intervertebral disc space). The navigation computer then plotted and saved the measured optimal trajectory through the triangular safe working zone between the traversing and exiting nerve roots of the foraminal annular window. The calculated path centered within the mediolateral aspects of the pedicle and intervertebral disc space. This was represented as a dotted color trajectory on the navigation display monitor (Fig. 11.5).

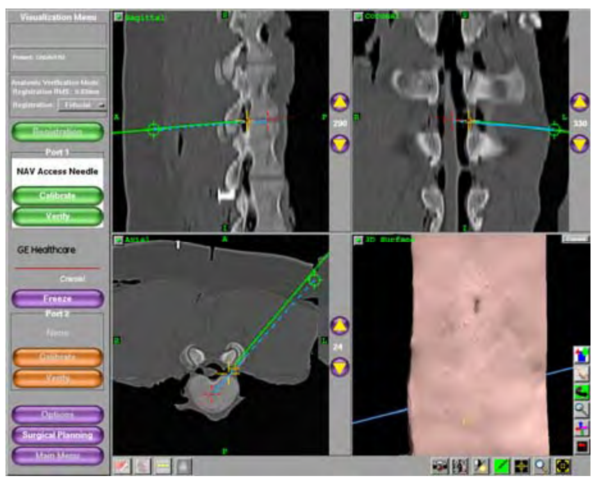

Figure 11.5 Nav screen shot showing the virtual trocar trajectory from the skin entry point to the nucleus.

Intraoperatively, the navigation trajectory was then enabled in real time to project and look beyond the virtual trocar tip into the specimen's CT slices at adjustable depths. We confirmed measurements starting at the level of the skin window and marked by a surgical pen and ruler to the corresponding anatomic target center of each disc level. At this point, a small dermal stab incision and infiltration of the subcutaneous tissue layers and muscle was made with the 18-gauge, 6-inch Nav Trocar. The tip was then retracted into its sleeve to shield against inadvertent contact with the nerve or dura as it was guided over the predetermined length of the target path at a 30- to 60-degree angle depending on anatomy. This was displayed on the workstation as traversing Kambin's triangle toward the dorsolateral aspect of the intervertebral disc.

The size of each small triangular zone decreased slightly at higher levels. Minor adjustments were made at each disc level for variations in the porcine anatomy to be parallel with the disc axis and as close as possible to midway between the superior and inferior endplates. At the point of contact with the spring-like posterior annular surface, the cannula was adjusted to reintroduce the trocar tip to penetrate the complete annulus. C-arm control shots were taken occasionally to correlate and measure tracking accuracy. The Nav Trocar was advanced 0.5–1.0 cm into the center of the spongy gelatinous-like disc nucleus. Once in position, the stylet was removed from the Nav Trocar, leaving a clear work channel to the disc space. The laser fiber with tubing was then inserted through the Nav cannula, and the laser irradiation was started. Various amounts of laser energy were delivered and calculated in joules.

11.3.4 Accuracy Measurement

Two methods were used to quantify the system tracking accuracy for this study. The first method uses a feature available on the navigation system in which a 3D point on the preoperative CT scan is identified and the distance from the navigated trocar tip to that anatomical point is measured. This distance is a measure of the accuracy error of the system when the navigated trocar tip is placed at the anatomical location (i.e.,, 2-mm spinous process fiducial pin, OsteoMEd®, Addison, Texas; mediolateral aspects of the pedicle; or the edge of the vertebral body) that corresponds to the 3D point identified previously. This method was used to quantify system accuracy with the surgical target point and is used once the trocar has reached the target point of the outer annulus and center of the intervertebral disc.

The second method used in this study to quantify system-tracking accuracy involved placing the navigated trocar in the inner-annular-nuclear junction of the target disc. A fluoroscopic control shot was taken on the C-arm to verify the placement of the trocar on the anatomy and correlate this location on the fluoroscopy to the preoperative CT to determine the same anatomical location on the CT scan displayed on the navigation system (Fig. 11.6). The distance from the navigation system's display of the virtual trocar tip overlaid on the CT to the identified anatomical location on the CT scan was estimated by using the 1-mm tick marks on the virtual trajectory of the trocar. This commensurable method was used to estimate accuracy multiple times as the Nav Trocar was advanced through the triangular working zone proportionally with spot fluoroscopy.

Figure 11.6 Photograph demonstrating the lab setup with the specimen undergoing C-arm correlation to the navigation and the laser setup at bottom right corner of photo.

In each irradiation, 20W repeat pulses were applied. In specimen 1, L1-L6 received the same laser irradiation doses. In specimen 2, L1-L6 discs received incremental laser irradiation (Fig. 11.7). Other than a few scout or control shots to correlate accuracy, the Nav Trocar can be guided without the need of repetitive C-arm fluoroscopy, minimizing exposure to intraoperative scatter of ionizing radiation.[56,63] Postoperative MR imaging was undertaken for comparison with preoperative MR images. The access to a veterinary research center equipped with CT scanners and MR suites specifically for animal studies as well as state-of-the-art mobile and ceiling-mounted C-arm fluoroscopes enabled the precision analyses of these animal specimens.

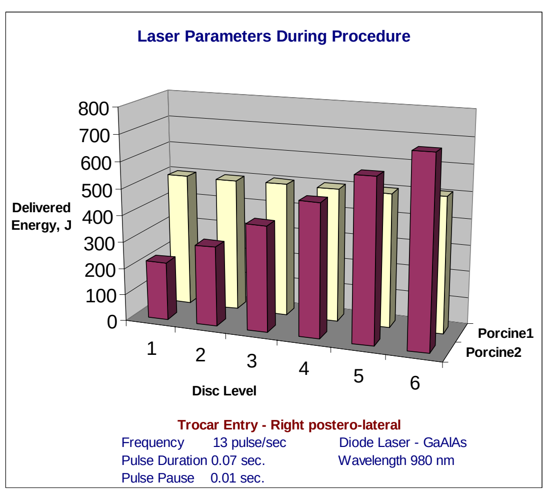

Figure 11.7 Graph demonstrating the laser energy mapping in the porcine specimens.

11.3.5 Preparation Of The Lumbar Spine And Disc Material

After the laser irradiation and CT and MR documentation, the lumbar intervertebral discs from each specimen were harvested and dissected (Fig. 11.8). Since the porcine disc is narrow, the discs were cut in half and photo-documented. Using a plastic template, same-size specimens from each intervertebral disc were excised for histological examination. The specimens were carefully numbered according to the irradiation doses. The material was placed in 10% buffered formalin solution. Routine histological preparation with hemotoxylin-and-eosin staining was used, and 10-µm sections were cut from the paraffin-embedded material.

Figure 11.8 Photo demonstrating the harvested spinal segments from the porcine specimen.

11.4 Results

Monitoring of a needle trocar is essential during percutaneous laser discectomy and the use of CT in this experimental study provided superior spatial and soft tissue resolution to that of the single-plane C-arm fluoroscopy views. The additional spatial configuration data provided by CT navigation facilitated the puncture position of the navigated trocar tip on axial and sagittal images, enabling for precision laser ablation of the intervertebral disc. We determined that the Nav Trocar was inserted into the intervertebral disc accurately with the aid of the computer-assisted surgical navigation system with 1.0–1.5 mm total system tip-tracking accuracy confirmed by spot x-ray fluoroscopy and further measured by the “distance from trocar” feature available on the navigation system.

The navigation computer also provided a registration root mean square (RMS) error of 0.50 mm and 0.80 mm in the two specimens using external fiducials. The postoperative MR study showed changes in the disc compared with images obtained before laser irradiation. Post-dissection macroscopic examination demonstrated that the insertion of the Nav Trocar was in the intended target area of the disc as planned by the computer software and correlated with low-dose pulse x-ray shots. Under magnification, visual dissection of the lumbar vertebrae showed no evidence of disruption to the adjacent nerve root and visceral or vascular structures. Furthermore, the microscopic examination revealed tissue coagulation changes in the uniformly and in the gradually irradiated discs (Figure 11.9). Total scout x-ray control time recorded for anteroposterior and lateral views on the C-arm for each disc level averaged less than 9 seconds. In this experimental study, our intention was not to evaluate quantitatively the effects of the disc irradiation, only the precision of the laser trocar insertion.

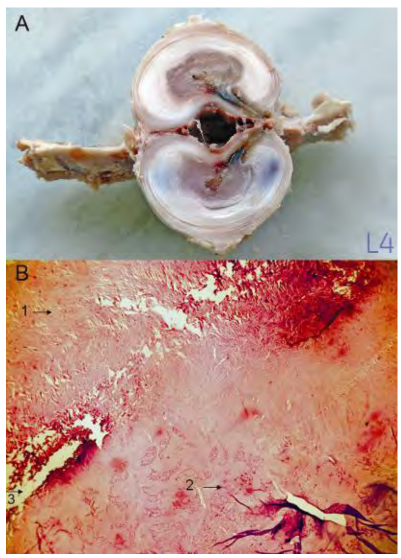

Figure 11.9 (A) Photograph showing macroscopic section of the vertebral level butterflied open with a visible Nav trocar channel and the irradiated nucleus pulposus matching the x-ray images. (B) Photomicrograph depicting at bottom the annulus fibrosus (1) and at top the nucleus pulposus (2). Between the two components the Nav-laser trocar channel (3) is clear, with the coagulation borders of the nucleus pulposus created by the thermal ablation procedure.

11.5 Discussion

The precision and accuracy demonstrated in this study indicate that my navigation trocar could be used to deliver other forms of percutaneous coagulating-ablating energy, such as CO_2 laser transmission with the new OmniGuide® flexible and hollow optical fiber,[92] intradiscal electrothermy, and plasma disc decompression with the coblation nucleoplasty® technique.[40,50,156,189,195,219] It is anticipated that newer tracking systems and further research will yield additional improvements and capabilities to deliver various types of laser energy to spinal surgery with the aid of computer-assisted surgical navigation.

11.5.1 Conclusion

We found that electromagnetic computer-assisted CT navigation can permit high-quality images for a safe, accurate puncture of the special laser Nav Trocar into the porcine intervertebral disc space and, other than for a few optional fluoroscopic confirmation shots to gauge system accuracy, its use obviates the need for continuous intraoperative C-arm fluoroscopy. As the technology advances, future expanded studies with larger sample sizes will help to further confirm these results and demonstrate clinical utility among interdisciplinary spine specialists.

CHAPTER 12. ORTHOPEDIC EXPERIMENT 1: FEMORAL/HIP FRACTURE FIXATION IN CADAVERS

12.1 Introduction

Fractures of the proximal femur, acetabulum, and pelvis are relatively common injuries in adults. Approximately 300,000 hip fractures occur annually in the United States, the vast majority requiring operative stabilization (American Association of Orthopedic Surgeons, Rosemont, IL). Hip fractures (intertrochanteric and femoral neck fractures) account for 30% of all hospitalized patients in the U.S., and the estimated cost for treatment is approximately $10 billion a year (Millennium Research Report, 2007, Toronto, Canada). Femoral neck fractures are increasing exponentially with the expanding general life expectancy. These fractures are associated with a substantial morbidity and mortality; approximately 15% to 20% of patients die within 1 year of fracture. In elderly individuals, most of these femoral fractures occur as a result of only moderate to minimal trauma, whereas in the young they are caused mostly by high-energy trauma. Femoral neck fractures and intertrochanteric fractures occur with about the same frequency and are more common in women than in men by a margin of 3 to 1.

Fractures of the neck of the femur have always presented great challenges to orthopedic surgeons and are said to remain the unsolved fracture as far as treatment and results are concerned. Since the first attempts in 1850 and with improvements with implant metal compatibility and X-rays after 1904, hip pinning has become a standard technique.

The technique for operative stabilization depends on the fracture pattern, but usually involves placement of one large compression hip screw (CHS) or three to four cannulated lag screws (CLS). Both procedures require frequent use of intraoperative fluoroscopy and image intensifier for placement of the guide wire, drilling and reaming, and insertion of the implant. The ability to use image-guidance (IG) and computer navigation would significantly decrease the radiation exposure secondary to fluoroscopy use.

12.2 Aims

We aimed to demonstrate the feasibility of stereotactic surgical navigation using fluoroscopy-based image guidance in the placement of cannulated lag screws in femoral neck fractures and intertrochanteric fractures in the region of the hip. We wanted to understand the practical needs to apply surgical navigation in the region of the proximal femur and to measure the accuracy of the screw placements, the insertion time, and the x-ray time between the navigation and conventional approach using fresh human cadavers.

12.3 Material And Methods

In August 2001, in the Pathology Department of Moritz Kaposi Medical Center in Kaposvar, Hungary I organized an investigational study in which we compared EMF-computer-assisted surgical navigation for the placement of 7.3 mm cannulated lag screws (CLS) in the proximal femora of five human cadavers with the use of fluoroscopic technique. Screws were placed on one side with standard technique using biplanar fluoroscopy and on the other side using navigation with EMF navigation. Left or right was determined randomly to void bias induced by the handedness of the surgeon.

The set-up time, total overall times, x-ray times, insertion times per method and side, and follow-up X-ray fluoroscopy accuracy assessments were all recorded as outcome measures.

We used three cannulated 7.3 x 1.10-mm lag screws (Figure 12.1) attached to a navigated custom Synthes hex-head driver made to be compatible with our navigated C-handle driver and receiver for distortion-free tracking. These were implanted bilaterally in each of the five cadavers for a total of 30 screws. We used a Synthes compact pneumatic drill for which we created a special adaptor for the navigational sensor to calibrate the drill for the cannulation of the femurs (Figure 12.2). With the drill, we used 2.8-mm guidewires. The Caspar-style bone pin can be seen in (Figure 12.3) of the x-ray attached to the proximal femur to which the reference transmitter is attached for automatic registration. (Figure 12.4) further depicts a multiplanar image for AP and lateral fluoroscopic images. In both x-ray planes, the virtual trajectory can be seen juxtaposed over the x-rays. The red trajectory line simulates the real-time position of the navigated instruments and/or implant. The extended green trajectory demonstrates a projection line forward into the bony anatomy. This can also be used to locate the proper skin entry and angle for drilling. These help obviate the need for x-ray and the time to acquire and maneuver between various x-ray images. Both virtual instrument lines are marked with depth markers to measure the length of the attached instruments or implant and the depth and direction into the given bone.

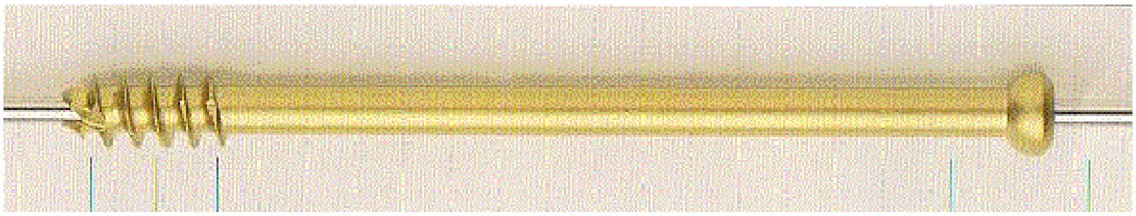

Figure 12.1 Photograph showing cannulated 7.3 x 1.10-mm lag screws.

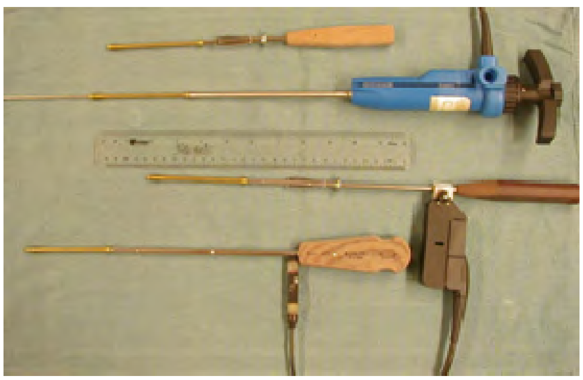

Figure 12.2 Photograph showing instruments I modified in a machine shop to be compatible with my navigation device and for use in facilitating the implant placement experiments.

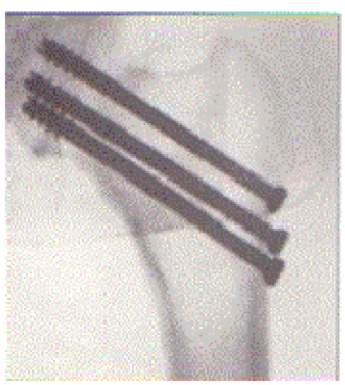

Figure 12.3 X-ray showing implanted cannulated lag screws.

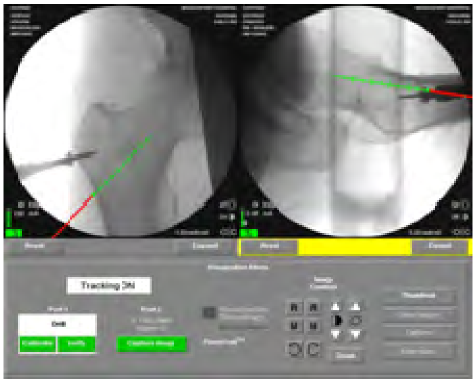

Figure 12.4 Screen shot illustrates virtual trajectory for the K-wire and lag screw path.

12.4 Results

We found that the transmitter is best located on the tip of the lesser trochanter (Figure 12.5) and that minimal EMF distortion from the drill occurs (Figures 12.4–12.14). All 30 cannulated lag screws were safely placed through the proximal femurs. (Figures 12.8 and 12.9) demonstrate the 2.8-mm cannulated T-handle receiver driving the custom Nav hex head Synthes cannulated screwdriver and the initial transmitter placement. Twenty-seven screws were accurately placed within 5 mm of the subchondral bone of the femoral head and 3 screws were within less than 5 mm of the subchondral bone but not intraarticular. All of the fracture lag screws were accurately placed. The C-arm Fluoroscopy time decreased from 53 seconds per side to 6 seconds per side.

Figure 12.5 Navigated Synthes drill insertion of the Steinman pins.

Figure 12.6 Alternating methods of navigation vs. non navigation of the proximal femurs.

Figure 12.7 EM sensor mounted and calibrated to the navigated Synthes pneumatic drill.

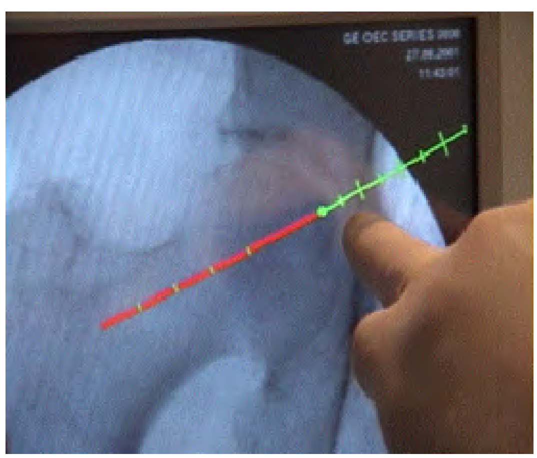

Figure 12.8 Virtual guidewire in red and extended tip projection in green providing the implant path.

Figure 12.9 Navigated and "cannulated" driver designed by RVJ.

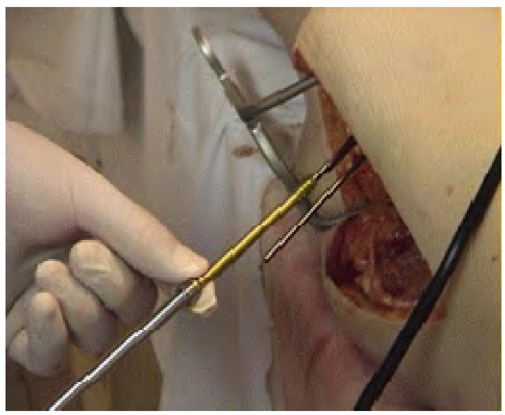

Figure 12.10 Navigated hex-head driving the 7.3mm x 110mm cannulated Synthes lag screw over guidewire.

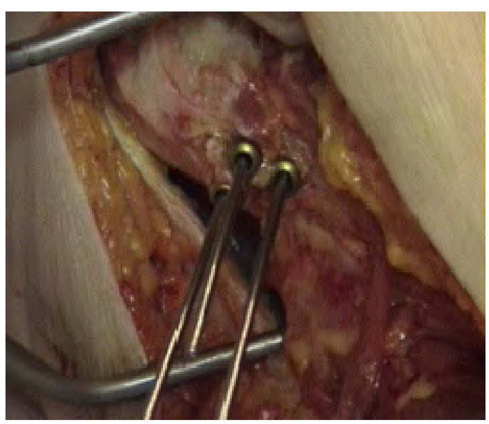

Figure 12.11 Final equidistant triangular positions of the titanium lag screws in the proximal femur.

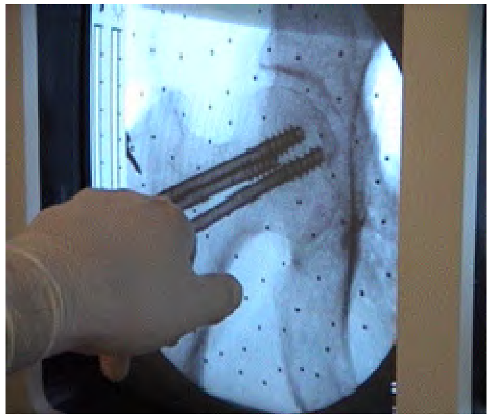

Figure 12.12 Fluoroscopic C-arm confirmation of the 3 lag screws correlated with virtual Navigation steps.

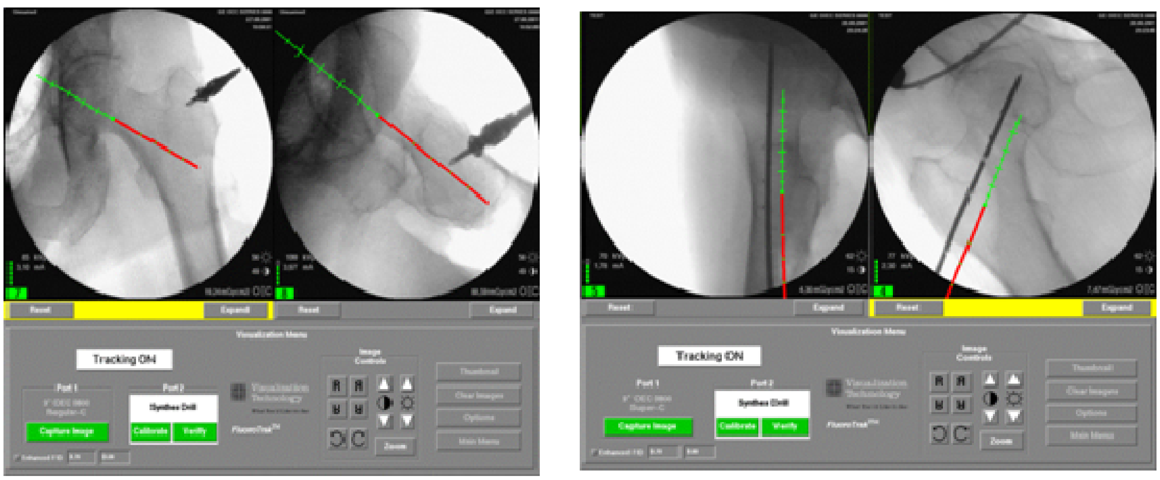

Figure 12.13 (A) Transmitter in greater trochanter and guided path; (B) saved trajectory line.

A simple guide tube for the 2- to 3-mm guide-wire was necessary (and necessarily made of plastic for EM compatibility). A tube with a concave serrated distal end was developed to reduce tissue trauma in the event of percutaneous placements. This helps to prevent bending of the wire when drilled into the bone. We found that a guide tube does not need to be tracked in the long run if there is a reliable and reproducible calibration and tracking accuracy for the powered or pneumatic drill. Our tracking of the drill provided the ideal information to the tip position whereas the tracking of only the guide tube gives only the entry point and estimated trajectory angle. However, the navigated guide tube is a simple option without a navigated power drill.

12.5 Discussion

In the U.S., there were almost 650,000 fractures of the proximal femur that required surgical intervention in 2006. Approximately one third of femoral fractures were treated with total joint replacements. Two thirds or 450,000 (2007 Medtech Insight IGS Report) are treated with internal fracture fixation using either cannulated screws or dynamic hip compression plates/nails. Internal fixation requires the use of an image intensifier to guide in placement of pins and/or screws. Emerging "less invasive" techniques are introducing percutaneous and small incision approaches to reduce bleeding, hospital stays, and outpatient recovery times.

Furthermore, there are 60,000 pelvic fractures annually. These fractures are the result of significant trauma and can be extremely debilitating and clinically challenging. Surgical goals using fluoroscopy are to restore near-perfect to perfect alignment and congruity of the joint surfaces. Only with accomplishment of the surgical goal can a patient hope to be restored to proper activities of daily living.

Approximately 10% of these fractures are currently navigated, primarily by optical tracking methods with inherent line of sight problems.[35,61,139] The standard fluoroscopy technique involves actively fluoroscope a patient while reducing the fracture, aligning any pins, drilling pins, or taps, and placing the screws. Confirmation shots follow placement. Total X-ray exposure time with this technique can vary, but tends to last minutes rather than seconds.[130]

As in the other procedures described in this paper, the introduction of EM navigation can eliminate the line-of-sight interference problems of the optical tracking methods[35,61,139] and provide future technology that can make sensors small enough to place on the guide wire for flexible tracking and for true percutaneous procedures as they further evolve.[226]

12.5.1 Conclusion

We demonstrated the feasibility of reducing radiation exposure to a patient and surgical team using the prototype instrument compared with current techniques for placing implants in proximal femur fractures. We showed that we could achieve accuracy equal to or better than current open/standard techniques for placement and implantation of medical devices and that insertion times were equivalent or better. The experiment demonstrated also that set-up times could be improved through refinement of instruments and techniques as expected in a natural learning curve.

CHAPTER 13. ORTHOPEDIC EXPERIMENT 2: CLINICAL INVESTIGATION OF FEMORAL/PELVIC FRACTURE FIXATION WITH NAVIGATION

13.1 Introduction

The results of our preclinical investigation proved to be encouraging enough to favor the navigational system for a clinical investigation in patients being treated with cannulated lag screws for valgus impacted femoral neck fractures and sacroiliac disruptions.

13.2 Methods And Results

I investigated with an experienced surgeon of Hungarian origin an L5-to-ilium bi-lateral spinal-to-pelvic fixation procedure using titanium the Universal Spine System Schanz screws (7.3 x 100 mm) and surgical EMF navigation with sacral laminectomy for sacral nerve root decompression. The patient was a 40-year-old man who was injured in a motor vehicle accident, sustaining a S2 U-shaped sacral fracture dislocation and spinal pelvic dislocation with cauda equina syndrome. The construct that was used allows for immediate bilateral weight bearing for the lower extremities.

Using the electromagnetic navigation system with custom instruments and a C-arm, a spinal clamp for transmitter registration was placed initially at the caudal end of the L4 spinous process in approximately 5 seconds and the reference dynamic frame pin-transmitter attached within seconds of that. The system was already initialized with receiver sensors attached to the hand tools. Six images were captured for a total of 12 seconds of C-arm time. Previous scout shots for C-arm positioning totaled 26 seconds. Five minutes were required to place two bilateral Schanz pedicle screws on the left side and nearly 10 minutes were required on the right side because of a slight deformity. It was estimated that the standard fluoroscopic technique here could have required 5–10 minutes of dose time. Total fluoroscopy time was 73 seconds.

13.3 Discussion And Conclusions

Successful placement of the screws was completed with the use of the EM navigation system. The navigation technology did not prolong the procedure and actually may have slightly shortened the overall time by obviating the need for AP oblique and lateral updated fluoroscopic views. A few images were captured to correlate the instrument artifact to the virtual tool and the extended distal tool-tip projection. This was useful in tracking the pedicle screws and subsequently the iliac screws using the awl and drill guide with navigation accuracy to 1 mm or better 95% of the tracked time as measured by the system software and correlated and controlled by spot fluoroscopy. Worst case was approximately 1.5 mm with the spine handle during rotation. I plan in the future to continue investigations using electromagnetic tracking for new custom drill guides and hand powered drills together with the application of a new mobile C-arm imagining technology based on digital flat panel producing CT-like images.

CHAPTER 14. SUMMARY CONCLUSION

We developed and tested an electromagnetic (EM) tracking system as an alternative to optical navigation systems. This avoids the line of site issues that are associated with the optical tracking[61,139]. We improved our EM system to minimize the potential for magnetic interference. The objectives of these preclinical and clinical experiments were to demonstrate that navigation coupled with a C-arm X-ray system intraoperatively can be integrated to record 2D images (where surgical anatomy is not entirely visualized without the axial plane, the most critical plane for ensuring spatial accuracy in geometrically challenging anatomy) and with 3D anatomical images to be saved for real-time surgical uses. Our aim was to also minimize X-ray exposure of the patient and staff while improving surgical precision through added visual dimensions, new tracking software and in the first uses of new percutaneous instrumentation.

The application of stereotactic computer-assisted surgical navigation in minimally invasive surgery can be used for less invasive procedures of the paranasal sinuses, cranial, spine, and orthopedic surgeries. Using a C-am navigational platform for paranasal sinus surgery has the intraoperative advantage of updating anatomical structural changes beyond endoscopic views after surgical dissection and manipulations of visible tissue landmarks, in three dimensions, something that is not possible with pre-operative and specially formatted CT data sets. My investigations on preclinical specimens and in patients performed by clinicians showed that the image quality was sufficient, but should be improved. We have planned protocols for future improvements.

For spine surgery we looked at the conventional fluoroscopic approach to pedicle screw fusion and instrumentation. We noted the incidence of misplaced pedicle screws with standard techniques to be reported from 3% to 55%[61,78,80,101,165,177.] In the thoracic spine literature we noted reports of a 25% pedicle screw misplacement rate in scoliosis patients,[133] whereas other studies have demonstrated a 41% pedicle wall disruption rate associated with thoracic pedicle screw insertion.[210] In contrast, various authors have demonstrated the use of stereotactic computer-assisted surgical navigation accuracy to range from 0 to 14%,[25,39,41,52,57,58,62,87,116,133,154,168,187,232] and others reported a 8.5% pedicle wall perforation rate when implementing navigation techniques in complex and prolonged thoracolumbar procedures.[230] We applied and tested our next generation electromagnetic tracking technology as an alternative to the previous generation of optical line of site navigation systems to determine clinically relevant tracking accuracy.

Under my direction, we designed and built custom instruments for the use in open and percutaneous spinal procedures. My experimental study with my collaborative team designed new instruments for navigation to improve the insertion of a fiber optics trocar for percutaneous laser discectomy and for pedicle fusion. We conducted 2D and 3D comparison studies between EM tracking and conventional C-arm placements for open and MIS pedicle screw approaches. Our results noted a substantial improvement in navigated mean accuracy vs. non-navigated spinal instruments and significantly lower critical perforation rates in comparison to conventional fluoroscopic implant placements.

We also measured the difference in x-ray exposure times and doses and found the results to be significantly less than with conventional fluoroscopy. In cases of placement of percutaneous pedicle screws, we noted that the surgeon is required to extrapolate the third dimension based on an interpretation of available images and knowledge of the pertinent anatomy. In our findings, we realized computer-assisted surgical navigation could be used as the link between visualized and non-visualized anatomical relationships, thereby minimizing guesswork associated with spinal surgery.

We also determined that the use of electromagnetic tracking in various open and transcutaneous thoracolumbar spinal procedures is feasible, safe and effective and therefore can add value in enhancing surgical precision while minimizing the need for additional use of ionizing radiation. More technical and clinical experiments with larger sample sizes, refined instruments, and software algorithms using the various experimental approaches described in this Thesis, may further improve stereotactic navigation in minimally invasive spine surgery. For this, we have created a spinal protocol for a future prospective minimally invasive multicenter randomized clinical trial to compare surgical navigation data with traditional C-arm fluoroscopy: in the accurate and expedient placement of thoracic and lumbar MIS instrumentation.

In orthopedic minimally invasive surgery of the femur, we designed and built electromagnetic compatible instruments to address the precision targeting and calculations of bony entry points. To accomplish this, we designed software for trajectories to measure the length and positioning of necessary guidewires and implants. During our experimentation we discovered materials for the instruments, which can be used to avoid electromagnetic field distortion (EMF). We also established the least invasive placement positions of a reference transmitter suitable for intraoperative registration and tracking. Our preclinical comparison studies resulted in substantial reductions of the overall need for fluoroscopy. We concluded through our experimental work and clinical evaluations that EM navigation technology can be used to enhance future emerging minimally invasive techniques.

APPENDIX.

1. Navigation Static-Dynamic Tracker Experiments

Introduction/Aims

We conducted bench tracker accuracy experiments in our corporate laboratory to assess the electromagnetic static and dynamic accuracies of our tracker system. In this experiment we not only measured static accuracy and precision, but also the dynamic accuracy, dynamic precision, and performance with metal distortion.

Static accuracy is measured by collecting data at known stationary locations and observing the variability, while dynamic accuracy involves collecting data while the sensor is in motion with respect to the transmitter.

This experimental investigation takes into account our tool-sensor configurations, tool tip calibrations, and motion of the surgical instrument tools to ensure that the accuracy is similar to a use case scenario of an image-guided stereotactic surgical navigation system.

Materials and Methods

Materials

Several trackers are in use to facilitate surgical navigation and most are optical based tracker boxes. The following navigation trackers were included in the study:

1. NDI Vicra™ Optical Tracker
2. NDI Aurora® EM Tracker
3. Ascension microBIRD™
4. Ascension pciBIRD™
5. Polhemus FASTRAK®
6. Polhemus Liberty™
7. GE InstaTrak® Gold

NIST certified granite block was used as the bench.

Methods

Static Precision

We positioned our EMF field transmitter and receiver on a flat surface 12 inches apart (Figure A1), and 1000 measurements were taken.

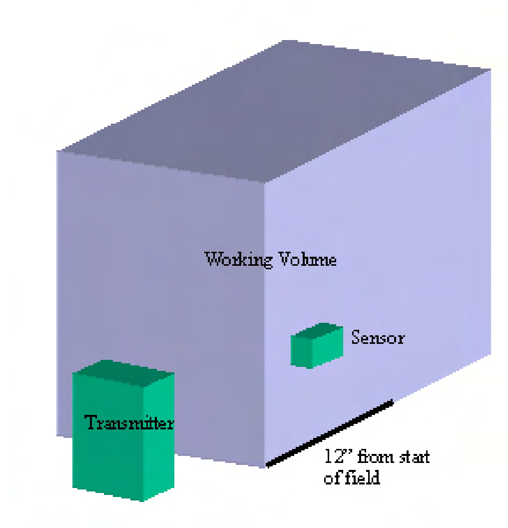

Figure A1. Static precision setup

The standard deviation, 95th percentile from the distance mean, and span (maximum distance – minimum distance reported) were calculated.

Tracker Configuration	**Std.Dev. [mm]**	**95% from mean [mm]**	**Span [mm]**
GE InstaTrak Gold	0.03	0.08	0.14

Static Accuracy

A 3-axis robot with a composite arm (Figure A2) was used to collect data on a 1-inch grid throughout a tracker's working volume (up to a 24x24x24-inch volume).

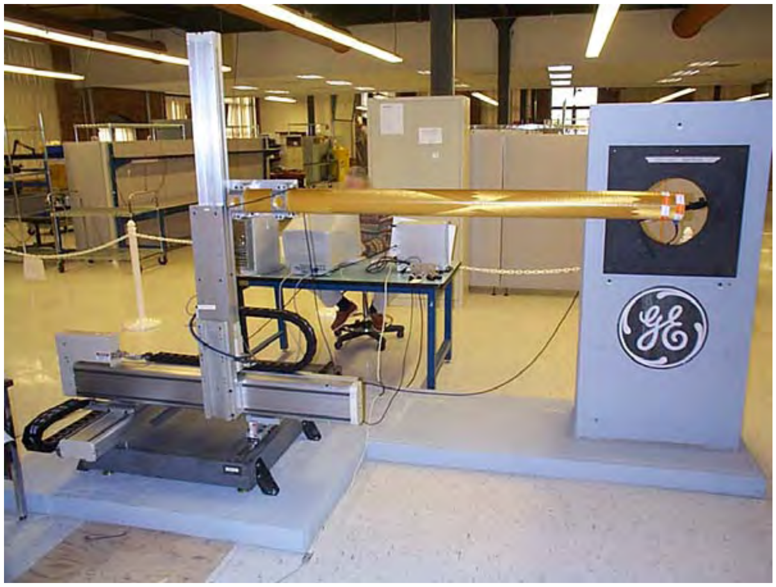

Figure A2.

Thirty samples were collected at each position. The resulting point cloud and the robot coordinate system were then aligned (registered). The standard deviation, RMS, 95 percentile, and maximum error were calculated.

Tracker Configuration	Std.Dev. [mm]	95% from mean [mm]	Span [mm]
GE InstaTrak Gold	0.03	0.08	0.14

Dynamic precision at different speeds

For systems supporting 2 or more sensors, two sensors were placed a fixed distance apart on a rigid board. The board containing the two sensors was moved in a random spiral pattern throughout the working volume (Figure A3). The spirals were done in different orientations.

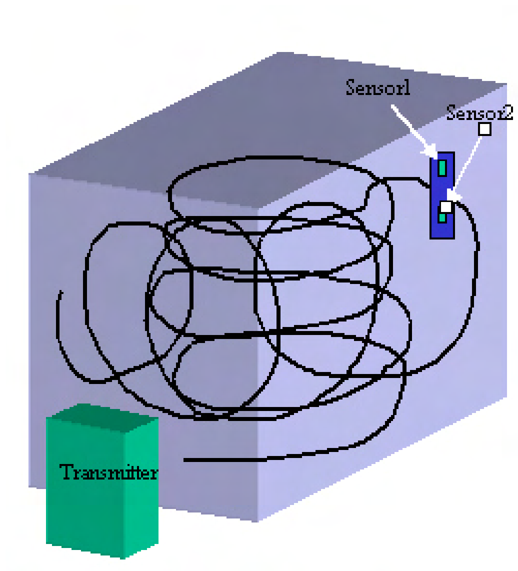

Figure A3.

Each data sample was time-stamped and an average velocity (mm/sec.) was calculated. One thousand samples were collected, and for each sample the distance between the sensors was calculated.

Tracker Configuration	**Std.Dev. @ 50mm/sec [mm]**	**95th % @ 50mm/sec [mm]**	**Span @ 50mm/sec [mm]**	**Std.Dev. @ 100mm/sec [mm]**	**95th % @ 100mm/sec [mm]**	**Span @ 100mm/sec [mm]**
GE InstaTrak Gold	0.14	0.27	0.79	0.20	0.38	1.07

Dynamic precision

A precision NIST traceable 6x6x9-inch granite block that has 6 finished faces was used (Figure A4). The front face of the block was placed 6 inches from the EM Transmitter.

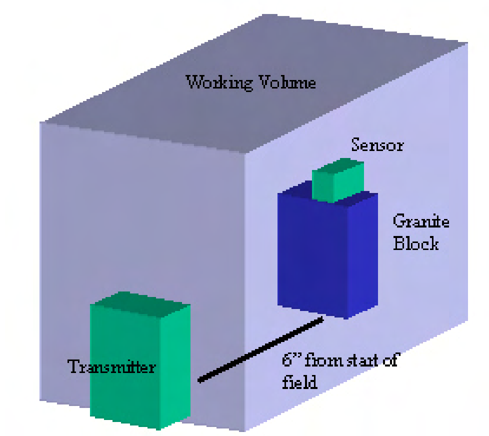

Figure A4.

A raw sensor or calibrated tool tip was "scribbled" on the five accessible surfaces. By "scribbling," we mean moving the sensor randomly over a precision flat surface of the granite block and collecting points as we move the sensor. The collected points were best-fit to planes.

Tracker Configuration	**Standard Deviation [mm]**	**RMS [mm]**	**95% [mm]**	**Maximum Error [mm]**	**Span [mm]**
GE InstaTrak Gold 4.7-cm pointer with 1.5-mm ball tip	0.13	0.13	0.26	0.57	1.11

Dynamic Accuracy

For tools such as pointers that have calibrated tips, thousands of points are collected on the faces of the granite block (Figure A5).

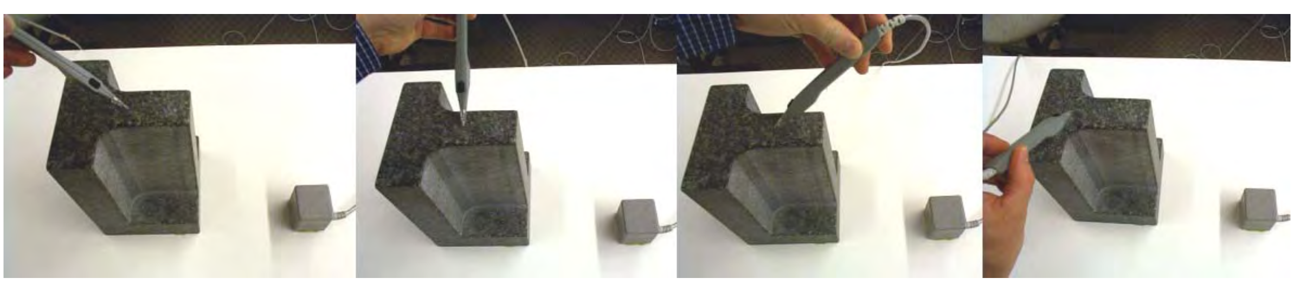

Figure A5.

The collected points are best-fit to a CAD model.

Tracker Configuration	Mean [mm]	Standard Deviation [mm]	RMS [mm]	95% [mm]	Maximum Error [mm]	Span [mm]
GE InstaTrak Gold Short pointer with 1.5-mm ball tip	-0.22	0.16	0.27	0.48	0.90	1.33

Dynamic metal distortion detection

We wanted to know how well EM trackers work around metal distorters. To create a baseline, we collected thousands of points on the granite block with no distortion. These data were best-fit to one or more planes

In the test case, we collected data on the granite block with distortion by introducing various objects (Figure A6). This point cloud is then compared with the reference plane(s). Only data that are considered “undistorted” by the tracker are used.

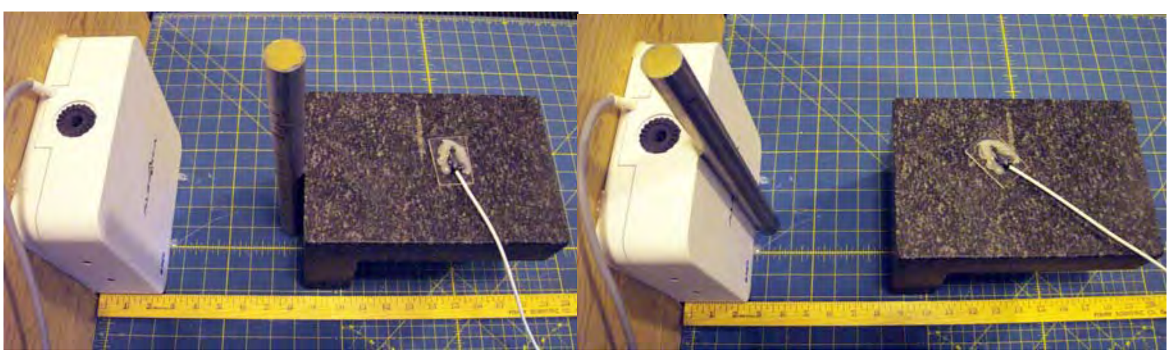

Figure A6.

Tracker Configuration	Distorter	Percentage of non-distorted points returned	Mean [mm]	Standard Deviation [mm]	RMS [mm]	95% [mm]	Maximum Error [mm]	Span [mm]	Trackable Area %
GE InstaTrak Gold Snap Receiver	None	100%	0.00	0.14	0.14	0.31	0.46	0.92	100%
	Type 17-4 Stainless Steel	90%	0.88	0.29	0.92	1.34	1.78	1.92	96%
	Type 304 Stainless Steel	59%	1.04	0.37	1.10	1.55	2.10	2.91	83%
	Type 440C Stainless Steel	98%	1.75	0.20	1.76	2.06	2.68	1.62	100%
	Nitronic Stainless Steel	53%	0.97	0.34	1.03	1.41	1.64	2.55	85%
	Titanium	69%	0.73	0.35	0.81	1.22	1.73	2.77	85%
	Spray Paint Can	0%							0%
	Aluminum soda can	0%							0%

Results and Discussion

The tests in this study gave us a good indication of tracker performance one would observe using an image guided surgical navigation system that includes an instrument tool-tip and registration. The tests also indicate that EM trackers can attain dynamic precision and accuracy results similar to those of the new generation of small optical trackers. Although EM trackers can be affected by metal distortion, they can usually detect the distortion and limit the number of bad points passed on to the application.

2. Overall System Accuracy Test

Introduction/Aims

We conducted a system accuracy assessment test to ensure that the transmitter, receiver, and tracker components were operating within the specifications we needed to proceed all the way to clinical environmental levels of at least 1 mm.

Materials and Methods

Materials

We used the InstaTrak IT3500 stereotactic computer-assisted navigation system by GE. We applied radiolucent blocks made of radiolucent material with a set of embedded ball bearings, which are numbered. Two radiolucent blocks with 10 and 66 embedded ball bearings were used.

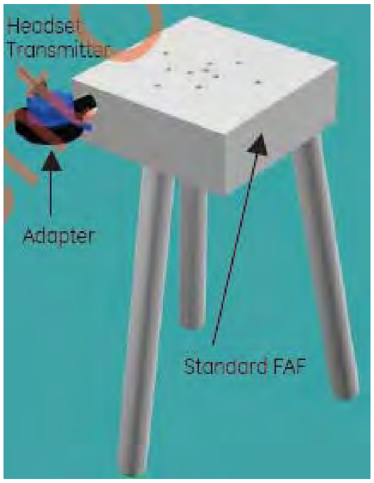

Figure A7. 10 ball bearings in a radiolucent block tripod

Other equipment included a CT image of the radiolucent blocks, a headset transmitter used in ENT/Cranial applications, and a short Pointer used in clinical procedures.

Methods

We loaded a CT image of the radiolucent block into the IT3500 InstaTrak navigation system. The short pointer was calibrated. Fiducial registration was performed. The short pointer was placed on each of the embedded ball bearings on the Field Accuracy Fixture block and positional data were collected. The location of each ball bearing was collected by placing the tip of the short pointer on top of the ball bearing in the radiolucent block. The collected locations were registered to the ball bearing locations in the CT scan of the radiolucent block. An RMS value was computed for the registration.

The test was conducting using a radiolucent block with 10 ball bearings and also a radiolucent block with 66 embedded ball bearings (Figure A7). The test was conducted in clean and distorted environments.

Figure A8a. 10 point block

Figure 8b. 66 point block

Results and Conclusion

We used an RMS value of 1.0 mm as the rejection criterion.

RMS values in clean and distorted environments.

RMS (40 point)	**RMS** (10 point)	**ENVIRONMENT**
0.216	0.159	Clean
0.220	0.192	Clean
0.290	0.217	Clean
0.262	0.325	Clean
0.099	0.135	Clean
2.321	2.053	Distorted
1.205	1.263	Distorted
1.621	2.570	Distorted

It was proven that using both radiolucent blocks in a distortion-free environment demonstrated that we were able to achieve an overall system accuracy of less than 1 mm RMS. At this point, we were confident to go forward with our experiments in cadavers to assess total system accuracy of the electromagnetic navigation system in looking at the clinical relevant accuracy of various ENT, spine, and orthopedic operations.

ACKNOWLEDGMENTS

The research performed for this Thesis was made possible through the contributions of several distinguished colleagues in both the United States and Hungary. I would like to extend my special thanks to Professor Gyorgy Weber for his encouragement, support, and many advices throughout the memorable years we worked together on new minimally invasive surgical (MIS) applications that later inspired my interest and enthusiasm to continue work in the area of MIS leading to the compilation of these experiments. Professor Weber's corrections and suggestions to this document are much appreciated. I would also especially like to thank Professor Erzsebet Roth for her tremendous support, expert guidance, and mentorship that are greatly appreciated in light of the many obstacles and setbacks common in experimental work. Additionally I extend my gratitude to the faculty of the Experimental Surgery Department of the University of Pecs for their hospitality and time during my various course studies at their laboratories. Anna Viski, MD Director of Pathology at Moritz Kaposi Medical Center, deserves my great appreciation for the help she provided to the femoral bone studies and the histological spine laser studies.

I would like to further thank my distinguished colleagues in medicine and in science for their endless hours of enthusiasm enduring the frigid colds of winter and sizzling heat of summer in the catacombs and bowels of various institutional laboratories we traveled to and from. My appreciation goes to friends and Drs. H. Yuan, H.C. Sagi, J. Carrino, R. Manos, N. Ordway, M. Fried, S. Brown and colleagues for early experiments. Also thanks to Drs. B. Selland, P. Sweeney, M. Perez-Cruet, K. Yonemura, J. Reagen, L. Khoo, F. Jolesz, D. Groszmann, P. Birkmeyer, Z. Cselik, I. Repa, and all my unnamed peers and different institutions for their outstanding support of this research.

I would also like to thank my Thesis committee members for their interest and for taking the time to be involved in the dissertation process. A special thanks also goes to my colleagues at GE Healthcare and Johnson and Johnson.

Finally, I wish to thank my parents, Geza and Maria, and my wife Ava and son Christian for their constant encouragement, patience, and devotion.

REFERENCES

1. http://www.polhemus.com/index_print.php?page=Military_Polhemus'_Military_History. Accessed on
2. FDA Public Health Advisory: Avoidance of serious x-ray induced skin injuries to patients during fluoroscopically guided procedures. September 9, 1994, in. Rockville, MD: Food and Drug Administration, 1994
3. Virtual cockpit's panoramic displays afford advanced mission capabilities, in **Aviation Week and Space Technology**, 1985, pp 143-152
4. What's Next? Nationwide Evaluation of X-ray Trends: 2000 computed tomography, in **CRCPD publication no. NEXT_2000CTT**: Conference of Radiation Control Program Directors, Department of Health and Human Services, 2006
5. Abdel-Malek K, McGowan DP, Goel V, Kowalski D, Smith S: Bone registration method for robot assited surgery: Pedicle screw insertion. **Proc Inst Mech Eng (H) 211:**221-233, 1997
6. Acosta FL, Jr., Thompson TL, Campbell S, Weinstein PR, Ames CP: Use of intraoperative isocentric C-arm 3D fluoroscopy for sextant percutaneous pedicle screw placement: case report and review of the literature. **Spine J 5:**339-343, 2005
7. Adamson TE: Microendoscopic posterior cervical laminoforaminotomy for unilateral radiculopathy: results of a new technique in 100 cases. **J Neurosurg 95:**51-57, 2001
8. Alker G, Kelly PJ: An overview of CT based stereotactic systems for the localization of intracranial lesions. **Comput Radiol 8:**193-196, 1984
9. American Academy of Otolaryngology Head and Neck Surgery Foundation and the American Rhinologic Society: in. Alexandria, VA
10. Amiot LP, Lang K, Putzier M, Zippel H, Labelle H: Comparative results between conventional and computer-assisted pedicle screw installation in the thoracic, lumbar, and sacral spine. **Spine 25:**606-614, 2000
11. Amulya K, Höllwarth M: History of Endoscopic Surgery, in. Berlin: Springer, 2008, pp 3-15
12. Arand M, Hartwig E, Hebold D, Kinzl L, Gebhard F: [Precision analysis of navigation-assisted implanted thoracic and lumbar pedicled screws. A prospective clinical study]. **Unfallchirurg 104:**1076-1081, 2001
13. Archer BR, Wagner LK: Protecting patients by training physicians in fluoroscopic radiation management. **J Appl Clin Med Phys 1:**32-37, 2000
14. Ascher P, Holzer P, Sutter B, Choy DS, Jury H: Percutaneous nucleus pulposus denaturation (abstract). **Lasers Surg Med 2:**149, 1983
15. Ascher PW: Status quo and new horizons of laser therapy in neurosurgery. **Lasers Surg Med 5:**499-506, 1985
16. Assaker R, Reyns N, Vinchon M, Demondion X, Louis E: Transpedicular screw placement: image-guided versus lateral-view fluoroscopy: in vitro simulation. **Spine 26:**2160-2164, 2001
17. Austin MS, Vaccaro AR, Brislin B, Nachwalter R, Hilibrand AS, Albert TJ: Image-guided spine surgery: a cadaver study comparing conventional open laminoforaminotomy and two image-guided techniques for pedicle screw placement in posterolateral fusion and nonfusion models. **Spine 27:**2503-2508, 2002

18. Barnett GH, Miller DW, Weisenberger J: Frameless stereotaxy with scalp-applied fiducial markers for brain biopsy procedures: experience in 218 cases. **J Neurosurg 91:**569-576, 1999
19. Baroud G: A brief update on the biomechanisms underlying cement injection and leakage in vertebroplasty. **Support Cancer Ther 2:**105-108, 2005
20. Baroud G, Crookshank M, Bohner M: High-viscosity cement significantly enhances uniformity of cement filling in vertebroplasty: an experimental model and study on cement leakage. **Spine 31:**2562-2568, 2006
21. Baroud G, Falk R, Crookshank M, Sponagel S, Steffen T: Experimental and theoretical investigation of directional permeability of human vertebral cancellous bone for cement infiltration. **J Biomech 37:**189-196, 2004
22. Baroud G, Vant C, Giannitsios D, Bohner M, Steffen T: Effect of vertebral shell on injection pressure and intravertebral pressure in vertebroplasty. **Spine 30:**68-74, 2005
23. Belmont PJ, Jr., Klemme WR, Dhawan A, Polly DW, Jr.: In vivo accuracy of thoracic pedicle screws. **Spine 26:**2340-2346, 2001
24. Berg O, Carenfelt C, Rystedt G, Anggard A: Occurrence of asymptomatic sinusitis in common cold and other acute ENT-infections. **Rhinology 24:**223-225, 1986
25. Bloch O, Holly LT, Park J, Obasi C, Kim K, Johnson JP: Effect of frameless stereotaxy on the accuracy of C1-2 transarticular screw placement. **J Neurosurg 95:**74-79, 2001
26. Bohner M, Gasser B, Baroud G, Heini P: Theoretical and experimental model to describe the injection of a polymethylmethacrylate cement into a porous structure. **Biomaterials 24:**2721-2730, 2003
27. Bolger C, Wigfield C: Image-guided surgery: applications to the cervical and thoracic spine and a review of the first 120 procedures. **J Neurosurg 92:**175-180, 2000
28. Bozzini P: Der Lichtleiter. **J. Prak. Heilk 24:**107, 1805
29. Brenner DJ, Hall EJ: Computed tomography--an increasing source of radiation exposure. **N Engl J Med 357:**2277-2284, 2007
30. Brodke DS, Dick JC, Kunz DN, McCabe R, Zdeblick TA: Posterior lumbar interbody fusion. A biomechanical comparison, including a new threaded cage. **Spine 22:**26-31, 1997
31. Brown SM, Sadoughi B, Cuellar H, von Jako R, Fried MP: Feasibility of near real-time image-guided sinus surgery using intraoperative fluoroscopic computed axial tomography. **Otolaryngol Head Neck Surg 136:**268-273, 2007
32. Buchelt M, Katterschafka T, Horvat R, Kutschera HP, Kickinger W, Laufer G: Fluorescence guided excimer laser ablation of intervertebral discs in vitro. **Lasers Surg Med 11:**280-286, 1991
33. Buchelt M, Kutschera HP, Katterschafka T, Kiss H, Schneider B, Ullrich R: Erb:YAG and Hol:YAG laser ablation of meniscus and intervertebral discs. **Lasers Surg Med 12:**375-381, 1992
34. Buchelt M, Schlangmann B, Schmolke S, Siebert W: High power Ho:YAG laser ablation of intervertebral discs: effects on ablation rates and temperature profile. **Lasers Surg Med 16:**179-183, 1995
35. Bucholz R, Smith K: A comparison of sonic digitizers vs. light emitting diode-based localization, in Maciunas R (ed): **Interactive Image Guided Neurosurgery.** Park Ridge, IL: American Association of Neurological Surgeons, 1993

36. Buchroeder R: An optical analysis of the Farrand VCASS helmet-mounted display. Air Force Aerospace Medical Research Laboratory Technical Report:ASAMRL-TR-83-072, in: Wright-Patterson AFB, Ohio, October 1983
37. Carl AL, Khanuja HS, Sachs BL, Gatto CA, vomLehn J, Vosburgh K, et al: In vitro simulation. Early results of stereotaxy for pedicle screw placement. **Spine 22:**1160-1164, 1997
38. Casper GD, Hartman VL, Mullins LL: Results of a clinical trial of the holmium:YAG laser in disc decompression utilizing a side-firing fiber: a two-year follow-up. **Lasers Surg Med 19:**90-96, 1996
39. Castro WH, Halm H, Jerosch J, Malms J, Steinbeck J, Blasius S: Accuracy of pedicle screw placement in lumbar vertebrae. **Spine 21:**1320-1324, 1996
40. Chen YC, Lee SH, Saenz Y, Lehman NL: Histologic findings of disc, end plate and neural elements after coblation of nucleus pulposus: an experimental nucleoplasty study. **Spine J 3:**466-470, 2003
41. Choi WW, Green BA, Levi AD: Computer-assisted fluoroscopic targeting system for pedicle screw insertion. **Neurosurgery 47:**872-878, 2000
42. Choy DS: Percutaneous laser disc decompression (PLDD): 352 cases with an 8 1/2-year follow-up. **J Clin Laser Med Surg 13:**17-21, 1995
43. Choy DS: Percutaneous laser disc decompression using the 1.06 and 1.32 µm Nd/Yag laser. **Spine State Art Rev 7:**41-48, 1993
44. Choy DS, Altman P: Fall of intradiscal pressure with laser ablation. **J Clin Laser Med Surg 13:**149-151, 1995
45. Choy DS, Case RB, Fielding W, Hughes J, Liebler W, Ascher P: Percutaneous laser nucleolysis of lumbar disks. **N Engl J Med 317:**771-772, 1987
46. Cinotti G, Gumina S, Ripani M, Postacchini F: Pedicle instrumentation in the thoracic spine. A morphometric and cadaveric study for placement of screws. **Spine 24:**114-119, 1999
47. Cleary K, Anderson J, Brazaitis M, Devey G, DiGioia A, Freedman M, et al: Final report of the technical requirements for image-guided spine procedures Workshop, April 17-20, 1999, Ellicott City, Maryland, USA. **Comput Aided Surg 5:**180-215, 2000
48. Cohen NA, Kennedy DW: Endoscopic sinus surgery: where we are-and where we're going. **Curr Opin Otolaryngol Head Neck Surg 13:**32-38, 2005
49. Davis JK: Percutaneous discectomy improved with KTP laser. **Clin Laser Mon 8:**105-106, 1990
50. Derby R, Eek B, Chen Y, O'Neill C, Ryan D: Intradiscal Electrothermal Annuloplasty (IDET): A Novel Approach for Treating Chronic Discogenic Back Pain. **Neuromodulation 3:**82-88, 2000
51. Deyo RA, Cherkin DC, Loeser JD, Bigos SJ, Ciol MA: Morbidity and mortality in association with operations on the lumbar spine. The influence of age, diagnosis, and procedure. **J Bone Joint Surg Am 74:**536-543, 1992
52. Dickman CA, Rosenthal D, Karahalios DG, Paramore CG, Mican CA, Apostolides PJ, et al: Thoracic vertebrectomy and reconstruction using a microsurgical thoracoscopic approach. **Neurosurgery 38:**279-293, 1996
53. Eichholz KM, Nioguy S, Samartzis D, von Jako R, Perez-Cruet MJ: Applications of image guidance in minimally invasive spine surgery, in Perez-Cruet MJ, Khoo LT,

Fessler RG (eds): **An Anatomic Approach to Minimally Invasive Spine Surgery.** St. Louis, MO: Quality Medical Publishing, 2007, pp 207-222
54. Esses SI, Sachs BL, Dreyzin V: Complications associated with the technique of pedicle screw fixation. A selected survey of ABS members. **Spine 18:**2231-2238; discussion 2238-2239, 1993
55. Farber GL, Place HM, Mazur RA, Jones DE, Damiano TR: Accuracy of pedicle screw placement in lumbar fusions by plain radiographs and computed tomography. **Spine 20:**1494-1499, 1995
56. Finn MA, Yonemura KS, von Jako R: Neuro-navigational image-guided applications, in Pimenta L, Beisse R, Kim D (eds): **Minimally Invasive Spine Fusion: Techniques and Operative Nuances.** St. Louis, MO: Quality Medical Publishing, 2008
57. Foley K, Silveri C, Vaccaro A, ea: Atlantoaxial transarticular screw fixation: Risk assessment and bone morphology using an image guidance system. **J Bone Joint Surg Br 80:**245, 1998
58. Foley K, Smith K, Smith M: Frameless stereotactic guidance of cervical spine lateral mass screw placement, in Nolte L, Ganz R (eds): **Computer Assisted Orthopaedic Surgery.** Bern: Hogrefe and Huber Publications, 1999, pp 89-98
59. Foley KT, Gupta SK: Percutaneous pedicle screw fixation of the lumbar spine: preliminary clinical results. **J Neurosurg 97:**7-12, 2002
60. Foley KT, Simon DA, Rampersaud YR: Virtual fluoroscopy: computer-assisted fluoroscopic navigation. **Spine 26:**347-351, 2001
61. Foley KT, Smith MM: Image-guided spine surgery. **Neurosurg Clin N Am 7:**171-186, 1996
62. Foley KT, Smith MM: Microendoscopic discectomy. **Tech Neurosurg 3:**301-307, 1997
63. Fraser JF, von Jako R, Carrino J, Hartl R: Electromagnetic navigation in minimally invasive spine surgery: Results of a cadaveric study to evaluate percutaneous pedicle screw insertion. **SAS J 2:**43-47, 2008
64. Fried MP, Hsu L, Topulos GP, Jolesz FA: Image-guided surgery in a new magnetic resonance suite: preclinical considerations. **Laryngoscope 106:**411-417, 1996
65. Fried MP, Kleefield J, Gopal H, Reardon E, Ho BT, Kuhn FA: Image-guided endoscopic surgery: results of accuracy and performance in a multicenter clinical study using an electromagnetic tracking system. **Laryngoscope 107:**594-601, 1997
66. Fried MP, Moharir VM, Shin J, Taylor-Becker M, Morrison P: Comparison of endoscopic sinus surgery with and without image guidance. **Am J Rhinol 16:**193-197, 2002
67. Friets EM, Strohbehn JW, Hatch JF, Roberts DW: A frameless stereotaxic operating microscope for neurosurgery. **IEEE Trans Biomed Eng 36:**608-617, 1989
68. Furness T: Visually-coupled information systems, in **ARPA Conference on Biocybernetic Applications for Military Systems.** Chicago, IL, 1978
69. Gaines RW, Jr.: The use of pedicle-screw internal fixation for the operative treatment of spinal disorders. **J Bone Joint Surg Am 82-A:**1458-1476, 2000
70. Gangi A, Kastler BA, Dietemann JL: Percutaneous vertebroplasty guided by a combination of CT and fluoroscopy. **AJNR Am J Neuroradiol 15:**83-86, 1994
71. Garfin SR, Reilley MA: Minimally invasive treatment of osteoporotic vertebral body compression fractures. **Spine J 2:**76-80, 2002

72. Gayet LE, Hamcha H, Charbonneau A, Texereau J, Bertheau D, Bellicaud D, et al: [Biomechanical study and digital modeling of traction resistance in posterior thoracic implants]. **Rev Chir Orthop Reparatrice Appar Mot 87:**459-468, 2001
73. Gejo R, Matsui H, Kawaguchi Y, Ishihara H, Tsuji H: Serial changes in trunk muscle performance after posterior lumbar surgery. **Spine 24:**1023-1028, 1999
74. Gertzbein SD, Robbins SE: Accuracy of pedicular screw placement in vivo. **Spine 15:**11-14, 1990
75. Gevargez A, Groenemeyer DW, Czerwinski F: CT-guided percutaneous laser disc decompression with Ceralas D, a diode laser with 980-nm wavelength and 200-microm fiber optics. **Eur Radiol 10:**1239-1241, 2000
76. Ginzburg L, Greenwald D, Cohen J: Complications of endoscopy. **Gastrointest Endosc Clin N Am 17:**405-432, 2007
77. Giorgi C, Luzzara M, Casolino D, Onagania E: A computer controlled stereotactic arm:virtual reality in neurosurgical procedures. **Acta Neurochir Suppl 58:**75-76, 1993
78. Girardi FP, Cammisa FP, Jr., Sandhu HS, Alvarez L: The placement of lumbar pedicle screws using computerised stereotactic guidance. **J Bone Joint Surg Br 81:**825-829, 1999
79. Glasser O: **Dr. W.C. Roentgen, ed 2.** Springfield, IL: Charles C. Thomas, 1958
80. Glossop ND, Hu RW, Randle JA: Computer-aided pedicle screw placement using frameless stereotaxis. **Spine 21:**2026-2034, 1996
81. Gottlob C, Kopchok GE, Peng SK, Tabbara M, Cavaye D, White RA: Holmium:YAG laser ablation of human intervertebral disc: preliminary evaluation. **Lasers Surg Med 12:**86-91, 1992
82. Gwaltney JM, Jr.: Acute community-acquired sinusitis. **Clin Infect Dis 23:**1209-1223; quiz 1224-1205, 1996
83. Halm H, Niemeyer T, Link T, Liljenqvist U: Segmental pedicle screw instrumentation in idiopathic thoracolumbar and lumbar scoliosis. **Eur Spine J 9:**191-197, 2000
84. Hart RA, Hansen BL, Shea M, Hsu F, Anderson GJ: Pedicle screw placement in the thoracic spine: a comparison of image-guided and manual techniques in cadavers. **Spine 30:**E326-331, 2005
85. Hiwatashi A, Ohgiya Y, Kakimoto N, Westesson PL: Cement leakage during vertebroplasty can be predicted on preoperative MRI. **AJR Am J Roentgenol 188:**1089-1093, 2007
86. Holly LT, Foley KT: Image guidance in spine surgery. **Orthop Clin North Am 38:**451-461; abstract viii, 2007
87. Holly LT, Foley KT: Three-dimensional fluoroscopy-guided percutaneous thoracolumbar pedicle screw placement. Technical note. **J Neurosurg 99:**324-329, 2003
88. Horsely V, Clarke R: The structure and functions of the cerebellum examined by a new method. **Brain 31:**45-124, 1908
89. Hott JS, Deshmukh VR, Klopfenstein JD, Sonntag VK, Dickman CA, Spetzler RF, et al: Intraoperative Iso-C C-arm navigation in craniospinal surgery: the first 60 cases. **Neurosurgery 54:**1131-1136; discussion 1136-1137, 2004
90. Hsu L, Fried MP, Jolesz FA: MR-guided endoscopic sinus surgery. **AJNR Am J Neuroradiol 19:**1235-1240, 1998

91. Isaacs RE, Podichetty VK, Santiago P, Sandhu FA, Spears J, Kelly K, et al: Minimally invasive microendoscopy-assisted transforaminal lumbar interbody fusion with instrumentation. **J Neurosurg Spine 3:**98-105, 2005
92. Jacobson AS, Woo P, Shapshay SM: Emerging technology: flexible CO2 laser WaveGuide. **Otolaryngol Head Neck Surg 135:**469-470, 2006
93. Jako GJ: ASLM Brochure on Laser Surgery and Medicine, in**.** Wausau, WI: American Society for Laser Medicine and Surgery, 1986, pp 1-30
94. Jako GJ: Laser surgery of the vocal cords. An experimental study with carbon dioxide lasers on dogs. **Laryngoscope 82:**2204-2216, 1972
95. Jako GJ: Minimally invasive direct access surgical technology---MIDAST^{TM}, in **International Developments in Surgery and Surgical Research. Surgical Technology International.** San Francisco: Universal Medical Press, 1999, Vol Book VIII
96. Jane JA, Jr., Thapar K, Alden TD, Laws ER, Jr.: Fluoroscopic frameless stereotaxy for transsphenoidal surgery. **Neurosurgery 48:**1302-1307; discussion 1307-1308, 2001
97. Jang JS, Lee SH: Minimally invasive transforaminal lumbar interbody fusion with ipsilateral pedicle screw and contralateral facet screw fixation. **J Neurosurg Spine 3:**218-223, 2005
98. Johnson RG, Murphy M, Miller M: Fusions and transfusions. An analysis of blood loss and autologous replacement during lumbar fusions. **Spine 14:**358-362, 1989
99. Kahler DM: Image guidance: fluoroscopic navigation. **Clin Orthop Relat Res:**70-76, 2004
100. Kalfas IH: Image-guided spinal navigation. **Clin Neurosurg 46:**70-88, 2000
101. Kalfas IH, Kormos DW, Murphy MA, McKenzie RL, Barnett GH, Bell GR, et al: Application of frameless stereotaxy to pedicle screw fixation of the spine. **J Neurosurg 83:**641-647, 1995
102. Kambin P, Zhou L: Arthroscopic discectomy of the lumbar spine. **Clin Orthop Relat Res:**49-57, 1997
103. Kang JD, An H, Boden S, Phillips F, Foley K, Abdu W: Cement augmentation of osteoporotic compression fractures and intraoperative navigation: summary statement. **Spine 28:**S62-63, 2003
104. Kaso G, Horvath Z, Szenohradszky K, Sandor J, Doczi T: Comparison of CT characteristics of extravertebral cement leakages after vertebroplasty performed by different navigation and injection techniques. **Acta Neurochir (Wien) 150:**677-683; discussion 683, 2008
105. Kawaguchi Y, Matsui H, Tsuji H: Back muscle injury after posterior lumbar spine surgery. A histologic and enzymatic analysis. **Spine 21:**941-944, 1996
106. Kawaguchi Y, Matsui H, Tsuji H: Back muscle injury after posterior lumbar spine surgery. Part 2: Histologic and histochemical analyses in humans. **Spine 19:**2598-2602, 1994
107. Kawaguchi Y, Yabuki S, Styf J, Olmarker K, Rydevik B, Matsui H, et al: Back muscle injury after posterior lumbar spine surgery. Topographic evaluation of intramuscular pressure and blood flow in the porcine back muscle during surgery. **Spine 21:**2683-2688, 1996
108. Keenan WN, Woodward AF, Price D, Eckloff K, Richards J, Powell J, et al: Manipulation under anaesthetic of children's fractures: use of the image intensifier

reduces radiation exposure to patients and theatre personnel. **J Pediatr Orthop 16:**183-186, 1996
109. Kelly P, Groes S: Magnetic field digitizer for stereotactic surgery, in US (ed), 1998, Vol U.S. Patent No. 5787856
110. Kelly PJ: Stereotactic craniotomy. **Neurosurg Clin N Am 1:**781-799, 1990
111. Kelly PJ: **Tumor Stereotaxis.** Philadelphia: W.B. Saunders, 1991
112. Kelly PJ, Kall BA, Goerss S: Transposition of volumetric information derived from computed tomography scanning into stereotactic space. **Surg Neurol 21:**465-471, 1984
113. Kennedy DW: Functional endoscopic sinus surgery. Technique. **Arch Otolaryngol 111:**643-649, 1985
114. Kennedy DW, Zinreich SJ, Rosenbaum AE, Johns ME: Functional endoscopic sinus surgery. Theory and diagnostic evaluation. **Arch Otolaryngol 111:**576-582, 1985
115. Kim DY, Lee SH, Chung SK, Lee HY: Comparison of multifidus muscle atrophy and trunk extension muscle strength: percutaneous versus open pedicle screw fixation. **Spine 30:**123-129, 2005
116. Kim KD, Patrick Johnson J, Bloch BO, Masciopinto JE: Computer-assisted thoracic pedicle screw placement: an in vitro feasibility study. **Spine 26:**360-364, 2001
117. Koh YH, Han D, Cha JH, Seong CK, Kim J, Choi YH: Vertebroplasty: magnetic resonance findings related to cement leakage risk. **Acta Radiol 48:**315-320, 2007
118. Kosmopoulos V, Schizas C: Pedicle screw placement accuracy: a meta-analysis. **Spine 32:**E111-120, 2007
119. Kothe R, Matthias Strauss J, Deuretzbacher G, Hemmi T, Lorenzen M, Wiesner L: Computer navigation of parapedicular screw fixation in the thoracic spine: a cadaver study. **Spine 26:**E496-501, 2001
120. Kozak J, Nesper M, Fischer M, Lutze T, Goggelmann A, Hassfeld S, et al: Semiautomated registration using new markers for assessing the accuracy of a navigation system. **Comput Aided Surg 7:**11-24, 2002
121. Krag MH, Beynnon BD, Pope MH, Frymoyer JW, Haugh LD, Weaver DL: An internal fixator for posterior application to short segments of the thoracic, lumbar, or lumbosacral spine. Design and testing. **Clin Orthop Relat Res:**75-98, 1986
122. Krebs J, Ferguson SJ, Bohner M, Baroud G, Steffen T, Heini PF: Clinical measurements of cement injection pressure during vertebroplasty. **Spine 30:**E118-122, 2005
123. Laine T, Lund T, Ylikoski M, Lohikoski J, Schlenzka D: Accuracy of pedicle screw insertion with and without computer assistance: a randomised controlled clinical study in 100 consecutive patients. **Eur Spine J 9:**235-240, 2000
124. Laine T, Makitalo K, Schlenzka D, Tallroth K, Poussa M, Alho A: Accuracy of pedicle screw insertion: a prospective CT study in 30 low back patients. **Eur Spine J 6:**402-405, 1997
125. Laine T, Schlenzka D, Makitalo K, Tallroth K, Nolte LP, Visarius H: Improved accuracy of pedicle screw insertion with computer-assisted surgery. A prospective clinical trial of 30 patients. **Spine 22:**1254-1258, 1997
126. Lane GJ, Prodoehl JA, Black J, Lee SH, Rhodes A, Sherk HH: An experimental comparison of CO_2, Argon, Nd:Yag and HO:Yag laser ablation of intervertebral discs. **Spine State Art Rev 7:**1-10, 1993
127. Ledlie JT, Renfro M: Balloon kyphoplasty: one-year outcomes in vertebral body height restoration, chronic pain, and activity levels. **J Neurosurg 98:**36-42, 2003

128. Leksell L: A note on the treatment of acoustic tumours. **Acta Chir Scand 137:**763-765, 1971
129. Leksell L: A stereotactic apparatus for intracerebral surgery. **Acta Chir Scand 99:**229-233, 1949
130. Liebergall M, Ben-David D, Weil Y, Peyser A, Mosheiff R: Computerized navigation for the internal fixation of femoral neck fractures. **J Bone Joint Surg Am 88:**1748-1754, 2006
131. Lieberman IH, Togawa D, Kayanja MM, Reinhardt MK, Friedlander A, Knoller N, et al: Bone-mounted miniature robotic guidance for pedicle screw and translaminar facet screw placement: Part I--Technical development and a test case result. **Neurosurgery 59:**641-650; discussion 641-650, 2006
132. Liljenqvist U, Hackenberg L, Link T, Halm H: Pullout strength of pedicle screws versus pedicle and laminar hooks in the thoracic spine. **Acta Orthop Belg 67:**157-163, 2001
133. Liljenqvist UR, Halm HF, Link TM: Pedicle screw instrumentation of the thoracic spine in idiopathic scoliosis. **Spine 22:**2239-2245, 1997
134. Lim MR, Girardi FP, Yoon SC, Huang RC, Cammisa FP, Jr.: Accuracy of computerized frameless stereotactic image-guided pedicle screw placement into previously fused lumbar spines. **Spine 30:**1793-1798, 2005
135. Linton OW: News of X-ray reaches America days after announcement of Roentgen's discovery. **AJR Am J Roentgenol 165:**471-472, 1995
136. Little J, Taveras J: **Radiology: Diagnosis, Imaging, Intervention.** Philadelphia: JB Lippincott, 1992
137. Lundsford L, Kondziolka D, Leksell D: The Leksell stereotactic system, in Tasker P, Gildenberg P (eds): **Textbook of Stereotactic and Functional Neurosurgery.** New York: McGraw-Hill, 1998, pp 51-64
138. Ma CM, Coffey CW, DeWerd LA, Liu C, Nath R, Seltzer SM, et al: AAPM protocol for 40-300 kV x-ray beam dosimetry in radiotherapy and radiobiology. **Med Phys 28:**868-893, 2001
139. Maciunas R: Interactive image guided neurosurgery7, in Tindall G, Cooper P, Barrow D (eds): **The Practice of Neurosurgery.** Baltimore: Williams and Wilkins, 1997
140. Manarey CR, Anand VK: Radiation dosimetry of the FluoroCAT scan for real-time endoscopic sinus surgery. **Otolaryngol Head Neck Surg 135:**409-412, 2006
141. Manchikanti L, Cash KA, Moss TL, Rivera J, Pampati V: Risk of whole body radiation exposure and protective measures in fluoroscopically guided interventional techniques: a prospective evaluation. **BMC Anesthesiol 3:**2, 2003
142. McGuire JE: Space, geometrical objects and infinity : Newton and Descartes on extension, in **Nature mathematized I. Dordrecht**: Kluwer Academic Publishers, 1995, pp 69-112
143. Mehlman CT, DiPasquale TG: Radiation exposure to the orthopaedic surgical team during fluoroscopy: "how far away is far enough?" **J Orthop Trauma 11:**392-398, 1997
144. Messerklinger W: **Endoscopy of the Nose.** Baltimore: Urban and Schwartzenberg, 1978
145. Munsterberg H: The X-Rays. **Science 3:**161-163, 1896
146. Murphy MA, McKenzie RL, Kormos DW, Kalfas IH: Frameless stereotaxis for the insertion of lumbar pedicle screws. **J Clin Neurosci 1:**257-260, 1994
147. National Cancer Institute: Interventional Fluoroscopy: Reducing Radiation Risks for Patients and Staff, in, 2005

148. Nerubay J, Caspi I, Levinkopf M, Tadmor A, Bubis JJ: Percutaneous laser nucleolysis of the intervertebral lumbar disc. An experimental study. **Clin Orthop Relat Res:**42-44, 1997
149. Neumann J, Morgenstern O: **The Theory of Games and Economic Behavior.** Princeton, NJ: Princeton University Press, 1944
150. Nickoloff EL, Alderson PO: Radiation exposures to patients from CT: reality, public perception, and policy. **AJR Am J Roentgenol 177:**285-287, 2001
151. Norris T: Radiation safety in fluoroscopy. **Rad Tech 73:**511-533, 2002
152. Odgers CJt, Vaccaro AR, Pollack ME, Cotler JM: Accuracy of pedicle screw placement with the assistance of lateral plain radiography. **J Spinal Disord 9:**334-338, 1996
153. Olson G, Citardi MJ: Image-guided functional endoscopic sinus surgery. **Otolaryngol Head Neck Surg 123:**188-194, 2000
154. Paramore CG, Dickman CA, Sonntag VK: The anatomical suitability of the C1-2 complex for transarticular screw fixation. **J Neurosurg 85:**221-224, 1996
155. Patil AA: Computed tomography plane of the target approach in computed tomographic stereotaxis. **Neurosurgery 15:**410-414, 1984
156. Pauza KJ, Howell S, Dreyfuss P, Peloza JH, Dawson K, Bogduk N: A randomized, placebo-controlled trial of intradiscal electrothermal therapy for the treatment of discogenic low back pain. **Spine J 4:**27-35, 2004
157. Perez-Cruet M, Wang M, Samartzis D: Microendoscopic cervical laminoplasty and laminectomy, in Kim DH, Fessler RG (eds): **Endoscopic Spine Surgery and Instrumentation.** New York: Thieme, 2004
158. Perez-Cruet MJ, Kim BS, Sandhu F, Samartzis D, Fessler RG: Thoracic microendoscopic discectomy. **J Neurosurg Spine 1:**58-63, 2004
159. Portenoy R: Opioid therapy for chronic nonmalignant pain: a review of the critical issues. **J Pain Sympt Manag 11:**203-217, 1996
160. Quinones-Hinojosa A, Robert Kolen E, Jun P, Rosenberg WS, Weinstein PR: Accuracy over space and time of computer-assisted fluoroscopic navigation in the lumbar spine in vivo. **J Spinal Disord Tech 19:**109-113, 2006
161. Raab FH, Blood EB, Steiner TO, Jones HR: Magnetic position and orientation tracking system. **Trans. Aerosp. Electron. Syst 15**, 1979
162. Raabe A, Krishnan R, Wolff R, Hermann E, Zimmermann M, Seifert V: Laser surface scanning for patient registration in intracranial image-guided surgery. **Neurosurgery 50:**797-801; discussion 802-793, 2002
163. Rafferty MA, Siewerdsen JH, Chan Y, Moseley DJ, Daly MJ, Jaffray DA, et al: Investigation of C-arm cone-beam CT-guided surgery of the frontal recess. **Laryngoscope 115:**2138-2143, 2005
164. Rajasekaran S, Vidyadhara S, Ramesh P, Shetty AP: Randomized clinical study to compare the accuracy of navigated and non-navigated thoracic pedicle screws in deformity correction surgeries. **Spine 32:**E56-64, 2007
165. Rampersaud YR, Foley KT, Shen AC, Williams S, Solomito M: Radiation exposure to the spine surgeon during fluoroscopically assisted pedicle screw insertion. **Spine 25:**2637-2645, 2000
166. Rampersaud YR, Simon DA, Foley KT: Accuracy requirements for image-guided spinal pedicle screw placement. **Spine 26:**352-359, 2001

167. Reidy DP, Houlden D, Nolan PC, Kim M, Finkelstein JA: Evaluation of electromyographic monitoring during insertion of thoracic pedicle screws. **J Bone Joint Surg Br 83:**1009-1014, 2001
168. Resnick DK: Prospective comparison of virtual fluoroscopy to fluoroscopy and plain radiographs for placement of lumbar pedicle screws. **J Spinal Disord Tech 16:**254-260, 2003
169. Rhodes A, Black J, Lane GJ, Lee SH, Sherk HH: Clinical use of the 2.1 µm Holmium:Yag laser and percutaneous lumbar discectomy. **Spine State Art Rev 7:**49-54, 1993
170. Richter M, Geerling J, Zech S, Goesling T, Krettek C: Intraoperative three-dimensional imaging with a motorized mobile C-arm (SIREMOBIL ISO-C-3D) in foot and ankle trauma care: a preliminary report. **J Orthop Trauma 19:**259-266, 2005
171. Ringel F, Stoffel M, Stuer C, Meyer B: Minimally invasive transmuscular pedicle screw fixation of the thoracic and lumbar spine. **Neurosurgery 59:**ONS361-366; discussion ONS366-367, 2006
172. Riskin DJ, Longaker MT, Gertner M, Krummel TM: Innovation in surgery: a historical perspective. **Ann Surg 244:**686-693, 2006
173. Roberts DW, Strohbehn JW, Hatch JF, Murray W, Kettenberger H: A frameless stereotaxic integration of computerized tomographic imaging and the operating microscope. **J Neurosurg 65:**545-549, 1986
174. Roberts T: The BRW/CRW stereotactic apparatus, in Tasker P, Gildenberg P (eds): **Textbook of Functional and Stereotactic Neurosurgery.** New York: McGraw-Hill, 1998, pp 65-71
175. Roentgen W: Sitzungsbenchte der WürzburgerPhysik-medico Gegellschraft, in: Eine Neue Art von Strahlen, 1895
176. Roessler K, Ungersboeck K, Dietrich W, Aichholzer M, Hittmeir K, Matula C, et al: Frameless stereotactic guided neurosurgery: clinical experience with an infrared based pointer device navigation system. **Acta Neurochir (Wien) 139:**551-559, 1997
177. Roh SW, Kim DH, Cardoso AC, Fessler RG: Endoscopic foraminotomy using MED system in cadaveric specimens. **Spine 25:**260-264, 2000
178. Roy-Camille R, Roy-Camille M, Demeulenaere C: [Osteosynthesis of dorsal, lumbar, and lumbosacral spine with metallic plates screwed into vertebral pedicles and articular apophyses]. **Presse Med 78:**1447-1448, 1970
179. Roy-Camille R, Saillant G, Mazel C: Internal fixation of the lumbar spine with pedicle screw plating. **Clin Orthop Relat Res:**7-17, 1986
180. Saal JA, Saal JS: Intradiscal electrothermal treatment for chronic discogenic low back pain: prospective outcome study with a minimum 2-year follow-up. **Spine 27:**966-973; discussion 973-964, 2002
181. Sagi HC, Kreig JC, Beauregard G-L, Kapur T, von Jako R: Electromagnetic navigation, in Corbin TP, Connolly PJ, Yuan HA, Bao Q-B, Boden SD (eds): **Emerging Spine Surgery Technologies: Evidence and Framework for Evaluating New Technology.** St. Louis, MO: Quality Medical Publishing, 2006, pp 239-252
182. Sagi HC, Manos R, Benz R, Ordway NR, Connolly PJ: Electromagnetic field-based image-guided spine surgery part one: results of a cadaveric study evaluating lumbar pedicle screw placement. **Spine 28:**2013-2018, 2003

183. Sagi HC, Manos R, Park SC, Von Jako R, Ordway NR, Connolly PJ: Electromagnetic field-based image-guided spine surgery part two: results of a cadaveric study evaluating thoracic pedicle screw placement. **Spine 28:**E351-354, 2003
184. Sanders R, Koval KJ, DiPasquale T, Schmelling G, Stenzler S, Ross E: Exposure of the orthopaedic surgeon to radiation. **J Bone Joint Surg Am 75:**326-330, 1993
185. Saringer WF, Reddy B, Nobauer-Huhmann I, Regatschnig R, Reddy M, Tschabitscher M, et al: Endoscopic anterior cervical foraminotomy for unilateral radiculopathy: anatomical morphometric analysis and preliminary clinical experience. **J Neurosurg 98:**171-180, 2003
186. Sasso RC, Cotler HB: Posterior instrumentation and fusion for unstable fractures and fracture-dislocations of the thoracic and lumbar spine. A comparative study of three fixation devices in 70 patients. **Spine 18:**450-460, 1993
187. Schulze CJ, Munzinger E, Weber U: Clinical relevance of accuracy of pedicle screw placement. A computed tomographic-supported analysis. **Spine 23:**2215-2220; discussion 2220-2211, 1998
188. Schwend RM, Dewire PJ, Kowalski TM: Accuracy of fluoroscopically assisted laser targeting of the cadaveric thoracic and lumbar spine to place transpedicular screws. **J Spinal Disord 13:**412-418, 2000
189. Sharps LS, Isaac Z: Percutaneous disc decompression using nucleoplasty. **Pain Physician 5:**121-126, 2002
190. Shea WR: **The Magic of Numbers and Motion: The Scientific Career of René Descartes** Canton, MA: Science History Publications, 1991
191. Sheikh H, Eichholz KM, Nioguy S, Samartzis D, von Jako R, Perez-Cruet MJ: Image guidance in minimally invasive spinal surgery, in Wolfa C, Resnick DK (eds): **Neurosurgical Operative Atlas: Spine and Peripheral Nerve, ed 2.** New York: Thieme, 2007, pp 308-313
192. Shepard S, Paul Lin P, ea: Quality Control in Diagnostic Radiology. **American Association of Physicists in Medicine 74:**10.13, 2002
193. Sherk HH, Rhodes A, Black J, Prodoehl JA: Results of percutaneous lumbar discectomy with lasers. **Spine State Art Rev 7:**141-150, 1993
194. Shope TB: Radiation-induced skin injuries from fluoroscopy. **Radiographics 16:**1195-1199, 1996
195. Singh V, Piryani C, Liao K, Nieschulz S: Percutaneous disc decompression using coblation (nucleoplasty) in the treatment of chronic discogenic pain. **Pain Physician 5:**250-259, 2002
196. Slomczykowski M, Roberto M, Schneeberger P, Ozdoba C, Vock P: Radiation dose for pedicle screw insertion. Fluoroscopic method versus computer-assisted surgery. **Spine 24:**975-982; discussion 983, 1999
197. Smith K, Frank K, Bucholz R: The NeuroStation – a highly accurate, minimally invasive solution to frameless stereotactic neurosurgery. **Comput Med Imaging Graph 18:**831-842, discussion 842-845, 1994
198. Spiegel EA, Wycis HT, Marks M, Lee AJ: Stereotaxic Apparatus for Operations on the Human Brain. **Science 106:**349-350, 1947
199. Stammberger H: Endoscopic endonasal surgery--concepts in treatment of recurring rhinosinusitis. Part I. Anatomic and pathophysiologic considerations. **Otolaryngol Head Neck Surg 94:**143-147, 1986

200. Steffee AD, Biscup RS, Sitkowski DJ: Segmental spine plates with pedicle screw fixation. A new internal fixation device for disorders of the lumbar and thoracolumbar spine. **Clin Orthop Relat Res:**45-53, 1986
201. Steinmann JC, Herkowitz HN, el-Kommos H, Wesolowski DP: Spinal pedicle fixation. Confirmation of an image-based technique for screw placement. **Spine 18:**1856-1861, 1993
202. Strong MS, Jako GJ: Laser surgery in the larynx. Early clinical experience with continuous CO 2 laser. **Ann Otol Rhinol Laryngol 81:**791-798, 1972
203. Suk SI, Lee CK, Kim WJ, Chung YJ, Park YB: Segmental pedicle screw fixation in the treatment of thoracic idiopathic scoliosis. **Spine 20:**1399-1405, 1995
204. Suk SI, Lee CK, Min HJ, Cho KH, Oh JH: Comparison of Cotrel-Dubousset pedicle screws and hooks in the treatment of idiopathic scoliosis. **Int Orthop 18:**341-346, 1994
205. Talairach J, Hecaen M, David M, Monnier M, Ajuriaguerra J: Recherches sur la coagulation therapuetique des structures souscorticales chez l'homme. **Rev Neurol 81:**4-24, 1949
206. Teller E: **Memoirs: A Twentieth Century Journey in Science and Politics.** New York: Perseus Publishing
207. Teller E: **The Pursuit of Simplicity.** Los Angeles: Pepperdine University Press, 1980
208. Teller E, Wilson K, Talley A, Higgins GH: **The Constructive Uses of Nuclear Explosives.** New York: McGraw Hill, 1968
209. Togawa D, Kayanja MM, Reinhardt MK, Shoham M, Balter A, Friedlander A, et al: Bone-mounted miniature robotic guidance for pedicle screw and translaminar facet screw placement: part 2--Evaluation of system accuracy. **Neurosurgery 60:**ONS129-139; discussion ONS139, 2007
210. Vaccaro AR, Rizzolo SJ, Allardyce TJ, Ramsey M, Salvo J, Balderston RA, et al: Placement of pedicle screws in the thoracic spine. Part I: Morphometric analysis of the thoracic vertebrae. **J Bone Joint Surg Am 77:**1193-1199, 1995
211. Villalobos H, Germano IM: Clinical evaluation of multimodality registration in frameless stereotaxy. **Comput Aided Surg 4:**45-49, 1999
212. von Jako R: Navigation and visualization of an access needle system, in Office USP (ed): **U.S. Patent Application Publication.** United States, 2006, Vol US 2006/0063998 A1
213. Wagner LK, Eifel PJ, Geise RA: Potential biological effects following high X-ray dose interventional procedures. **J Vasc Interv Radiol 5:**71-84, 1994
214. Watanabe E, Mayanagi Y, Kosugi Y, Manaka S, Takakura K: Open surgery assisted by the neuronavigator, a stereotactic, articulated, sensitive arm. **Neurosurgery 28:**792-799; discussion 799-800, 1991
215. Watanabe E, Watanabe T, Manaka S, Mayanagi Y, Takakura K: Three-dimensional digitizer (neuronavigator): new equipment for computed tomography-guided stereotaxic surgery. **Surg Neurol 27:**543-547, 1987
216. Webb S: In the beginning, in Webb S (ed): **The Physics of Medical Imaging.** Bristol: Adam Hilger, 1988, pp 8-19
217. Weinstein JN, Spratt KF, Spengler D, Brick C, Reid S: Spinal pedicle fixation: reliability and validity of roentgenogram-based assessment and surgical factors on successful screw placement. **Spine 13:**1012-1018, 1988

218. Weisskopf M, Herlein S, Birnbaum K, Siebert C, Stanzel S, Wirtz DC: [Kyphoplasty - a new minimally invasive treatment for repositioning and stabilising vertebral bodies]. **Z Orthop Ihre Grenzgeb 141:**406-411, 2003
219. Welch WC, Gerszten PC: Alternative strategies for lumbar discectomy: intradiscal electrothermy and nucleoplasty. **Neurosurg Focus 13:**E7, 2002
220. Welch WC, Subach BR, Pollack IF, Jacobs GB: Frameless stereotactic guidance for surgery of the upper cervical spine. **Neurosurgery 40:**958-963; discussion 963-954, 1997
221. Wiesner L, Kothe R, Ruther W: Anatomic evaluation of two different techniques for the percutaneous insertion of pedicle screws in the lumbar spine. **Spine 24:**1599-1603, 1999
222. Wiesner L, Kothe R, Schulitz KP, Ruther W: Clinical evaluation and computed tomography scan analysis of screw tracts after percutaneous insertion of pedicle screws in the lumbar spine. **Spine 25:**615-621, 2000
223. Wigland M: **Transnasal Endoscopic surgery of th eAnterior Skull Base: Proceedings of the Twelfth ORL World Congress, Budapest, 1981. .** Budapest: Publ House Hungary Acad Sci, 1981
224. Wolfsberger S, Rossler K, Regatschnig R, Ungersbock K: Anatomical landmarks for image registration in frameless stereotactic neuronavigation. **Neurosurg Rev 25:**68-72, 2002
225. Wolgin M, Finkenberg J, Papaioannou T, Segil C, Soma C, Grundfest W: Excimer ablation of human intervertebral disc at 308 nanometers. **Lasers Surg Med 9:**124-131, 1989
226. Wood BJ, Zhang H, Durrani A, Glossop N, Ranjan S, Lindisch D, et al: Navigation with electromagnetic tracking for interventional radiology procedures: a feasibility study. **J Vasc Interv Radiol 16:**493-505, 2005
227. Xu R, Ebraheim NA, Shepherd ME, Yeasting RA: Thoracic pedicle screw placement guided by computed tomographic measurements. **J Spinal Disord 12:**222-226, 1999
228. Yeung AT: Considerations for the use of the KTP laser for disc decompression and ablation. **Spine State Art Rev 7:**67-93, 1993
229. Yonezawa T, Onomura T, Kosaka R, Miyaji Y, Tanaka S, Watanabe H, et al: The system and procedures of percutaneous intradiscal laser nucleotomy. **Spine 15:**1175-1185, 1990
230. Youkilis AS, Quint DJ, McGillicuddy JE, Papadopoulos SM: Stereotactic navigation for placement of pedicle screws in the thoracic spine. **Neurosurgery 48:**771-778; discussion 778-779, 2001
231. Yuan HA, Garfin SR, Dickman CA, Mardjetko SM: A Historical Cohort Study of Pedicle Screw Fixation in Thoracic, Lumbar, and Sacral Spinal Fusions. **Spine 19:**2279S-2296S, 1994
232. Yuguchi T, Nishio M, Akiyama C, Ito M, Yoshimine T: Posterior microendoscopic surgical approach for the degenerative cervical spine. **Neurol Res 25:**17-21, 2003
233. Zamorano L: The Zamorano-Dujovny Multipurpose localizing unit, in **Advances Neurosurgical Navigation.** New York: Thieme, 1999, pp 255-256
234. Zindrick MR, Wiltse LL, Widell EH, Thomas JC, Holland WR, Field BT, et al: A biomechanical study of intrapeduncular screw fixation in the lumbosacral spine. **Clin Orthop Relat Res:**99-112, 1986

PERSONAL PUBLICATIONS

Articles In Refereed Journals Related to Navigation

1) ***"Percutaneous Laser Discectomy with Stereotactic Computer-Assisted Surgical Navigation."*** **von Jako, RA**; Cselik, Z; J. Lasers in Surgery and Medicine, 41: 42-51, 2009. IF: 2.771

2) ***"Electromagnetic navigation for percutaneous guide-wire insertion; Accuracy and Efficiency Compared to Conventional Fluoroscopy Technique."*** **von Jako R**; Carrino JA; Yonemura KS; Noda GA; Zhu W; Blaskiewicz D; Raju M; Groszmann DE; Weber G; J. NeuroImage; Accepted. 5/2009. IF:5.565

3) ***"Electromagnetic Navigation in Minimally Invasive Spine Surgery: Results of a Cadaveric Study to Evaluate Percutaneous Pedicle Screw Insertion",*** Fraser J; **von Jako R**; Hartl R. J. Of Spine Arthroplasty Society,2:43-47, 2008.

4) ***"Method for evaluating compatibility of commercial electromagnetic tracking systems with surgical imaging tables***". Nafis C, Jensen V, **von Jako R**, SPIE Medical Imaging, 6918:Visualization, Image-Guided Procedures and Modeling, Bellingham WA. 2008. IF: 3.084

5) ***"Feasibility of Real-Time Image Guided Sinus Surgery Using Intra-operative Fluoroscopic Computed Axial Tomography"***, Brown SM; Sadoughi B; Cuellar H; Brook A; **Von Jako R**; Fried MP; Cover Page. Journal of Otolaryngology – Head and Neck Surgery.136:268–73,2007. IF: 1.339

6) ***"Image Guidance offers Additional Power in the Endoscopic Solution of Extended Cranio-Facial Malformations: Hungarian Experience with Computer Assisted Endoscopic Sinus Surgery"***. Hirshberg A, Fent, Z, H, K, Rezek, O, **von Jako R,** Repassy, G**,** International Journal of Pediatric Otolaryngology, 1: 181-84, 2006. IF: 0.851

7) ***"Electromagnetic Field-Based Image Guided Spine Surgery, Part Two: Results of a Cadaveric Study Evaluating Thoracic Pedicle Screw Placement".*** Sagi HC, Manos R, Park SC, Von Jako R, Ordway NR, Connolly PJ. SPINE, 28: E351-4, 2003 Lippincott & Williams. IF: 2.676

Related Articles Pending Submission

1) ***"Electromagnetic Surgical Navigation and Fixation of Femoral Neck Fractures. A Cadaveric Study on Accuracy and Efficiency.***" Sagi HC; **von Jako R.** J. Orthopedic Trauma, 2009.

2) "***The Evolution of Image-Guided and Computer-Aided Orthopaedic Surgery"***. Sagi HC, **von Jako R**, Yuan HA. J. American Academy of Orthopaedic Surgeons,2009.

General Articles In Refereed Journals

1) ***"Minimally Invasive Direct Cardiac Surgery with a Jakoscope® Retractor - Minimalisan invaziv direkt szivsebeszet jakoszkop feltaroval",*** Galajda Z, Jako G, **von Jako R**, Peterffy A, Orvosi Hetilap, 149:111-14, 2008.

2) ***"Minilaparotomies with a new special instrument"***. Privera TF, Nemeth L, **von Jako** R. American Journal of Obstetrics & Gynecology, 175:1078-79,1996. IF: 2.917

3) ***"Short Historical Note Connection between Varicella and Herpes Zoster"***. **Jako, G, Jako R**. Journal of Medicine, 17 267-69, 1986. IF: 2.510

Supplements and Other Publications

1) ***"Clearing the Way to Sinus Surgeries,"*** **von Jako R**. Interviewed by Author/Editor; *USA Today*, September 10, 2006.

2) ***"Use of a new Fat Pad sparing minimally invasive incision and a fiberoptic retractor*** **(Jakoscope®)** ***in the treatment of cruciate ligament and chondral injuries"***. Preliminary report presented at the 8th International Eurosurgery Congress in Budapest, Hungary. June 1998. Kish G, Hangody L, **von Jako R**. The British Journal of Surgery, vol. 85, supplement 2, July 1998.

3) ***"Minimal and Direct Access in Thoracic Diagnosis and Surgery"***. Nabrady Z, **von Jako R**, Wain J, Boni J. The British Journal of Surgery, vol. 85, supplement 2. July 1998.

4) ***"Minimal and Direct Access Endoscopic Surgery in Gynecology"***. Bodis J,. Jako G, Lehoczky T, Dyevich T, **von Jako R**. The British Journal of Surgery, vol. 85, supplement 2, July 1998.

5) ***"Howard-Jako Technique for Minimally Invasive Direct Access Surgery (MIDAST™) for Anterior Interbody Spine Fusion."*** Howard D, Haynes H, **von Jako R**. The British Journal of Surgery, vol. 85, supplement 2. July, 1998.

6) ***FDA Common Generic Device Names Beginning with "AR" –*** Proprietary Device Name; ***Jakos****cope® JS 200*, FDA Medical Specialty Code (SU-General Plastic Surgery), FDA Product Code (GAD), FDA Device Classification Code (General Controls), FDA Regulation Number (878.4800), FDA Establishment Registration Number (2249254), FDA listing date (12-27-01).

7) ***"Preliminary Report: Endoscopic Laser-Microsurgical Removal of Human Gallbladder"***. Journal of Laparoendoscopic Surgery, Vol. 1, Number 4 (1991) Acknowledged.

Abstracts

1) ***"Electromagnetic navigation and radiation exposure in the placement of percutaneous pedicle screws".*** Finn MA, Yonemura KS, Araghi A, Khoo LT, Perez-Cruet M, Carrino JA, **von Jako R**. Abstract; 35th Annual Lende Snowbird Neurosurgery Conference. Jan30-Feb 4th, 2009.

2) ***"Surgical Electromagnetic Navigation in Musculoskeletal Procedures"*** IEEE Engineering in Medicine and Biology Society (EMBS). **Von Jako, RA**;Abstract IEEE. MIT Nov 2008.

3) ***"An Invitro Study Comparing Minimally Invasive Spine Fusion between the Conventional Fluoroscopic Technique and Surgical Navigation, Results for Accuracy, Insertion Time, X-ray Time and Dose Reduction"***. Yoneumra KS, Carrino JA; **von Jako R**; Perez-Cruet M; Araghi A; Khoo L University of Utah, Johns Hopkins University School of Medicine, Baltimore, MD, Providence Hosp, Detroit, MI, Texas Back Institute, Phoenix, AZ, UCLA Medical Center, Los Angeles, CA. Abstract; North American Spine Society, Austin, Texas. 2007.

4) ***"Navigation Surgery in Cochlear Implantation".*** Repassy G, Kustel M, Hrabak K, Fent Z, **von Jako R**. Semmelweis University Medical Faculty of Medicine, Dept of ORL and HNS, Budapest, Hungary and GE Healthcare Surgery, Lawrence, MA., 8th International Conference of the European Society of Pediatric Otorhinolarnygology, ESPO 2008. June 8-11th. Presented abstract published 2008.

5) ***"Percutaneous Pedicle Screw Insertion via Electromagnetic Navigation"***. Fraser J; **von Jako R**; Carrino J, Hartl R, Weill Medical College of Cornell University, NYNY; Johns Hopkins University School of Medicine, Baltimore, MD; Cornell University, NYNY. Abstract; North American Spine Society, Austin, Texas. 2007.

6) ***"Electromagnetic Surgical Navigation for the Placement of Transcutaneous Pedicle Screws into the Thoracolumbar Spine, A comparison to Freehand Fluoroscopy"***. Perez-Cruet M; Yonemura KS; Carrino JA; Araghi A; Khoo L; **von Jako R**; Providence Hosp, Detroit, MI, University of Utah, Johns Hopkins University School of Medicine, Baltimore, MD, Texas Back Institute, Phoenix, AZ, UCLA Medical Center, Los Angeles, CA. Abstract/Poster; Congress of Neurological Surgeons, San Diego. CA. 2007.

7) ***"Method for evaluating compatibility of commercial Electromagnetic (EM) catheter tracking systems with surgical and imaging tables",*** Nafis C, Jensen V, **von Jako R**, abstract. SPIE, 2007, Bellingham WA.

8) ***"Navigation Surgery in Cochlear Implantation***. Kustel M, Hrabak K, Fent Z, von Jako R, Abstract 50. Collegium Oto-Rhino-Laryngologicum AmicitiaeSacrum 27-30 August 2006, Moscow, Russia.

9) ***"Surgical Navigation for Cochlear Implantation, Results for first Twelve Clinical Uses"***. Repassy G; Krustel M; Fent Z; **von Jako R**; World Congress for Cochlear Implantation and Research. Abstract and Presentation. Vienna, Austria, June 2006.

10) ***"Feasibility of Real-Time Image-Guided Sinus Surgery using Intraoperative Fluoroscopy"***, Brown SM; Sadoughi B; Cuellar H; Brook A; **Von Jako R;** Fried MP; Montefiore Medical Center. American Rhinological Society annual meeting, 2005 Abstract.

11) ***"Image Guided Spine Surgery Reduces Radiation Exposure and Fluoroscopic Time"***. Yonemura K, Carrino J**,** **von Jako R**. American Association of Neurological Surgeons / Congress of Neurological Surgeons, Abstract 2004.

12) ***"Computer-Assisted Endoscopic Pedicle Fixation: Evaluation of Electromagnetic Virtual Fluoroscopy and FluoroCAT in a Cadaver Model"***, Regan J, Villavicenocio A, **von Jako R**. North American Spine Society, Poster and Abstract, 2004.

Book Chapters

1) Finn, MA, Yonemura, K, **von Jako, R**: ***"Neuro-Navigational Image Guided Applications"***, Chapter 10 In Minimally Invasive Spine Fusion: Techniques and Operative Nuances. by Mick Perez-Cruet, Rudolf Beisse, Luiz Pimenta, and Daniel Kim, Quality Medical Publishing, Inc., 2009.

2) Hormoz, S, Eichholz, KM, Nioguy, S, Samartzis, D, **von Jako, R**, Perez-Cruet, M: ***"Image Guidance in Minimally Invassive Spinal Surgery"***, Chapter 52 In Neurosurgical Operative Atlas, by Wolfa and Resnick., 2nd Edition: Thieme Medical Publishers, Inc and American Association of Neurological Surgeons, 2007.

3) Eichholz, K, Nioguy, S, Samartzis, D, **von Jako, R,** Perez-Cruet, M: ***"Applications of Image Guidance in Minimally Invasive Spine Surgery"***, Chapter 10 In An Anatomical Approach to Minimal Access Spine Surgery, by Perez-Cruet, Khoo, and Fessler, Quality Medical Publishing, Inc., 2006.

4) Sagi, HC, Krieg, JC, Beauregard, GL, Kapur, T, **von Jako, R:** ***"Electromagnetic Navigation"***, Chapter 15 In Emerging Spine Technologies: Evidence and Framework for Evaluating New Technology, by Corbin and Connolly, Quality Medical Publishing, Inc., 2005.

5) Jako, G, **von Jako, R**: ***"Minimally Invasive Direct Access Surgical Technology – MIDAST"™***, In Surgical Technology International. Book VIII, 1999. Universal Medical Press Inc. San Francisco, CA.

GE Healthcare White Papers

1) "Posterior Cervical Fusion C1-C2 Using Electromagnetic Image Guidance" – Medical University of Syracuse
2) "Anterior Cervical Disk Surgery" Miami Baptist Hospital
3) "C5 Cervical Corpectomy – Treating Cervical Spondylotic Myelopathy" – Carney Hospital, Boston
4) "Use of Image Guided Surgery in MIS Cochlear Implantations – A Work in Progress" – Semmelweis Medical University, Budapest
5) "Minimally Invasive Pedicle Screw Placement with FluoroTrak Guidance" – Medical University of Utah
6) " Pediatric Hip Dysplasia with 3D Intra-Operative Fluoroscopic Imaging" – Boston Medical Center
7) "3D Fluoroscopic Image Guided Kyphoplasty" – Medical University of Syracuse
8) "Use of Image Guidance With Cranio-Facial Malformations" – Semmelweis Medical University, Budapest
9) "IIlio-sacral Screw Placement for Traumatic SI Dislocation" – Tampa General Hospital Dept. of Trauma
10) "Posterior Pedicle Fixation, T11-L5" -Medical University of Syracuse
11) "Justification for Navigation Hazard Harm Matrix Acceptability" – GEHC-Surgery
12) "Image Guided Surgery for future vascular applications" – GEHC-Surgery
13) "Intraoperative Risks with Sinus Surgery and the Use of Surgical Navigation" – GEHC-Surgery
14) "Executive Summary for the Indications of C-arm Fluoroscopy Uses" – European TUV CE Mark
15) "The Evolution of Surgical Spinal Navigation" – GEHC -Surgery

Presentations & Exhibits

1) ***"Uses of Electromagnetic Surgical Navigation in Orthopedic Surgery",*** Invited Guest Speaker: **"** Massachusetts Institute of Technology and Engineering in Medicine and Biology Society (EMBS). Nov 2008.

2) ***"Surgical Instrumentation and Navigation Techniques in Open and MIS Spine Surgery- a didactic and Practical Session".*** Proctor: GE Healthcare-Surgery Engineering and Technology Forum at Brown University School of Medicine and Rhode Island Hospital Orthopedic Foundation. Oct 2008.

3) ***"Mechanism of Spinal Disease: An Overview".*** GE Healthcare Forum, Boston Sept 19^{th}, 2008.

4) ***"Applications of Electromagnetic Image Guidance in Spine Surgery",*** University of California, California NanoSystems Institute and the 5^{th} Annual World Congress of the International Brain Mapping and Intraoperative Surgical Planning Society. Invited Keynote Speaker, Aug 2008.

5) ***"Anatomy and Pathophysiology of Lumbar Spinal Disease"***, Harvard University – Massachusetts Institute of Technology Division of Health Sciences and Technology, HST.572 Future Medical Technologies, Spring 2007 semester invited lecturer, Course Chairman Prof. Jim Weaver.

6) ***"Computer Assisted Surgical Navigation in Spine, Orthopedic and Otorhinolaryngology"*** Sept–June, 2000–2007 North American Spine Society, College of Neurosurgeons, American Association of Neurosurgeons, American Association of Orthopedic Surgeons, American Association of Otorhinolaryngology, American Rhinology Society, Spine Arthroplasty Society, Society of Computer Assisted Orthopedic Surgery.

7) ***"Feasibility of Real-Time Image-Guided Sinus Surgery using Intraoperative Fluoroscopy"***, Seth M. Brown, MD, MBA; Babak Sadoughi, MD; Hernando Cuellar, MD; Alan Brook, MD; **Ron Von Jako, MD;** Marvin P. Fried, MD; Montefiore Medical Center. American Rhinological Society, Poster Exhibit, 2005.

Presentations & Exhibits continued

8) ***"Electromagnetic Spinal Navigation",*** von Jako R, Reagan J. Second Annual Symposium on Current Concepts in Spinal Disorders; Cedars-Sinai Medical Center, Department of Surgery, Institute for Spinal Disorders, La Quinta, CA, February 28-March 2, 2003.

9) ***"Techniques in Electromagnetic Spinal Navigation."*** von Jako R. Thirteenth Annual International Bethesda Spine Workshop, USUHS, Bethesda, MD, June 3-6, 2001.

10) ***"Progress in Angioscopy Minimally Invasive and Endovascular Surgery"***. Dec. 6–8, 1998. p. 85–97. Beth Israel Deaconess Medical Center. Harvard – Deaconess Surgical Service. Harvard Center for Minimally Invasive Surgery. Invited exhibitor & practical session instructor; precinical CME lab course.

11) Technical Exhibitor: ***"27th Annual Meeting, International Congress of Gynecologic Endoscopy"***, Atlanta, Georgia. November 10–15, 1998.

12) ***MIDAST™ in "Aortobifemoral bypass surgery"***. (scientific exhibit) American College of Surgeons 84th Annual Clinical Congress. Orlando, Florida, October, 1998.

13) Invited guest speaker for the ***"Eighth European Congress of Surgery"***, European Main Session, Budapest, Hungary, July 1998. Abstract indexed in The British Journal of Surgery Vol. 85. Supplement 2, July 1998.

14) Invited exhibitor for the ***"Arnold F. Fenton Annual Conference of Female Pelvic Anatomy and Reconstructive Surgery"***. Department of Obstetrics & Gynecology, North Shore University Hospital, Manhasset, New York. October 10, 1998.

15) Preclinical Surgical Workshop: ***"Minimally Invasive Vascular Bypass Surgery"***, Department of Cardio-Vascular Surgery, New England Medical Center. Tufts Medical School, Boston, Massachusetts. 1997.

16) Presented Senior Surgical Faculty In-service on ***"History of Minimally Invasive Direct Access Surgery"***. University of Massachusetts Medical Center, Worcester, MA. 1997.

17) ***"The History of Minimally Invasive Coronary Bypass Surgery". "Minimally Invasive Direct Access Surgery in Abdominal Vascular Reconstruction"***. (*5* scientific exhibits); vascular surgery, cardiac surgery, thoracic lung surgery, general and MIS esophageal surgery. American College of Surgeons 83rd Annual Clinical Congress, Chicago, IL, October 12–17, 1997.

18) ***"Exhibits for Jakoscope® & MIDAST™ in Gynecological Surgery"***. Las Vegas Convention Center, April 1997. American College of Obstetrics & Gynecology Annual Clinical Congress. (ACOG).

19) ***"International Meeting on Advanced Spine Techniques"***. July 10–12, 1997. Bermuda. (Scientific Exhibits) Medical Education Resource, Inc. & The Scoliosis Research Society.

20) Invited speaker & exhibitor to ***"Medical DATA International's Annual Emerging Medical Technologies East conference & Exhibition"***. September 29–30, 1997. Arlington, Virginia.

21) Invited co-speaker for the ***"Twelfth International Symposium on Minimal Intervention in Spinal Surgery"***. Allegheny University of the Health Sciences. Nov.21–23, 1997. Philadelphia, Pennsylvania.

22) American College of Surgeons 82nd Annual Clinical Congress, San Francisco, CA. October, 1996. (Scientific exhibits): ***Minimally Invasive Surgery (MIDAST)™*** for: vascular surgery, general surgery , thoracic surgery, urological surgery, minicholecystectomy, cardiac surgery, orthopedic spinal surgery, G.I. surgery, and gynecological surgery.

Presentations & Exhibits continued

23) ***Round table discussion for minimally invasive vascular bypass surgery***. Sponsored by GSI, Inc. American College of Surgeons 81st Annual Clinical Congress. New Orleans, LA. Oct. 22–27, 1995.

24) American College of Surgeons 80th Annual Clinical Congress. (2 Scientific Exhibits) Chicago, IL. October 1994.

    a. ***Microlaparotomy Cholecystectomy*** – A Simple, Rapid, and Inexpensive Alternative to Lapcholy.
    b. ***Minimal and Direct Access*** – Video Assisted – Aortoiliac Reconstructive Surgery.

25) Preclinical Surgical Workshop: ***"Minimally Invasive Aortobifemoral Bypass Surgery and M.I.S. Thoracic Surgery with the Jako-retractor endoscope"***. Massachusetts General Hospital, Department of Vascular and Thoracic Surgery. 1994.

26) ***"Annual College of International Hungarian Physicians Meeting"***. (Scientific Exhibits) Annual Meeting, August 1994, Budapest, Hungary.

    a. New Concepts in Instrumentation in Minimal Access Surgery of the Thorax. (Lecture and Video Abstract).
    b. Anterior Interbody Fusion of the Lumber Spine Using a Rigid Titanium Housing: Via a New Minimal and Direct Access Technique, by use of a Special Retractor Scope. (Lecture and Video Abstract).

27) ***"New Developments in Endoscopic Minimal Access Surgery"***: A Clinical and Experimental Study. (3 Scientific Exhibits) American College of Surgeons 79th Annual Clinical Congress, October 10–15, 1993. San Francisco, CA.

    a. ***Microlaparotomy Cholecystectomy*** – A Simple, Rapid, and Inexpensive Alternative to Lapcholy.
    b. ***Anterior Interbody Fusion of the Lumbar Spine using a rigid titanium housing:*** Open and minimally invasive surgical approaches.
    c. ***Minimal and Direct Access*** – Video Assisted – Aortoiliac Reconstructive Surgery.

28) ***"Non-Open Heart Coronary Bypass Surgery"***. (Abstract) American Society for Laser Surgery and Medicine. April 1993, New Orleans, Louisiana.

29) ***"Endoscopic Aorto-Bifemoral Bypass Surgery"***. ***"Non-Open Heart Coronary Bypass Surgery"***. International Society for Cardiovascular Surgery, XXI World Congress (Abstract) September 1993, Lisbon Portugal.

30) ***"New Concepts and Instruments for Minimal Access Surgery"***. (Scientific Exhibit) American College of Surgeons Annual Meeting, October 1993, San Francisco, California.

Intellectual Property: United States Patent and Trade Mark Office. * von Jako, RA

1. **Title:** Tissue Tracking Probe And Delivery System.
    a. Method and device to facilitate stereotactic surgical registration and navigation of soft tissue, i.e. visceral organs.
    Status: Filed

2. **Title:** Electro-magnetic computer assisted navigation of intraluminal endovascular instruments, using virtual and stereotactic imaging modalities.
    Status: Pending File

3. **Title:** A Method For Electromagnetic Image Guided Cochlear Implantation
    Status: Pending File

4. **Title:** Expert C-arm system
    Abstract: An expert image-guided surgical system and method for accessing, storing and sharing medical information between expert imaging apparatus for use during the planning and performance of surgical procedures.
    Status: Published

5. **Title:** Intraoperative Measurements On Navigated Placements Of Implants
    Abstract: Certain embodiments provide systems and methods for intraoperative implant measurement. Certain embodiments of a method include noting a location of a first implant, noting a location of a second implant, measuring a distance between the first and second implants based on the location of the first implant and the location of the second implant, and displaying the distance to a user. Certain embodiments of a system include a processor configured to determine a distance between a first implant and a second implant based on tracking information for a location of the first implant and a location of the second implant and a display configured to display an image including the first and second implants and the distance to a user.
    Status: Published

6. **Title:** Reference Platform and System for Head and Neck Wired and Wireless Registration for Electromagnetic Computer Assisted Surgical Navigation
    Abstract: A reference platform adapted to facilitate the attachment of a reference unit to a patient is disclosed herein. The reference platform includes a top surface adapted to contact a reference unit, and a bottom surface generally opposite the top surface. The bottom surface is adapted to contact a patient. The reference platform also includes a spike extending in a direction away from the bottom surface. The spike is configured to penetrate the patient in order to secure the reference platform to the patient. A corresponding method for mounting the reference unit to the patient is also provided.
    Status: Published

7. **Title:** Navigation And Visualization Of A Guide System For Instrumentation Used In Spinal Surgery, NAV Guide System
    Abstract: An instrument guide system for use with a surgical navigation system, the instrument guide system comprising a handle assembly, an instrument attachment assembly, a shaft connecting the handle assembly to the instrument attachment assembly, an electromagnetic sensor assembly removably mounted within an opening in the handle assembly, and an instrument removably attachable within a bore of the instrument attachment assembly.
    Status: Published

Intellectual Property continued:

8. **Title:** Computer Navigated One-Step Spine Pedicle Preparation Instrument, For Open And Percutaneous Spine Fusion Incisions (Awl, Tap, Probe In One)
Abstract: The present application discloses aA medical device adapted to facilitate pedicle screw fusion surgery is disclosed herein. The medical device includes a proximal end and a sharp distal end opposite the proximal end. The distal end is configured to allow the medical device to function as an awl. The medical device also includes a body portion defined between the proximal end and the distal end, and a threaded section defined by the body portion near the distal end. The threaded section is configured to allow the medical device to function as a tap. Accordingly, the medical device provides a single tool adapted to function as both an awl and a tap. A corresponding method for securing a pedicle screw to a vertebra is also provided.
Status: Published

9. **Title:** Method For Calibration And Surgical Navigation Of Straight And Angled Ring Curettes For The Purpose Of Skull Base Procedures
Abstract: A calibration apparatus for a medical device is disclosed herein. The calibration apparatus includes a locating member configured to locate a first predetermined portion of the medical device. The calibration apparatus also includes a calibration member positioned relative to the locating member such that, when the calibration apparatus is attached to the medical device, the calibration member aligns with a second predetermined portion of the medical device. A corresponding method for determining the location of the second predetermined portion of the medical device is also provided.
Status: Published

10. **Title:** Computer Navigation Planning Method For Percutaneous Spine Instrumentation
Abstract: A system and method for placement of at least one implant comprising an imaging system configured for taking at least one image of a patient; a navigation system configured for tracking position and orientation of at least one implant; a computer configured to measure and calculate the position and orientation of the at least one implant; and a display configured to display the at least one image of the patient and superimpose a graphical representation of the at least one implant with position and orientation information of the at least one implant on the at least one image of the patient.
Status: Filed

11. **Title:** Registration Clamp For Percutaneous Spinal Navigation (MIS Spine Clamp; Straight And Right Angle Designs)
Abstract: A percutaneous registration apparatus and method for use in minimally invasive spinal surgery. The apparatus including a holding member, first and second clamping members, first and second gripping members, and an adjustment mechanism for closing and opening the first and second gripping members.
Status: Published

12. **Title:** Method for Surgical Navigation of Artificial Spine Disk, Nucleus and Interbody Fusion Cage Placement and Orientation
Abstract: An image guided surgical system and method for targeting the precise patient specific anatomical placement of surgical instruments and motion preservation implants with surgical navigation. The system and method comprising a surgical navigation system; at least one imaging system coupled to the surgical navigation system; at least one computer coupled to the surgical navigation system and the imaging system having planning software for measuring clinical parameters of anatomy of a subject to be operated on; and at least one display for displaying imaging data, planning data and tracking data.
Status: Published

13. **Title:** Navigation And Visualization Of A Combination Needle/Cannula And Stylet/Trocar "NAV Access Needle System" For Intraosseous Bone Access. **Status: Published**

Intellectual Property continued:

14. **Title:** Navigation and Visualization with X-ray and or CT
    Abstract: Described herein are one or more implementations for a percutaneous spinal registration-and-access tool for minimally invasive spinal surgery involving lumbar pedicle screw fixation and registration (which is the set-up process for spinal computer navigation). This spinal registration-and-access tool aids registration by allowing more precise targeting of the spinous process (of the vertebrae) and safe working channel for percutaneous placement of a sharp tool (e.g., a bone pin) through the protected subcutaneous tissue.
    Status: Pending publication

15. **Title:** Mobile single unit surgical table with integrated computer navigation and 3-D flat panel digital fluoroscopy. ID10777
    Status: Filed

Medical and Technical Memberships

1) Massachusetts Medical Society
2) American Medical Association
3) American Academy of Otolaryngology Head and Neck Surgery
4) Spine Arthroplasty Society (International Society for the Advancement of Spine Surgery)
5) North American Spine Society
6) International Skeletal Society
7) International Brain Mapping and Intraoperative Surgical Planning Society
8) Institute of Electrical and Electronics Engineers
9) Society of Photo Optical Instrument and Engineering
10) Global Medical Affairs and Clinical Strategy – General Electric Healthcare
11) Hungarian Medical Association of America

Reviewer

2009: International Journal of Computer Assisted Radiology and Surgery (JCARS);
Springer Berlin / Heidelberg

2009: Center for Integration of Medicine and Innovative Technology (CIMIT); Boston / Massachusetts.
CIMIT is a consortium of Boston teaching hospitals and engineering schools. It provides grants and fellowships for early stage, collaborative research projects leading to publications and to improving patient care.

CME [126 AMA PRA Category 1 Credits] Course and Workshops in Related Surgery:

1. North American Spine Society Annual Meeting 2008. Common spinal Pathology: Operative and Non-operative Options. Degenerative Lumbar Spondylolisthesis, Evolution in the Treatment of Cervical Disc Disease, Hands-on Cervical And Lumbar Instrumentation, Applying Evidence-Based Medicine into Your Practice, Interventional Treatment, Lessons Learned from Disc Arthroplasty.
[18 CME credit points for AMA PRA Category 1 credits™.]

2. American Academy of Orthopedic Surgeons 2008. Instructional Courses/Scientific Programs.
[31 CME credit points for AMA PRA Category 1 Credits™.]

3. Spine Arthroplasty Society 2008. SAS-8 Global Symposium on Motion Preservation Technology.
[23 CME credit points for AMA PRA Category 1 Credits™.]

4. American Association of Otolaryngology Head and Neck surgery 2008.
[21 CME credit points for AMA PRA Category 1 Credits™]

5. Massachusetts General Hospital Symposium for Otolaryngology 2008.
[10 CME credit points for AMA PRA Credits™.]

6. International Musculoskeletal Radiological Society meeting Budapest Hungary 2007.
[23 CME credit points for AMA PRA Category 1 Credits™.]

7. International Conference on Cochlear Implants and Related Sciences 2006.
[**18 CME credit points** of postgraduate medical education officially approved by the Austrian Medical Council.**]**

Total CME Credit points 126 for AMA PRA Category 1 Credits 2007-2008

Awards

1. American College of Surgeons Scientific Exhibition Award, "MIS in Abdominal Vascular Reconstruction"
2. American College of Surgeons Scientific Exhibition Award, "History of Minimally Invasive Coronary Bypass"
3. America's Distinguished Physicians Research Award
4. GE Healthcare President's Award
5. GE Healthcare U.S. Multi-Center MIS Clinical Spine Study Grant Award
6. GE Healthcare Broad-Based Grant Award, 2002, 2004, 2006, 2007, 2008
7. GE Healthcare Surgery Leadership Award 2008
8. GE Healthcare Surgery Thinker Award 2008
9. GE Healthcare Patent Award 2004, 2005, 2006, 2007, 2008
10. GE Healthcare Surgery Technology Award, 2005 – 2007
11. GE Healthcare Surgery Leadership Award 2007
12. GE Healthcare OEC Engineering Award, 2006